

Soil Quality Dynamics and Spatial Heterogeneity in Grasslands and Cropping Systems in
Western Canada

by

Mina Kiani

A thesis submitted in partial fulfillment of the requirements for the degree of

Master of Science

in

Soil Science

Department of Renewable Resources
University of Alberta

© Mina Kiani, 2016

Abstract

Managing the land properly should lead us to conserve the soil which is a critical substance for sustaining our life and the global society. Quantifying the effects of land management and land-use conversion on soil physical and biological properties can aid to identify best management practices that can reverse the trend of declining soil quality. Additionally, underlying heterogeneity in soil properties can impose and amplify existing management challenges in common land use systems. Therefore, this study was conducted to identify sensitive soil quality indicators among contrasting land managements and also to characterize the spatial heterogeneities of key soil attributes using ordinary kriging (OK), regression-kriging (RK), cokriging (coK), and regression-cokriging (RcoK) geostatistical approaches. Our results demonstrated an improved hierarchical fractal aggregation (D_m) in soils covered by perennial legumes and grasses ($D_m = 0.97$) compared to nonfractal aggregation under fallow phases ($D_m = 0.99$). Our results proved that complex crop rotations including perennials enhanced soil quality which was concurrently associated with higher crop production. Long-term cattle manure additions had strong positive effect on nutrient cycling, while balanced fertilization beneficially influenced soil-water relationships and physical condition. Our results suggest that the D_m value, S-index, plant available water (PAW), soil organic C (SOC) concentration, and microbial biomass C (MBC) are highly responsive soil quality indicators, and hence, useful for evaluating management options. Collectively, our results indicate that conversions from either natural forest or native grassland to cultivated lands detrimentally alter the soil structural characteristics through substantially lowering macroporosity, saturated water content, and S-index. Such land-use conversions into cultivated lands also appear to increasing MBC in soils. Furthermore, fungi and Gram-negative bacteria were found to be distinctive biomarkers in the natural forest and

native grassland soils, respectively, perhaps suggesting a paradigmatic shift in microbial community composition when long-term cultivation is established. Comparison of OK, RK, coK, and RcoK approaches at our field scale revealed that the combination of kriging with certain terrain covariates [e.g., elevation and depth-to-water (DTW)] as implemented in the coK method delivers enhanced soil mapping while reducing prediction uncertainty.

Keywords: geostatistics, land-use, mass fractal dimension, NPKS fertilization, predictive mapping, secondary variable, soil quality evaluation

Acknowledgements

I would like to express my sincere gratitude to my supervisor Dr. Guillermo Hernandez Ramirez for the continuous support of my MSc study, for his patience, motivation, and immense knowledge. His guidance helped me in all the time of research and writing of this thesis. I would also like to acknowledge my committee member Sylvie Quideau for her precious contributions.

I thank my fellow labmates and research assistants, Lewis Fausak, Karin Lindquist, Kris Guenette, Catherine Pocklington, and Sisi Lin for their assistance during field sampling and laboratory analyses and for all the fun we have had in the last two years. I am also grateful for the assistance of our funding partners Alberta Livestock and Meat Agency (ALMA) Sustainability, and Rangeland Research Institute (RRI) University of Alberta.

Finally, I must express my very profound gratitude to my family for providing me with their support and continuous encouragement throughout my years of study and through the process of researching and writing this thesis. This accomplishment would not have been possible without them.

Table of Contents

Title Page	i
Abstract	ii
Acknowledgements	iv
Table of Contents	v
List of Tables	vii
List of Figures	viii
Introduction	1
CHAPTER ONE	5
1. Abstract	7
2. Introduction.....	9
3. Materials and Methods.....	12
3.1. Study sites	12
3.2. Soil sample collection and analysis	12
3.3. Statistical analysis.....	17
4. Results.....	20
4.1. Fractal dimension (Dm)	20
4.2. Water retention characteristics, pore size distribution, S-index, and hydraulic parameters	20
4.3. Soil microbial biomass C, microbial communities, pH, SOC, STN, and C:N.....	22
4.4. Correlation analyses among soil properties	24
4.5. The linkage between plant productivity and soil quality	24
5. Discussion	25
5.1. Land managements influence soil quality.....	25
5.2. Fractal aggregation, S-index, MBC, SOC, and PAW showed clear sensitivity to management.	30
6. Conclusion	35
7. Acknowledgement	36
8. References.....	37
9. Tables and figures	44
10. Figure captions.....	56
CHAPTER TWO	57
1. Abstract.....	59
2. Introduction.....	61

3. Materials and Methods.....	65
3.1. Study sites	65
3.2. Soil sample collection	66
3.3. Soil sample analysis	67
3.3. Classical statistical analysis	69
3.4. Geostatistical analysis	71
4. Results.....	74
4.1. Classical statistical analyses of soil properties.....	74
4.2. Variographic analyses of soil properties	75
5. Discussion	80
5.1. Soil quality changes in contrasting land use systems.....	80
5.2. Gaussian model fits better for PAW, SOC, and MBC variographies.	83
5.3. Co-kriging approach enhances spatial predictions.....	84
5.4. Optimization of field sampling designs	88
6. Conclusion	90
7. Acknowledgement	92
8. References.....	93
9. Tables and figures	100
10. Figure captions.....	113
Conclusion	114
References.....	117
Appendices.....	134

List of Tables

Chapter one

Table 1-1A	Effect of crop rotation and nutrient management on selected soil attributes at the 5 to 10 cm soil increment depth from Breton site. Within a column, treatment means with different letters differ, $P < 0.05$.
Table 1-1B	Effect of crop rotation and nutrient management on selected soil attributes at the 5 to 10 cm soil increment depth from Breton site. Within a column, treatment means with different letters differ, $P < 0.05$. Ks: saturated hydraulic conductivity; Unsat. K: hydraulic conductivity at 100 hPa; SOC: soil organic carbon; STN: soil total nitrogen; C:N: carbon to nitrogen ratio; MBC: microbial biomass carbon.
Table 1-2A	Effect of crop rotation type on selected soil attributes at the 5 to 10 cm soil depth increment from Lethbridge site. Within a column, treatment means with different letters differ, $P < 0.05$.
Table 1-2B	Effect of crop rotation on selected soil attributes at the 5 to 10 cm soil depth increment from Lethbridge site. Within a column, treatment means with different letters differ, $P < 0.05$. Ks: saturated hydraulic conductivity; Unsat. K: hydraulic conductivity at 100 hPa; SOC: soil organic carbon; STN: soil total nitrogen; C:N: carbon to nitrogen ratio; MBC: microbial biomass carbon.
Table 1-3	Multi-response permutation procedure results for microbial community structure (PLFA) in both sites. Only comparisons that were found to be significantly different are presented.
Table 1-4	Distinctive indicator species analysis for microbial community structure (PLFA) associated with treatments in Breton site. Each value represents the mean indicator with standard deviation in parentheses, and the highest indicator value is in bold. Only PLFAs that were found to be significantly different among groups are presented.
Table 1-5	Distinctive indicator species analysis for microbial community structure (PLFA) associated with treatments in Lethbridge site. Each value represents the mean indicator with standard deviation in parentheses, and the highest indicator value is in bold. Only PLFAs that were found to be significantly different among groups are presented.
Table 1-6	Pearson correlation coefficients (r-values) for relationships among soil properties in both sites.

Chapter two

Table 2-1	Descriptive statistics of soil properties at native grassland (NG) and irrigated cultivated land (IC) and optimal sample sizes at various confidence intervals.
Table 2-2	Spearman correlation coefficients (ρ -values) for relationships among selected soil properties at native grassland (NG) and irrigated cultivated land (IC).
Table 2-3	Spearman correlation coefficients (ρ -values) for relationships among soil properties of interest and terrain covariates (as derived from Light Detection and Ranging; LiDAR) at native grassland (NG) and irrigated cultivated land (IC).
Table 2-4	Deterministic and variographic (semivariogram and cross-semivariogram) models, fitting statistical indicators, and resulting validation parameters as a function of five geostatistical approaches in both native grassland (NG) and irrigated cultivated land (IC).
Table 2-5	Distinctive phospholipid fatty acid (PLFA) indicator species analysis associated with whether native grassland (NG) or irrigated cultivated land (IC). Each value represents the mean indicator with standard deviation in parentheses, and the highest indicator value is in bold. Only PLFAs that were found to be significantly different among groups are presented.

List of Figures

Chapter one

- Figure 1-1 Mass fractal dimension (D_m , unitless) of the natural log transformed aggregate mass (g) versus natural log normalized aggregate volume (cm^3) for phases within simple and complex rotations and adjacent forest (A. Breton, B. Lethbridge). D_m values are derived as slopes of linear regressions. Shown p-values are for regression coefficients against one as the non-fractal constant for mass vs. volume; $H_0: \beta_1 = 1$. Lower D_m values imply increasing development of hierarchical aggregation, and hence improved soil quality. Figures A and B have different y-axes scales.
- Figure 1-2 Mass fractal dimension (D_m , unitless) of the natural log transformed aggregate mass (g) versus natural log normalized aggregate diameter (cm) for two nutrient managements (A. balanced fertilization, B. control). The n value is the number of scanned aggregates. D_m values are derived as slopes of linear regressions. Shown p-values are for regression coefficients against one as the non-fractal constant for mass vs. volume; $H_0: \beta_1 = 1$.
- Figure 1-3 NMS ordination biplots for phospholipid fatty acid (PLFA) analysis for phases within simple and complex rotations and adjacent forest (A. Breton, B. Lethbridge). 89 iterations, stress= 13, and 2-dimensional solution for Breton and 69 iterations, stress= 11, 3-dimensional solution for Lethbridge.
- Figure 1-4 Fig. 4. Wheat grain yield ($\text{kg dry matter ha}^{-1}$) for simple and complex rotations in 2014 (A. Breton site, B. Lethbridge site). The wheat grain yield in complex rotation of Lethbridge site is the yield of first year of wheat at the mentioned rotation. There are three nutrient regimes in Breton, and the NPKS is referred in this study as balanced fertilization.

Chapter two

- Figure 2-1 Nested cyclic sampling design. The sampling intervals were every 10, 35, 85, 100 m for west to east direction and every 10, 35, 85, 95, 120, 170 m for north to south direction ($n = 36$; main panel). A 0.5, 2, 4.5 m cycle was applied in both directions for the smaller scale nest ($n = 20$) as showed in the inset. There are also two additional sampling points (highlighted in green) which were strategically located in the field plots to increase the sampling efficiency.
- Figure 2-2 Number of pairs of measured data points for each lag class assuming a uniform lag class size of 5 m distance interval. The dash line shows the 70% of the total distance which is taken as the maximum allowable active lag distance.
- Figure 2-3 (A) Square root of plant available water (PAW; $\text{m}^3 \text{ m}^{-3}$) versus soil organic carbon concentration (SOC; g C kg^{-1} soil) for native grassland (NG) site, and (B) logarithmic microbial biomass carbon (MBC; nmol g^{-1} soil) versus carbon to nitrogen ratio (C:N; unitless) for irrigated cultivated (IC) site.
- Figure 2-4 Terrain elevation derived from airborne LiDAR (Light Detection and Ranging) with vertical accuracy of 30 cm and spatial resolution of 2 m x 2 m [A. native grassland (NG), B. irrigated cultivated land (IC)]. The green dots are the locations of the 56 measured points in each field site. As customary, terrain elevation units are in meters above mean sea level.
- Figure 2-5 Maps of (a) plant available water (PAW; $\text{m}^3 \text{ m}^{-3}$), (b) soil organic carbon concentration (SOC; g C kg^{-1} soil), and (c) microbial biomass carbon (MBC; nmol g^{-1} soil) concentration by cokriging (coK) method in native grassland. The green dots are the locations of 56 measured points.
- Figure 2-6 Generalized visualization of the uncertainty prediction [standard deviation (SD)] for plant available water (PAW; $\text{m}^3 \text{ m}^{-3}$) using (a) ordinary kriging (OK), (b) regression-kriging (RK), (c) cokriging (coK), and (d) regression-cokriging (RcoK) approaches in an irrigated cultivated land site. The green dots are the 56 measured points.

Introduction

Land management practices can largely impact various soil properties which in turn are intrinsically linked to the sustainability of agroecosystem functions and productivity (Di et al., 2013; Garrigues et al., 2012). Moreover, an enhanced soil quality can build resiliency in land-based production systems. This will bolster buffering and adaptation capacities in agroecosystems which in turn enable managing the detrimental impacts of escalating climate variability (de Paul Obade and Lal, 2014; Garrigues et al., 2012). In an attempt to reverse the trend of declining soil quality, it is essential to focus on quantifying the effects of contrasting land management options and land-use conversions on soil properties (D'Hose et al., 2014; Geisseler et al., 2016). In addition, spatial heterogeneity in soil properties can represent management challenges to policymakers and producers where soil properties could differ from one sampling point to other nearby sampling points within the same management unit (Nyamadzawo et al., 2008; Robertson et al., 1993). Therefore, there is a need for comprehensive understanding and documentation of the spatial structure of soil properties and its linkage with ecosystem functions such as nutrient cycling and water regulation.

Conceptually, soil quality depends on the extent to which soils fulfill the role or goal for what they are being used (Karlen et al., 2003). Certain management choices such as rotation type and nutrient regime influence multiple specific functions of the soil. Earlier studies have suggested the implementation of diversified rotations as a part of conservation agriculture strategies to enhance soil quality (Munkholm et al., 2003; Ehlers and Claupein, 1994). They also reported that soil quality can be benefited by balanced fertilization recommendations (Chakraborty et al., 2011). In addition, common land use systems have been shown to have wide-ranging impacts on individual soil properties (Hebb et al., 2016; Teferi et al., 2016).

Conversion of native grasslands to annual croplands can lead to the physical disruption and loss of soil structure, thereby reducing macroporosity and increasing bulk density (Bodhinayake et al., 2002; Li et al., 2007; Jones et al., 2016). However, significant soil quality changes may generally be realized and noticeable over the long term due to the inherently slow rates of soil change with time (de Paul Obade and Lal, 2014), and therefore, there is a paucity of information regarding the long-term integrated effects of contrasting land managements and land-use changes on soil quality.

Soil quality cannot be directly measured and its assessment is typically inferred from observed or modelled soil physical, chemical, or biological attributes (Lal, 2001). Therefore, an on-going methodological challenge is to identify a relevant, standard set of specific properties as meaningful indicators of the soil quality which are sensitive to management-induced changes (Ahamadou and Huang, 2013). Conceptually, soil quality depends on the extent to which soils fulfil the role or goal for what they are being used (Karlen et al., 2003). Therefore, it is vital to identify a new soil health metrics to integrate and document changes in soil properties and associated several soil functions. In addition, such quantification of soil functions in various land uses can also inform the potential outcome of valuable ecosystem services including carbon sequestration, water cycling and filtration as well as grain and forage productivity.

Development of soil quality changes is gradual, and it typically takes a reasonable time to achieve a long-term steady state after a change of management (Chakraborty et al., 2011). Therefore, we focused on the comparative effects of contrasting natural ecosystems and agricultural systems in long-term study sites to detect changes that are likely absent or may not be evident in the short term. Moreover, a comprehensive soil characterization entails multiple attributes and functions (O'Sullivan et al., 2015). Hence, we investigated a wide range of soil

properties (e.g., aggregation, water conductivity, macroporosity, carbon and nitrogen, and microbial communities) and their responses to various land managements to test and identify the sensitivity of soil quality indicators to contrasting agroecosystems. New information on soil quality responses to land managements can improve methods by which land owners will be better able to measure and manage soil quality, and this may eventually lead to more sustainable agroecological systems.

Site-specific management endeavors to manage spatial and temporal variability within fields in order to optimize profitability, sustainability, and environmental protection (Duffera et al., 2007; Lowenberg-DeBoer and Swinton, 1997). Soil classification and survey have been traditionally used to document and characterize the spatial variation by generating maps of soil classes that represents soil properties estimated within a defined region or generalized mapping unit (Webster, 1985). Different geostatistical methods have been recently applied to interpolate soil properties from sparse sampling points into continuous surfaces by modeling the spatial correlation with minimum variance (Cambardella et al., 1994; Hengl et al., 2004; Lark, 2002; Wang et al., 2009). However, insufficient attention has been paid to comparing the spatial structure of specific soil properties such as plant available water (PAW), soil organic carbon (SOC), and microbial biomass carbon (MBC) which are closely related to key soil functions such as soil pore water relationships and nutrient cycling. Different geostatistical methods have been employed to map soil properties whether merely based directly on available measured data (e.g., ordinary kriging) or based on spatial distribution of a secondary variate (e.g., cokriging, regression cokriging) (Mirzaee et al., 2016; Wang et al., 2013; Hengl et al., 2004; Odeh et al., 1995). However, there are discrepancies across these available reports regarding the performance of these various geostatistical methods, and hence, the existing literature substantiates the need

for further comparison of these various geostatistical approaches under contrasting agroecosystems and for multiple biophysical attributes.

We hypothesized that soil quality will increase (e.g., higher macroporosity and microbial biomass carbon) in the following pattern: cropland < native prairie and the spatial variability of soil quality indicators is higher in native prairie comparing with irrigated cultivated land. Regarding contrasting land managements, we hypothesized that soil quality increases in the following pattern: controls with no nutrient added < Nitrogen fertilizer < Manure. Also, crop rotations including leguminous crops would increase soil quality more than simple wheat-fallow rotations.

The aims of this study were to: i) determine the long-term effects of contrasting land managements (i.e., crop rotations and nutrient regimes) and divergent land-use types (native grassland versus cultivated land) on selected soil physical, chemical and biological properties, ii) identify soil quality indicators that can provide robust metrics of sustainability by testing whether they can detect and distinguish among contrasting land managements and land-use systems, iii) capture and upscale new spatial knowledge of key soil biophysical attributes (i.e., PAW, SOC, and MBC) from point measurement to field landscapes by extracting their spatial variability patterns while comparing several geostatistical approaches (i.e., OK, coK, RK, and RcoK).

CHAPTER ONE

**Quantifying the Sensitive Soil Quality Indicators across contrasting Long-term Land Management
Systems: Crop Rotations and Nutrient Regimes**

1. Abstract

Managing the land properly can lead us to conserve the soil which is a critical substance for sustaining our life and the global society. However, measuring the quality of the soil explicitly is still a challenge. Therefore, this study was conducted to identify suitable soil quality indicators among contrasting land managements (i.e., simple vs. complex crop rotations; manure vs. balanced fertilization) at long-term experimental fields. The fractal structure of soils was documented by the mass-diameter relationship of soil aggregates using 3D laser scanning. Hydraulic conductivity (K), pore size fractions, and S-index were determined from moisture retention curves using a HYPROP system. Soil microbial community structure was also characterized using phospholipid fatty acid (PLFA) analysis. Our results demonstrated an improved hierarchical fractal aggregation in soils covered by perennial legumes and grasses ($D_m = 0.97$) compared to nonfractal aggregation under fallow phases ($D_m = 0.99$). In addition, across nutrient managements, balanced fertilization was the only management exhibiting significantly enhanced fractal aggregation. Moreover, complex crop rotations and balanced fertilization also improved S-index, saturated water content (sat. WC), and plant available water (PAW) compared to their counterparts ($P_s < 0.05$). Similarly, significant differences between simple and complex rotations were evident for microbial community composition and biomass carbon (MBC) with 1.5 times higher MBC in the soils under complex rotations compared to both the adjacent forest soil and the simple 2-yr rotations. Our results proved that complex crop rotations including perennials enhanced soil quality, and this outcome was associated with higher crop productivity. Both balanced fertilization and manure had contributed to improving soil functions where cattle manure had stronger positive effect on nutrient cycling, while the balanced fertilization beneficially influenced water relationships and physical condition in the

soil. Our results suggest that the Dm, S-index, PAW, soil organic C, and MBC are highly responsive indicators useful for evaluating management options that also influence agricultural productivity.

Keywords: grain yield, mass fractal dimension, NPKS fertilization, PLFA, soil quality evaluation

2. Introduction

Enhancing and sustaining the quality of soils is essential to ensure agricultural productivity, water availability and an overall environment quality (de Paul Obade and Lal, 2014; Garrigues et al., 2012). Moreover, an enhanced soil quality can build resiliency in land-based production systems to enable buffering and adaptation capacities that can diminish the detrimental impacts of escalating climate variability and frequency of extreme weather events such as droughts or flooding (de Paul Obade and Lal, 2014; Garrigues et al., 2012). Likewise, agricultural management practices can largely impact the quality of the soil which in turn is intrinsically linked to the sustainability of agroecosystem functions and productivity (Di et al., 2013).

In an attempt to reverse the trend of declining soil quality, recent studies focused on identifying suitable soil management practices (D'Hose et al., 2014; Sharma et al., 2008). However, soil quality cannot be directly measured and soil quality information is typically inferred from observed or modelled soil physical, chemical, or biological attributes (Lal, 2001). Therefore, an on-going methodological challenge is to identify a relevant, standard set of specific properties as meaningful indicators of the soil quality which are sensitive to management-induced changes (Ahamadou and Huang, 2013). Conceptually, soil quality depends on the extent to which soils fulfil the role or goal for what they are being used (Karlen et al., 2003). Therefore, within the context of agricultural production, high soil quality is rather equivalent to long-term high productivity and system resiliency without significant soil or environmental degradation (Karlen et al., 2006).

Crop rotation is one of the fundamental management factors influencing soil quality and thus the overall sustainability of cropping systems (Munkholm et al., 2013). Many reports have

suggested the use of diverse rotations as part of the conservation agriculture concept to enhance the soil quality particularly in weakly structured soils (Munkholm et al., 2003; Ehlers and Claupein, 1994). However, significant soil quality changes may only be realized and noticeable over the long term due to the inherently slow rates of soil change with time (de Paul Obade and Lal, 2014), and therefore, there is a paucity of information regarding the long-term integrated effects of contrasting rotation types and different nutrient management regimes on soil quality.

Appropriate fertilizer application is an important management practice to manage soil fertility in croplands (Sradnick et al., 2013). Soil quality can also benefit from balanced fertilization recommendations as indicated by Chakraborty et al. (2011), who reported increasing contents of soil organic matter, microbial biomass, and plant nutrient elements. It has been suggested that soil quality is directly linked to microbial activity, as microbial metabolic capabilities are linked to nutrient cycling and other key soil functions (Sradnick et al., 2013). The majority of the existing nutrient studies focused mostly on fertility and microbial aspects of the soil. Nevertheless, organic matter can be formed and accrued in soils due to recurrent fertilizer applications in the long-term which stimulate plant productivity (including roots and harvest residues) as well as microbial and faunal activities in the soil (Chakraborty et al., 2011; Hati et al., 2008). Consequently, implementation of long-term balanced fertilization in cropland could hypothetically improve also soil physical conditions by increasing water holding capacity, macroporosity, infiltration capacity, aggregation and decreasing the bulk density (Hati et al., 2008; Metzger and Yaron., 1987).

Certain management choices such as rotation type and nutrient regime influence various specific functions of the soil, and hence, measuring merely one physical or biological property of the soil could not reveal the entire impacts of management options. Therefore, it is vital to

identify and model critical indicators of soil quality and agro-ecosystem sustainability (de Paul Obade and Lal, 2014). There is also a need for new soil health metrics to integrate and document changes in soil properties and associated soil functions. In addition, such quantification of soil functions in croplands can also inform the potential outcome of valuable ecosystem services including carbon sequestration, water cycling and filtration as well as grain and forage productivity.

Development of soil quality changes is gradual, and it typically takes a reasonable time to achieve a long-term steady state after a change of management (Chakraborty et al., 2011). Therefore, our study is focusing on the comparative effects of contrasting crop rotations and nutrient managements in long-term agricultural field experiments to detect changes that are likely absent or may not be evident in the short term. Moreover, a comprehensive soil characterization entails multiple attributes and functions (O'Sullivan et al., 2015). Hence, we investigated a wide range of soil properties responses (e.g., aggregation, water conductivity, macroporosity, carbon and nitrogen, and microbial communities) to various land managements to test and identify the sensitivity of soil quality indicators to contrasting agroecosystems. New information on soil quality responses to land managements can improve methods by which land owners are better able to measure and manage soil quality, and this may eventually lead to more sustainable agroecological systems.

Specific objectives of this study were to: i) determine the long-term effects of contrasting crop rotations and nutrient managements on soil physical and biological properties, and ii) identify soil quality indicators that can provide robust metrics of sustainability by testing whether they can detect and distinguish among contrasting land managements and also by examining the associations among these soil quality measures and other soil properties and crop productivity.

3. Materials and Methods

3.1. Study sites

The study was conducted at two sites, the University of Alberta Breton Plots, located approximately 100 km southwest of Edmonton (53.089°N, 114.442°W) and the Agriculture Agri-Food Canada's Lethbridge Research Centre located approximately 500 km south of Edmonton (49.705°N, 112.775°W). The Breton plots were established on Orthic Gray Luvisol, and the Lethbridge plots were established on Orthic Dark Brown Chernozemic soil according to the Canadian System of Soil Classification (Soil Classification Working Group, 1998) (AGRASID, 2015). The granulometric distribution for Breton loamy soil was: sand (1000–50 µm size diameter) 362, silt (50–2 µm) 444, and clay (<2 µm) 194 g kg⁻¹ soil and for Lethbridge loamy soil was: sand 432, silt 304, and clay 264 g kg⁻¹ soil. Based on 20 years data from Breton and Lethbridge on-site permanent weather stations (Alberta - Weather Conditions and Forecast, 2016), the mean annual precipitation is 547 and 402 mm in Breton and Lethbridge plots, respectively. The annual average of air temperature was 2.1 °C in Breton and 5 °C in Lethbridge.

3.2. Soil sample collection and analysis

In Breton long-term classical plots, two rotations were selected for this study including a 2-yr wheat–fallow rotation and a 5-yr wheat–oat–barley/hay–hay₁–hay₂ rotation which were established in 1930. The hay phases included alfalfa and brome grass since 1967 to present. Each rotation was managed with three nutrient managements including balanced fertilization (N-P-K-S fertilizer), manure, and control receiving no nutrient addition. Detailed information about fertilization rates for each crop phase has been previously described by Dyck et al. (2012). Our field sample collections were conducted in early spring 2015. We collected soil samples at the fallow phase in 2-yr rotation, oat and Hay₂ phases within the 5-yr rotation because this sampling

timing allowed for examination of the carry over effects from the immediate preceding growing seasons: wheat_{2yrR}, wheat_{5yrR}, and Hay_{1-5yrR}, respectively. As a reference benchmark in the Breton site, we also collected soil samples at an adjacent natural forest. A total of ten sampling plots were conducted at the Breton site. At the Lethbridge long-term experiment (known as Rotation 120) we also sampled two rotations: a 2-yr wheat–fallow rotation (established in 1985) and a 6-yr fallow–wheat₁–wheat₂–alfalfa₁–alfalfa₂–alfalfa₃ rotation [established in 1951(Lafond and Harker, 2012)]. The alfalfa phases included alfalfa and crested wheat grass. This experiment is arranged in a randomized complete block design with 4 replicates. All the phases of the two rotations were sampled except for alfalfa₂ in the 6-yr rotation for a total of 28 sampling plots.

Within each field sampling plot, undisturbed soil samples were collected using stainless steel cylindrical cores (8 cm inner diameter) with three samples per plot for Breton, and two for Lethbridge. Soil undisturbed clods (~ 500 cm³) were also excavated from each plot with a shovel at the 5 cm depth (three samples per plot for Breton, and two for Lethbridge). Clods were wrapped in aluminum foil and plastic sampling bags to prevent significant moisture loss, and placed in a plastic container to minimize disturbance during transport from the field. For chemical and microbial analyses, we also collected disturbed soil samples in each field plot by composing 4 subsamples taken using a 2 cm inner diameter push probe (three samples per plot for Breton, and one for Lethbridge). These disturbed samples were placed in the Whirl-Pak[®] (Nasco, Fort Watkins, Wisconsin) sterile sampling bags and were transported in an icebox to the laboratory. Samples for microbial characterization were kept frozen at –86 °C until they were freeze-dried in preparation for analysis. Within each sampling plot, all soil samples were taken at randomly selected sampling points and at the depth increment of 5-10 cm.

Using the undisturbed clods, mass fractal dimension of soil aggregates was determined using multistriple laser triangulation scanning (3D Scanner Ultra HD, NextEngine, California). Fractal dimension is a measure of how soil aggregates are hierarchically organized in soils. Larger aggregates have a lower mass to volume ratio as explained by the porosity exclusion principle (Hirmas et al., 2013); denser micro-aggregates are bonded to form macro-aggregates with greater porosity. The procedure for measuring fractal dimension is described in detail by Hirmas et al, 2013. Briefly, a parent clod (~500 cm³) was progressively broken down into five smaller size classes (i.e. 4-8, 2-4, 1-2, 0.5-1, and 0.25-0.5 cm diameter). Two aggregates from each class were randomly selected and scanned to obtain a 3D image to determine aggregate volume. We assessed the precision of our volume measurements using repeated laser scanning (n= 20). The method performed well for determining multiple volumes ranging from 0.1 to 270 cm³ as shown by coefficient of variations lower than 5% and standard deviations lower than 0.04 cm³.

Fractal dimension was obtained using the following equation:

$$M(v) = k_m v^{D_m} \quad [1]$$

where $M(v)$ is the mass of aggregates (g) with volume v (cm³), k_m is a constant representing the mass of aggregate unit volume, and D_m is the fractal dimension. Lower D_m values imply increasing hierarchical aggregation, and hence development of improved soil structure.

Using the undisturbed cores, water retention was determined with the evaporation method (Schindler et al., 2010) using a HYPROP device (UMS GmbH, Munich, Germany) for tensions < 1000 hPa. Matric potential was automatically recorded every minute for the first hour and each 10 minute afterwards by two tensiometers at two depths within the saturated soil cores. The

gravimetric water content of the samples was recorded twice daily for up to 14 days. Data points of the retention and unsaturated hydraulic conductivity (unsat. K) curves were calculated with the HYPROP 2011 software (UMS GmbH, Munich, Germany) based on the mean tension potential of the two tensiometers and water contents.

The water content for moderate to dry moisture ranges was evaluated with a WP4-T potentiometer (Decagon Devices, Inc., PullmanWA, USA) based on the chilled-mirror dew point technique (Schelle et al., 2013). Seven different amounts of water were added to 5 mg dry weight of soil in plastic cups. Each sample cup represents one point on the curve. The cups were closed tightly and samples allowed equilibrating for 24 hours. When the water potential of the sample was in equilibrium with the vapor pressure of the WP4-T measurement chamber, water tension was recorded. Sample weight was determined immediately after measurement and related to the oven-dry weight (at 105 °C) to obtain the corresponding water content. The constrained van Genuchten (1980) model was fitted to the results from the evaporation method and WP4-T measurements.

$$\theta_g = (\theta_s - \theta_r)[1 + (\alpha h_m)^n]^{-m} + \theta_r \quad [2]$$

where θ_g is the volumetric water content ($\text{cm}^3 \text{ cm}^{-3}$), θ_s and θ_r are the saturated and residual water content ($\text{cm}^3 \text{ cm}^{-3}$), respectively, h_m is the matric potential (hPa), α (hPa^{-1}) is a reciprocal suction that is characteristic for the soil, and n and m ($m = 1 - \frac{1}{n}$) are dimensionless variables that describe the shape of the curve.

Soil pore size distribution data was computed from the soil water retention data for tensions of approximately -30, -60, and -330 hPa using the procedure outlined in Hernandez-Ramirez et al. (2014). These tensions correspond to pore diameters of 100, 50, and 9 μm . Pore volume fractions were quantified from the change in volumetric water content using these pore

diameters as class boundaries. Plant available water was also calculated as the volumetric water content between field capacity (-330 hPa) and permanent wilting point (-15000 hPa).

Dexter (2004) introduced the S-index as an index of soil physical quality where S is the slope of the water retention curve at the inflection point when logarithm of water suction (h) is plotted against water content. S-index is calculated from the modelled van Genuchten parameters as follows:

$$S = n (\theta_s - \theta_r) \left(1 + \frac{1}{m}\right)^{-(1+m)} \quad [3]$$

The hydraulic conductivity (k) was calculated according to the Darcy-Buckingham law (Schindler et al., 2010):

$$k(h) = \frac{\Delta V}{2A \Delta T i_m} \quad [4]$$

where h is the mean pressure head averaged of both tensiometers, ΔV is the soil water volume difference, A is surface area, ΔT is time interval, and i_m is the hydraulic gradient calculated based on the pressure head readings. Unsaturated hydraulic conductivity was calculated as the conductivity of the sample at the tension of approximately 100 hPa. At the end of each measurement campaign, the soil samples were oven dried at 105 °C for 24 h to derive the total porosity and the bulk density assuming a particle density of 2.65 g cm⁻³.

After grinding a portion of the composited, disturbed samples, we determined the content of soil organic carbon (SOC) and soil total nitrogen (STN) by dry combustion method using a Costech ECS 4010 Elemental Analyzer (Costech Analytical Technologies Inc., Valencia, CA, USA). Soil pH was measured using a 1:2 soil to water ratio (Mclean, 1982).

Using composited samples, we characterized soil microbial communities using phospholipid fatty acid (PLFA) analysis. Polar lipids were extracted from freeze-dried samples

using a modified Bligh and Dyer protocol (Hannam et al., 2006). The resulting fatty-acid methyl esters were separated using an Agilent 6890 Series capillary gas chromatograph (Agilent Technologies, Wilmington, DE, USA). Individual peaks were identified and quantified (nmol g⁻¹) using the MIDI peak identification software (MIDI, Inc., Newark, DE, USA). The standardized X: Y ω Z nomenclature for fatty acids was used to identify PLFAs, where X is the number of carbon atoms, Y is the number of double bonds, and Z is the position of the first double bond from the aliphatic end (ω) of the molecule. Prefixes “i” and “a” indicate branching at the second and third carbon atom, respectively, from the ω end, and the suffix “c” corresponds to a c transfiguration. Taken together, all of the PLFA biomarkers were considered to be representative of the total PLFA of the soil microbial community.

3.3. Statistical analysis

We used non-metric multi-dimensional scaling (NMS) ordinations to identify potential patterns in the soil microbial community compositions. The ordination technique presents the advantage of not requiring normal distribution, nor does it assume linear relationships among variables (McCune and Grace, 2002). NMS organizes complex datasets in a reduced dimensional space (typically two or three dimensions) as to reveal similarities or dissimilarities in the original dataset structure. An optimal NMS solution results from the iterative search for the best representation within the reduced space. The strength of the NMS solution is expressed by the stress value, which indicates differences between the original data structure and the NMS solution. Generally, a NMS solution with a stress value <10 is determined to be reliable. All analyses were conducted using PCORD software (version 5, MjM Software Design, Gleneden Beach, OR, USA).

All PLFAs with <20 carbons were used for analysis of the microbial communities. Data groupings were tested for significant differences in the NMS analysis using a multi-response permutation procedure (MRPP). Analyses were completed using the Sorensen distance. In addition to the probability value p , the MRPP test generates a T value, which indicates separation among groups, with a larger T reflecting a stronger separation, and an A value, which is an index of within-group homogeneity compared to random expectation, with a larger A indicating greater homogeneity (McCune and Grace, 2002). Moreover, indicator species analyses were performed using the data groupings shown to be different by MRPP. This statistical method generates an indicator value based on the abundance and frequency of a particular PLFA in a given data grouping. A larger indicator value represents a stronger relationship between the PLFA and the given data grouping. The statistical significance of the indicator value was tested against a randomized Monte Carlo test.

Using Bartlett's and Shapiro-Wilk's tests, Lethbridge data were tested and passed normality and equal variance tests. Analyses of variance (ANOVA) with mixed models were used to test differences among rotations and phases (fixed effect) with plot as a random source of variation for the Lethbridge site. When there was a significant effect in the ANOVA models ($p < 0.05$), Tukey HSD tests were subsequently run to compare means and identify any grouping structure. Plots at Breton site do not have an experimental design to allow for conventional parametric statistical tests. Therefore, we used nonparametric Dunn's test following by rejection of a Kruskal–Wallis test to test differences in Breton plots between rotations and among phases and also the three different nutrient managements. All statistical analyses were completed using R software and an alpha critical level of 5 %.

Linear regression was used to assess the scaling relationship of mass-volume for all soil clods and aggregates. Data were natural log transformed to reduce bias of large clods on fitted parameters (Hirmas et al., 2013). A t-test determined if the regression coefficients [i.e., slopes of mass fractal dimension (D_m)] of the linear regressions were significantly different from a value of 1 (i.e., the non-fractal constant for mass versus volume is 1; $H_0: \beta_1 = 1$).

Fitted soil moisture retention curves and hydraulic conductivity were modelled from the measured data. Root mean square error (RMSE) was used as a criterion for model selection. Parameters for the van Genuchten (VG) model (Tables 1A, 1B, 2A, and 2B) and hydraulic conductivity were first derived from each individual measured data set and subsequently analyzed to statistically test for differences between rotations and among phases and also the three different nutrient managements.

Pearson correlation was used for all dataset to assess the association among all available properties and soil quality metrics.

4. Results

4.1. Fractal dimension (Dm)

Linear regression analyses revealed the clear existence of fractal aggregation in the soils under forest and extended complex crop rotations (Fig. 1). Furthermore, Tukey test detected a significant difference in fractal aggregation between forest and simple rotation ($P < 0.05$; Table 1B).

We also conducted Dm estimations separately for each crop rotation phases. Soils were not significantly fractal at fallow phases of both simple and complex rotations in Lethbridge (0.987 and 0.993, respectively). Similarly, the wheat phase in the simple wheat-fallow rotation was also nonfractal in Breton (0.992). On the contrary, the wheat phases in complex rotations exhibited clear fractal aggregation (Fig. 1A and 1B; Dm values significantly different than one). This result demonstrates an overall improved hierarchical fractal aggregation in soils managed with rotation including perennial legumes and grasses. In addition, among manure, balanced fertilization, and control, the balanced fertilization was the only nutrient regime that exhibited significantly fractal aggregation (Dm= 0.965, $P = <0.001$ for test $H_0: \beta_1 = 1$; Fig. 2).

4.2. Water retention characteristics, pore size distribution, S-index, and hydraulic parameters

Overall means of the van Genuchten (VG) parameters for the moisture retention curves differed between forest and croplands (Table 1A), but there was no significant difference neither between the simple and complex rotation nor among the phases of the rotations. Root mean square errors for the moisture curve of each land use system ranged from 0.005 to 0.021 $\text{cm}^3 \text{cm}^{-3}$ indicating effective fitting of the VG model to measured data.

Saturated water content and PAW were 1.3 times higher in forest than the croplands (Table 1A). When comparing the two crop rotation types, they differed significantly with up to 8

% greater saturated water content in complex rotation soils compared to simple rotation; however, there was no significant difference among rotation phases at both sites. Plant available water (PAW) also differed between rotations, with 1.2 times greater PAW in complex rotation than simple rotation ($P < 0.05$) at the Breton site (Table 1A). With regards to nutrient managements, the saturated water content was greater in plots receiving long term applications of fertilizer or manure compared to the control treatment with no nutrient addition ($P < 0.01$). Consequently, it became evident that PAW was 7-18% higher where balanced fertilization was recurrently applied.

Clear significant difference was found in the S-index (i.e., slope of moisture curves at their inflection point) between forest and cropland ($P < 0.001$) (Table 1A). Additionally, crop rotation affected the S-index, with a 10% numerical increase in S-index for the complex rotations compared to simple rotations (Tables 1A and 2A) although this tendency was not statistically significant. Furthermore, balanced fertilization had greater S-index than manure additions (0.024 vs. 0.022; $P < 0.05$).

Pore size distribution results did not translate into differences in soil pore fractions among land managements, with the unique exception of significantly more abundant small pores ($< 9 \mu\text{m}$ diameter) in balanced fertilization than the control soil (Table 1B). With respect to the phases of the complex rotation, a greater presence of large pores ($>100 \mu\text{m}$ diameter) in soils under perennial legumes than other cropping phases indicates an overall tendency for increased soil space for roots, air, and water in these soils.

Root mean square error values of modelled hydraulic conductivity (K) were high over all measured soils ($0.218 \text{ cm day}^{-1}$; Tables 1A and 2A) indicating modest fitting in part as a result of extrapolation into the saturated zone of the retention curve. Unsaturated hydraulic conductivity at

100 hPa did not differ among land managements, with the only exception of the manured soils which had about half unsat. K compared to both the balanced fertilization and control soil ($P < 0.001$; Table 1B). Conversely, saturated hydraulic conductivity (sat. K) was more than 1.5 times faster in complex rotations than the simple rotations. Forest soil was also clearly different than cropland soils with 26 times faster sat. K ($P < 0.001$).

Complex rotation had a lower soil bulk density than simple rotation ($P < 0.001$; Tables 1A and 2A). Bulk density was also much lower in soils receiving manure compared to the control soil. As expected, total porosity revealed the reverse responses to rotation and nutrient management ($P_s < 0.001$).

4.3. Soil microbial biomass C, microbial communities, pH, SOC, STN, and C:N

At the Breton site, MBC was nearly 1.5 times greater in the complex rotation compared to the forest and simple rotation soils ($P < 0.05$; Table 1B). Lethbridge soils exhibited a similar tendency with 19% numerically greater MBC concentration in the complex crop rotation than in the simple rotation (Table 2B). Different phases of rotations also did not significantly influence MBC. Nevertheless, when focusing on our nutrient management comparisons at the Breton site, a sharp increase in MBC was observed when contrasting the control fields with a basal concentration of 1982 nmol g^{-1} versus a peak of 3018 nmol g^{-1} in the manured soils ($P < 0.05$).

The ordinations attained a low stress (≤ 13) after 70–90 iterations indicating resolution convergence. Solution for the microbial communities in Breton soils was two-dimensional and the axes explained more than 90% of the data variance. Analysis of the microbial communities led to a three-dimensional solution for the Lethbridge site, where the two axes presented in Fig. 3 accounted for 61% of the variance.

Separations between forest and croplands and also between the simple and complex rotations in both experimental sites were significant for the PLFA data (as a proxy to microbial community structure) as evidenced by the p-values smaller than the 0.01 obtained from the MRPP analyses (Table 3). Similarly, the A value, which indicates within-group homogeneity, was 0.15 for the microbial communities among all treatments. With regards to rotation phases, not only there was no significant difference among the phases within the complex rotations but also the wheat phases in the simple and the complex rotations were also similar with each other (Table 3). These inferences were further supported by the evident overlaps of the data clusters of the phases within the complex rotations as shown on the NMS graphic visualizations (Fig. 3). However, the fallow phases in both simple and complex rotations at the Lethbridge site resulted in two distinctive clusters clearly separated on the NMS visualization (Fig. 3B), yielded fairly large T value (> 3.2) and p value lower than 0.001 in the pairwise comparisons (Table 3).

Significant PLFA biomarkers were detected in both Breton and Lethbridge sites (Tables 4 and 5). The presence of Gram-negative bacteria associated with 16:1 ω 9c, 18:1 ω 5c, and 19:0 Cyc ω 8c PLFAs (Zelles, 1999) was seen in croplands, while forest was characterized by unique protozoa and fungal biomarkers (20:4 ω 6c and 18:3 ω 6c PLFAs, respectively).

The SOC and STN concentrations were affected by rotations and nutrient management (Tables 1B and 2B). Both SOC and STN were significantly higher in the complex crop rotations. Manure addition also had significantly greater SOC and STN than both inorganic balanced fertilization and the control soils. Although the soil C:N ratio did not statistically differ across cropping systems, this parameter was 1.5 times wider in the forest soil than the croplands ($P < 0.001$; Table 1B).

The pH was lower in the complex 5-yr crop rotation than simple 2-yr rotation particularly in the Breton site. Long-term application of inorganic balanced fertilization decreased the pH by a magnitude difference of roughly one pH unit (Table 1B).

4.4. Correlation analyses among soil properties

Several associations were found among soil parameters within the different land managements. Fractal aggregation – Dm value – was inversely correlated to abundance of large pores, sat. WC, sat. K, SOC, and S-index ($-0.35 > \rho > -0.47$; $P < 0.05$; Table 6) in Breton soils while there was no significant correlation between Dm value and other soil properties in Lethbridge site. Soil MBC was inversely correlation with C:N ratio and pore size fraction of 9-50 μm diameter. The MBC had also inverse association with S-index in particular in the Breton site (-0.35 ; $P < 0.05$).

4.5. The linkage between plant productivity and soil quality

In our study, comparison of wheat grain yields in simple wheat-fallow rotation versus in complex rotation indicated a rotation effect trending towards numerically higher yield levels with the complex rotation (Fig. 4). This yield difference was 40 and 14% for Breton and Lethbridge sites, respectively. The balanced fertilization also had higher grain yields than manure – on average 3500 and 2500 kg dry matter ha^{-1} for balanced fertilization and manure, respectively. It is noteworthy that these two nutrient managements had 2 to 3 times greater wheat yield compared to the control field.

5. Discussion

5.1. Land managements influence soil quality.

5.1.1. Complex crop rotation improves soil quality and plant productivity.

Complex crop rotations improve overall soil quality compared to simple rotations as evidenced by enhanced SOC, STN, MBC, sat. WC, PAW and fractal aggregation (Tables 1B and 2B; Fig. 1). The higher values of PAW and sat. WC in our complex long rotations which included alfalfa as a legume phase are directly associated with the greater soil porosity in this rotation type. Perennial legumes have heavy tap roots that burrow deep into the ground, lifting soil for better tilth and water holding capacity (Danga et al., 2009). Our results showed that in complex long rotations with better soil structure and water availability, microbial biomass was 1.3 times more abundant than in the simple 2-yr rotations (Tables 1B and 2B). Soil moisture content and availability directly impact the presence and activity of microorganisms. In general, microbial activity and growth in soils decrease as the soil becomes dry (Curtin et al., 2012; Paul and Clark, 1989). In addition, more diverse and extended crop rotations would improve the quality and quantity of the plant residues that can be incorporated into the soil, which subsequently become available to microbial communities as substrates (Tiemann et al., 2015). When microbial abundance and activity are increased, soil aggregation is typically enhanced (Bossuyt et al., 2001). In keeping with this notion, our Dm value results reveal that the complex rotations – which increased MBC – had also improved soil aggregation and structure as indicated by significantly fractal Dm, while the simple rotations did not exhibit these responses (Fig. 1). Furthermore, enhanced formation of soil aggregates can feedback into storing and protecting additional organic carbon and nitrogen in the soil (Oades, 1984). Such increased SOC and STN suggest an enhanced soil fertility status (Tiemann et al., 2015). Leguminous crop phases are frequently linked to increases in N availability as well as aggregate formation and stability

(McDaniel et al., 2014). In our study, complex rotations including perennial legume phases had much greater hierarchical aggregation (i.e., lower Dm), SOC, and STN than simple wheat-fallow rotations. Having higher soil aggregation in more diverse rotations can also increase abundance of larger soil pores, which had a direct contribution to our higher saturated water content and hydraulic conductivity under the complex rotation types. We further postulate that such enhancement in soil aggregation could also improve surface water infiltration, providing adaptation to drought and resistance to erosion (Bot and Benites, 2005).

Soil health is the foundation of productive farming practices. More diverse and extended crop rotations contribute to enhanced productivity (Smith et al., 2008; Wienhold et al., 2006). In our study, comparison of wheat grain yields in simple wheat-fallow versus complex rotations indicated an effect trending towards numerically higher yield levels with complex rotations (Fig. 4). This specific finding can reinforce the notion that the beneficial effects of diverse rotations on plant productivity may be associated with the enhancement of soil quality by protecting SOC and soil aggregation, storing available water, and providing a favorable microclimate conditions for biological activities including the decomposition and recycling of plant residues into available nutrients.

As noted above, there were no clear differences across the two assessed rotation phases within the complex rotations (i.e., wheat vs. hay) for various soil properties in particular for the Breton site. It became evident that implementation of complex rotations in the long term (i.e., more than 80 and 60 years in Breton and Lethbridge, respectively) provide the benefits derived from the perennial legumes and grasses to all the phases within these rotations. These differences among rotation phases were still slightly distinguishable in the Lethbridge site probably because this experiment has been established more recently than Breton. For instance, we notice that

PAW was significantly increased in the second year of wheat in Lethbridge (6-yr wheat₂), and this effect was specifically attributed to a higher volume of medium and small pores (i.e., < 9 µm in diameter; Table 2B). Higher PAW in this rotation phase might be the result of two consecutive wheat crops as wheat is known to have a dense and far reaching root system favoring ample soil aggregation and C input within the rhizosphere which may subsequently feedback into increasing water retention and availability (Norman et al., 2016).

Our comparative results between croplands and the adjacent native forest support the notion that conversion of forest to agricultural land can result in a significant alteration in soil properties including depletions of soil structure and SOC concentrations, thereby declining porosity, saturated hydraulic conductivity, and plant available water (Beheshti et al., 2012). Annual tillage and cropping practices can cause soil compaction and having lower SOC which would lead to the predominance of micro-aggregates (Ashagrie et al., 2007; Yang et al., 2009). Our results show that cropping, in particular the 2-yr simple rotations, had a significant effect on deteriorating soil structural quality (i.e., S-index, saturated water content, bulk density; Tables 1A and 2A). Furthermore, agricultural equipment traffic may lead to compaction in the soil (Schwen et al., 2011); this effect can be inferred in our study from the pronounced loss of large pores (i.e., > 100 µm in diameter). Congruently, this decrease in the volume of large pores was associated with degradation of key soil structure parameters (i.e., declining fractal aggregation, S-index, and SOC; Table 6). Significant losses in SOC concentration, porosity, and soil structure following conversion of forest to cropland would detrimentally impact critical soil functions such as greenhouse gases mitigation (Beheshti et al., 2012).

In our study, microbial biomass-C (MBC) concentration was much enriched in the complex rotation soils compared to both forest and simple rotation (Table 1A). Provided that the

management as well as the quantity and quality of organic matter inputs in forest vs. complex rotation are different, microbial biomass growth and accumulation seem to be facilitated in soils recurrently receiving nutrients – in particular manure – and covered by perennial legumes and grasses (Ohtonen et al., 1997). By contrast, the boreal forest soils could remain nutrient limited (Quideau et al., 2013) which would prevent such MBC accumulation even though when the assessed native forest ecosystem received much lesser disturbance than the croplands. The 1.5 times wider C:N ratio in our forest soils underpins the nutrient limitation hypothesis as postulated by Quideau et al. (2013). In general, the capacity of organic matter to decompose can be assessed by C:N ratio (Kaye and Hart, 1998). High C:N ratio in soils has been found in systems that have recalcitrant organic matter that decomposes very slowly and N is unavailable and tightly bound within the organic compounds (Inglett et al., 2011). Moreover, fungal biomass is known to have relatively high C:N ratio, and fungi development can be inhibited by increased N availability (Inglett et al., 2011). Therefore, N-limiting conditions in this native forest ecosystem can potentially explain our finding of fungal biomarker in the forest soil, whereas Gram-negative bacteria were the characteristic biomarkers of the cropland soils. Bossuyt et al (2001) also reported a clear difference between fungal and bacterial populations with fungi dominating in the low-quality residue treatment and bacteria dominating in the high-quality residue treatment.

5.1.2. Long-term inorganic balanced fertilization leads to enhanced soil structure.

Fertilization is an important means for improving crop productivity by meet nutrient requirements (Hati et al., 2011). This positive effect of nutrient additions using manure or inorganic fertilizers was confirmed in our study (Fig. 4). Organic amendments such as cattle manure can greatly contribute to the soil fertility (Sradnick et al., 2013). This response can be

attributed in part to the combined effect of a great number and diversity of microbes and an additional input of organic carbon and nitrogen resulting in increased soil fertility compared to inorganic fertilization (Chakraborty et al., 2011; Sradnick et al., 2013). This is consistent with our study where SOC, STN, and MBC were much higher in manured soils compared to fertilized soils receiving balanced rates of inorganic N, P, K, and S nutrient inputs (Table 1B).

Inorganic fertilization can also facilitate the addition of crop nutrient requirements and the long-term accretion of organic residues and organic matter in the soils through enhanced biomass production and root growth (Hati et al., 2011). In our study, improved fractal aggregation and structural quality (i.e., lower Dm value and higher S-index) in soils receiving balanced fertilization compared to manured fields indicates that the balanced fertilization can develop hierarchical aggregation leading to an overall, enhanced soil physical quality to greater extent than manure additions. Furthermore, we found that plant available water capacity was 7% higher in soils where long-term balanced fertilization has been applied, which also reflects a better soil structure and pore connectivity (Table 1A). This implies an enhanced capacity of the soil to intake, maintain and move available water within the topsoil during the growing season. Considering the fact that water is one of the most crucial limiting factor impacting crop yields (Oweis et al., 2004; Kiani et al., 2016a), the higher crop productivity in our balanced fertilized fields points out that water availability may be a key factor driving crop productivity under this nutrient management.

Soils are known to integrate multiple attributes and functions (O'Sullivan et al., 2015). Different land managements can affect distinct specific functions of the soil. Both balanced fertilization and manure additions contributed to improving certain specific soil functions better than the control soils; cattle manure had an even stronger effect on enhancing nutrient cycling as

indicated by increased SOC, STN, and MBC, while balanced fertilization influenced beneficially the pore water relationships and physical conditions of the soil as shown by a lower Dm value as well as higher S-index and PAW (Tables 1A, 1B, 2A, and 2B; Fig. 2). Our study extends the existing literature by documenting these clear but divergent differences in soil structure versus microbial functions across contrasting nutrient sources.

Long-term application of urea decreased the soil pH considerably, while manure amendments markedly increase the contents of SOC, STN, and other available nutrients, and reduced soil acidification (Chakraborty et al., 2011; Dong et al., 2012). Very acid soils (pH less than 5) cause microbial activity and numbers to be considerably lower than neutral soils (McCauley et al., 2009). Moreover, available studies have shown that certain microorganisms, such as nitrifying bacteria and nitrogen-fixing bacteria associated with many legumes, generally perform poorly when soil pH falls below 6 (Sylvia et al., 1998). This could be a reason for the lower response of SOC, STN, and MBC to balanced fertilization compared to manure addition in the Orthic Gray Luvisol soils of Breton where the naturally-acidic soil pH originated via pedogenesis under native forest vegetation gradually becomes even more acidic with long-term balanced fertilization (Dyck et al., 2012).

5.2. Fractal aggregation, S-index, MBC, SOC, and PAW showed clear sensitivity to management.

Indicators of soil quality can inform how well goals related to soil functions are being achieved. Indicators should be self-explanatory, sufficiently sensitive for its purpose, readily available, and relatively easy to compute (Bremer, 2004). Soil quality depends on the interactions of physical, chemical and biological characteristics and a proper assessment of soil quality requires measurement of a high number of parameters (Marzaioli et al., 2010). Specialists have agreed to search for a minimum data set to reduce the cost of soil quality assessment (Liu et

al., 2014). Overall, our findings indicate soil indicators including soil organic carbon, microbial biomass-C, S-index, and fractal aggregation are dynamic and highly responsive to contrasting land managements. Our synthesis is consistent with comparisons of soil quality indicators for land managements by de Paul Obade and Lal (2014) and Gülser (2006).

Examination of aggregate size distribution gives essential information for assessing the formation and development of soil aggregation and structure (Gülser, 2006). In our study, mass-volume fractal dimension of aggregates was strongly influenced by crop rotation types. Soils under the complex long rotations exhibited significantly fractal aggregation ($D_m < 1$) while the simple rotation was not (Fig. 1). Hierarchical aggregation peaked under the perennial legume and grass phases, followed by wheat crops. No hierarchical aggregation was found under fallow phases. Additionally, the significant inverse correlation between D_m values and macroporosity (i.e., $>100 \mu\text{m}$ in diameter; Table 6) indicates better soil physical quality when macroaggregates and macroporosity are concurrently abundant in soils. Likewise, increments in SOC contents due to more diverse and longer rotations in our study were clearly associated with a marked increase in the proportion of large aggregates exhibiting favorable reduced densities. A significant inverse correlation between the D_m value and SOC content further substantiates this mechanistic linkage (Table 6). Our study is one of the few available reports evaluating the effectiveness of fractal aggregation model for detecting soil quality changes as a function of contrasting land management options.

Focusing on our nutrient regime comparison, fractal aggregation approach effectively detected that balanced fertilization was the only nutrient regime exhibiting significant fractal aggregation which may be due to the greater amount of crop residues and roots derived from higher plant productivity (Fig. 2). Aggregation of soil particles into larger units such as peds or

aggregates has major impacts on transport processes in soils. The significant inverse relationships between D_m value versus saturated hydraulic conductivity, macropore volume, and saturated water content corroborates the ability of fractal aggregation approach to detect and inform water filtering, movement and storage capacity functions in the soil. These results show that fractal aggregation is a robust method to assess the structure and quality of the soil as affected by land managements.

The soil physical parameter S is an index to assess soil structural quality (e.g., pore size distribution, compaction, PAW) (Dexter, 2004; Naderi-Boldaji and Keller, 2016). An S -index value of 0.035 is considered as a threshold separating soils of favorable structure (> 0.035) from those with relatively deficient structure (< 0.035), and soils with much lower S -index (< 0.02) are considered to have very degraded structure (Dexter, 2004). In our study, the increase in S -index when comparing complex rotation vs. simple rotation, and also the significant increase when contrasting forest vs. cropland as well as balanced fertilization vs. manure further supports the clear sensitivity and utility of this integrated metric of soil physical quality. The multiple significant inverse correlations of S -index with D_m value, bulk density, and PWP as well as the several direct correlations of S -index with sat. WC, PAW, sat. K, volume of pores larger than 9 micrometer in diameter, and SOC consistently show that the S -index can be a meaningful, suitable indicator for soil structural and water movement assessment in our assessed fine-textured soils. Similar to in our study, Reynolds et al. (2009) had previously reported good agreement between S -index and their physical quality results including field capacity, plant available water, air permeability, and macroporosity for rigid to moderately expansive loamy soils.

The structural and functional relationships of soil microbial communities have been considered as indicators for soil quality (Bastida et al., 2008). Soil microbial biomass is ascertained as one of the most sensitive indicators of changes in soil quality (Stenberg, 1999). In our study, the 1.3-fold increase in MBC in the complex versus simple rotations, and also in the manure soils further supports the clear sensitivity and usefulness of this integrated metric of soil quality. The MBC also correlated well with other soil attributes such as S-index, sat. K, medium pore volume, and C:N ratio. It is noteworthy that forest soil exhibited improved soil S-index compared to croplands, but by contrast, the microbial biomass carbon declined in natural forest. These findings imply that distinct soil functions are affected by different land uses in different directions.

As noted above, cattle manure had strong effect on improving soil nutrient cycling function while balanced fertilization beneficially impacted soil physical conditions. This comparative result across management choices and key soil functions emphasizes the importance of considering several soil quality indicators for assessing multiple soil functions. This outcome also highlights the usefulness of Dm value, S-index, PAW, SOC, STN, and MBC as an insightful set of soil quality indicators.

It is noteworthy that although the forest soil has the highest SOC concentration and also this soil has strong fractal aggregation compared to the cropland soils, the microbial biomass carbon is the lowest. This result could be in part explained by the type of organic carbon substrates suitable for microbes to grow is different from the type of organic carbon which helps the soil structure improvement. Labile soil organic C is usually described as the fraction of SOC with a turnover time of less than a few months or years and this C pool is considered to be readily decomposable components that act as a primary energy source for most soil

microorganisms (Zou et al., 2005). Perhaps the most representative labile soil microbial components are carbohydrates (González-Chávez et al. 2010). On the other hand, recalcitrant C has a longer turnover time (i.e., decades to centuries) and an interesting group of these organic compounds are those produced by arbuscular-mycorrhizal fungi which are also known to have a strong participation in soil aggregate formation and stability (González-Chávez et al. 2010). These notions can collectively imply that the majority of SOC in forest is recalcitrant C rather than labile soil C. This recalcitrant C can contribute to the improvement of soil structure, and consequently, leading to enhanced hierarchical fractal aggregation as in our study ($D_m < 1$). Moreover, indicator analysis of microbial species determined fungi as a distinctive biomarker in our forest soil which further supports our interpretation of fungal-facilitated formation of macro-aggregation in forest soils (Table 5). In addition, protozoa was another biomarker in forest soil which is a microfauna and it is more directly linked to soil aggregation and porosity than other microbes. Collectively, these results emphasize the importance of quantifying both MBC and fractal aggregation (D_m) as key indicators to reveal and document a comprehensive assessment of soil quality. Future studies can focus on examining the effects and mechanisms of different types of organic C input and availability on the various key soil functions including microbial-mediated nutrient cycling, aggregation formation, and pore water relationships.

6. Conclusion

Long-term implementation of more diverse and extended crop rotations contributed to soil quality by improving soil aggregation, increasing porosity, and accruing soil organic matter, nitrogen and microbial biomass, which in turn interacted collectively to provide substantial benefits on plant water availability, soil water conductivity, and crop productivity. The various crop phases of the assessed rotations did not caused pronounced differences in terms of most of the measured soil properties, with the only noticeable exception of fractal aggregation which revealed clear differences across phases of the crop rotations. Fallow phases exhibited non-fractal aggregation, while the most fractal soils were found under the perennial leguminous phases of these rotations. Overall, the inclusion of perennial plants in the crop rotation amply benefited soil structural parameters.

Although long-term nutrient additions contributed in general to improving soil functions compared to the control fields that received no nutrient additions, cattle manure addition had even stronger effect specifically on improving nutrient cycling functions while the balanced fertilization benefited directly water availability and overall soil physical condition.

A collective assessment of the measured physical and biological properties of forest and cropland soils can indicate that the distinctive fungal presence in the forest soils is associated with a well-defined hierarchical soil aggregation. Moreover, this is contrasting with the noticeable presence of Gram-negative bacteria as the characteristic biomarker in cropland soils. Fractal aggregation (Dm value), S-index, PAW, SOC, and MBC were identified as a valuable representative subset of highly responsive indicators of soil quality which are useful for comparing management options that influence agricultural productivity. It is suggested to

explore the applicability of these indicators in an even wider range of land managements and agroecological conditions.

7. Acknowledgement

The authors are grateful for the assistance of our funding partners Alberta Livestock and Meat Agency (ALMA) Sustainability, and Rangeland Research Institute (RRI) University of Alberta.

The authors also wish to thank Lewis Fausak, Karin Lindquist, and Kris Guenette for their assistance during field sampling at Breton and Lethbridge sites as well as Jela Burkus and Catherine Pocklington for laboratory analyses.

8. References

- AGRASID. Agricultural Region of Alberta Soil Inventory Database, 2015. URL: [http://www1.agric.gov.ab.ca/\\$department/deptdocs.nsf/all/sag3249](http://www1.agric.gov.ab.ca/$department/deptdocs.nsf/all/sag3249).
- Alberta-Weather Conditions and Forecast, 2016. URL: <http://agriculture.alberta.ca/acis/alberta-weather-data-viewer.jsp>.
- Ahamadou, B. and Huang, Q., 2013. Impacts of Agricultural Management Practices on Soil Quality. In *Molecular Environmental Soil Science* (pp. 429-480). Springer Netherlands.
- Ashagrie, Y., Zech, W., Guggenberger, G., Mamo, T., 2007. Soil aggregation, and total and particulate organic matter following conversion of native forests to continuous cultivation in Ethiopia. *Soil Tillage Res.* 94, 101–108. doi:10.1016/j.still.2006.07.005
- Bastida, F., Zsolnay, A., Hernández, T., García, C., 2008. Past, present and future of soil quality indices: A biological perspective. *Geoderma* 147, 159–171. doi:10.1016/j.geoderma.2008.08.007
- Beheshti, A., Raiesi, F., Golchin, A., 2012. Soil properties, C fractions and their dynamics in land use conversion from native forests to croplands in northern Iran. *Agric. Ecosyst. Environ.* 148, 121–133. doi:10.1016/j.agee.2011.12.001
- Bossuyt, H., Deneff, K., Six, J., Frey, S.D., Merckx, R., Paustian, K., 2001. Influence of microbial populations and residue quality on aggregate stability. *Appl. Soil Ecol.* 16, 195–208. doi:10.1016/S0929-1393(00)00116-5
- Bremer, E., Ellert, K., 2004. Soil quality indicators: a review of implications for agricultural ecosystems in Alberta. Technical report, Symbio Ag Consulting, Lethbridge, Alberta, Canada. AESA.
- Chakraborty, A., Chakrabarti, K., Chakraborty, A., Ghosh, S., 2011. Effect of long-term fertilizers and manure application on microbial biomass and microbial activity of a tropical agricultural soil. *Biol.*

Fertil. Soils 47, 227–233. doi:10.1007/s00374-010-0509-1

Curtin, D., Beare, M.H., Hernandez-Ramirez, G., 2012. Temperature and Moisture Effects on Microbial Biomass and Soil Organic Matter Mineralization. Soil Sci. Soc. Am. J. 0, 0. doi:10.2136/sssaj2012.0011

D'Hose, T., Cougnon, M., De Vlieghe, A., Vandecasteele, B., Viaene, N., Cornelis, W., Van Bockstaele, E., Reheul, D., 2014. The positive relationship between soil quality and crop production: A case study on the effect of farm compost application. Appl. Soil Ecol. 75, 189–198. doi:10.1016/j.apsoil.2013.11.013

Danga, B.O., Ouma, J.P., Wakindiki, I.I.C., Bar-Tal, A., 2009. Chapter 5 Legume-Wheat Rotation Effects on Residual Soil Moisture, Nitrogen and Wheat Yield in Tropical Regions, 1st ed, Advances in Agronomy. Elsevier Inc. doi:10.1016/S0065-2113(08)00805-5

de Paul Obade, V., Lal, R., 2014. Soil quality evaluation under different land management practices. Environ. Earth Sci. 72, 4531–4549. doi:10.1007/s12665-014-3353-z

Dexter, a R., 2004. Soil physical quality Part I. Theory, effects of soil texture, density, and organic matter, and effects on root growth. Geoderma 120, 201–214. doi:10.1016/j.geodermaa.2003.09.005

Di, H.J., Cameron, K.C., Shen, J., Winefield, C.S., Callaghan, M.O., Bowatte, S., He, J., 2013. Molecular Environmental Soil Science. doi:10.1007/978-94-007-4177-5

Dong, W., Zhang, X., Wang, H., Dai, X., Sun, X., Qiu, W., Yang, F., 2012. Effect of Different Fertilizer Application on the Soil Fertility of Paddy Soils in Red Soil Region of Southern China. PLoS One 7, 1–9. doi:10.1371/journal.pone.0044504

Garrigues, E., Corson, M.S., Angers, D.A., Van Der Werf, H.M.G., Walter, C., 2012. Soil quality in Life Cycle Assessment: Towards development of an indicator. Ecol. Indic. 18, 434–442.

doi:10.1016/j.ecolind.2011.12.014

Gülser, C., 2006. Effect of forage cropping treatments on soil structure and relationships with fractal dimensions. *Geoderma* 131, 33–44. doi:10.1016/j.geoderma.2005.03.004

Hannam, K. D., Quideau, S. A., Kishchuk, B. E., 2006. Forest floor microbial communities in relation to stand composition and timber harvesting in northern Alberta. *Soil Biology and Biochemistry*, 38, 2565- 2575.

Hati, K.M., Swarup, A., Mishra, B., Manna, M.C., Wanjari, R.H., Mandal, K.G., Misra, A.K., 2008. Impact of long-term application of fertilizer, manure and lime under intensive cropping on physical properties and organic carbon content of an Alfisol. *Geoderma* 148, 173–179. doi:10.1016/j.geoderma.2008.09.015

Hernandez-ramirez, G., Lawrence-smith, E.J., Sinton, S.M., Schwen, A., Brown, H.E., 2014. Root Responses to Alterations in Macroporosity and Penetrability in a Silt Loam Soil. *Soil Sci. Soc. Am. J.* 78, 1392–1403. doi:10.2136/sssaj2014.01.0005

Hirmas, D.R., Giménez, D., Subroy, V., Platt, B.F., 2013. Fractal distribution of mass from the millimeter- to decimeter-scale in two soils under native and restored tallgrass prairie. *Geoderma* 207-208, 121–130. doi:10.1016/j.geoderma.2013.05.009

Inglett, K.S., Inglett, P.W., Ramesh Reddy, K., Reddy, K.R., 2011. Soil Microbial Community Composition in a Restored Calcareous Subtropical Wetland. *Soil Sci. Soc. Am. J.* 75, 1731–1740. doi:10.2136/sssaj2010.0424

Karlen, D.L., Andrews, S.S., Weinhold, B.J., Doran, J.W., 2003. Soil quality : Humankind ' s foundation for survival 171–179.

Karlen, D.L., Hurley, E.G., Andrews, S.S., Cambardella, C.A., Meek, D.W., Duffy, M.D., Mallarino,

- A.P., 2006. Crop rotation effects on soil quality at three northern corn/soybean belt locations. *Agron. J.* 98, 484–495. doi:10.2134/agronj2005.0098
- Kiani, M., Gheysari, M., Mostafazadeh-Fard, B., Majidi, M.M., Karchani, K., Hoogenboom, G., 2016a. Effect of the interaction of water and nitrogen on sunflower under drip irrigation in an arid region. *Agric. Water Manag.* 171, 162–172. doi:10.1016/j.agwat.2016.04.008
- Liu, Z., Zhou, W., Shen, J., Li, S., Ai, C., 2014. Soil quality assessment of yellow clayey paddy soils with different productivity. *Biol. Fertil. Soils* 50, 537–548. doi:10.1007/s00374-013-0864-9
- Marzaioli, R., D’Ascoli, R., De Pascale, R.A., Rutigliano, F.A., 2010. Soil quality in a Mediterranean area of Southern Italy as related to different land use types. *Appl. Soil Ecol.* 44, 205–212. doi:10.1016/j.apsoil.2009.12.007
- McCauley, A., Jones, C., Jacobsen, J., 2009. Soil pH and Organic Matter. Nutrient management modules 8, #4449-8. Montana State University Extension Service, Bozeman, Montana, pp. 1–12.
- McDaniel, M.D., Tiemann, L.K., Grandy, A.S., 2014. Does agricultural crop diversity enhance soil microbial biomass and organic matter dynamics? A meta-analysis. *Ecol. Appl.* 24, 560–570. doi:10.1890/13-0616.1
- Melean, E.O., 1982. Soil pH and lime requirement. *Methods Soil Anal.* 9, 595– 624. doi:10.2134/agronmonogr9.2.2ed.c12
- Munkholm, L.J., Heck, R.J., Deen, B., 2013. Long-term rotation and tillage effects on soil structure and crop yield. *Soil Tillage Res.* 127, 85–91. doi:10.1016/j.still.2012.02.007
- Munkholm, L.J., Schjøning, P., Rasmussen, K.J., Tanderup, K., 2003. Spatial and temporal effects of direct drilling on soil structure in the seedling environment. *Soil Tillage Res.* 71, 163–173. doi:10.1016/S0167-1987(03)00062-X

- Naderi-Boldaji, M., Keller, T., 2016. Degree of soil compactness is highly correlated with the soil physical quality index S. *Soil Tillage Res.* 159, 41–46. doi:10.1016/j.still.2016.01.010
- Norman, C.R., Brye, K.R., Gbur, E.E., Chen, P., Rupe, J., 2016. Long-term Management Effects on Soil Properties and Yields in a Wheat-Soybean Double-Crop System in Eastern Arkansas. *Soil Sci.* 181, 1–12.
- O’Sullivan, L., Creamer, R.E., Fealy, R., Lanigan, G., Simo, I., Fenton, O., Carfrae, J., Schulte, R.P.O., 2015. Functional Land Management for managing soil functions: A case-study of the trade-off between primary productivity and carbon storage in response to the intervention of drainage systems in Ireland. *Land use policy* 47, 42–54. doi:10.1016/j.landusepol.2015.03.007
- Oweis, T., Hachum, A., Pala, M., 2004. Lentil production under supplemental irrigation in a Mediterranean environment. *Agric. Water Manag.* 68, 251–265. doi:10.1016/j.agwat.2004.03.013
- Quideau, S.A., Swallow, M.J.B., Prescott, C.E., Grayston, S.J., Oh, S.W., 2013. Comparing soil biogeochemical processes in novel and natural boreal forest ecosystems. *Biogeosciences* 10, 5651–5661. doi:10.5194/bg-10-5651-2013
- Reynolds, W.D., Drury, C.F., Tan, C.S., Fox, C.A., Yang, X.M., 2009. Use of indicators and pore volume-function characteristics to quantify soil physical quality. *Geoderma* 152, 252–263. doi:10.1016/j.geoderma.2009.06.009
- Schelle, H., Heise, L., Jänicke, K., Durner, W., 2013. Water retention characteristics of soils over the whole moisture range: A comparison of laboratory methods. *Eur. J. Soil Sci.* 64, 814–821. doi:10.1111/ejss.12108
- Schindler, U., Durner, W., von Unold, G., Muller, L., 2010. Evaporation Method for Measuring Unsaturated Hydraulic Properties of Soils: Extending the Measurement Range. *Soil Sci Soc Am J* 74, 1071–1083. doi:10.2136/sssaj2008.0358

- Schwen, A., Hernandez-Ramirez, G., Lawrence-Smith, E.J., Sinton, S.M., Carrick, S., Clothier, B.E., Buchan, G.D., Loiskandl, W., 2011. Hydraulic Properties and the Water-Conducting Porosity as Affected by Subsurface Compaction using Tension Infiltrometers. *Soil Sci. Soc. Am. J.* 75, 822–831. doi:10.2136/sssaj2010.0257
- Sharma, K.L., Grace, J.K., Mandal, U.K., Gajbhiye, P.N., Srinivas, K., Korwar, G.R., Hima Bindu, V., Ramesh, V., Ramachandran, K., Yadav, S.K., 2008. Evaluation of long-term soil management practices using key indicators and soil quality indices in a semi-arid tropical Alfisol. *Soil Res.* 46, 368–377. doi:http://dx.doi.org/10.1071/SR07184
- Smith, R.G., Gross, K.L., Robertson, G.P., 2008. Effects of crop diversity on agroecosystem function: Crop yield response. *Ecosystems* 11, 355–366. doi:10.1007/s10021-008-9124-5
- Sradnick, A., Murugan, R., Oltmanns, M., Raupp, J., Joergensen, R.G., 2013. Changes in functional diversity of the soil microbial community in a heterogeneous sandy soil after long-term fertilization with cattle manure and mineral fertilizer. *Appl. Soil Ecol.* 63, 23–28. doi:10.1016/j.apsoil.2012.09.011
- Stenberg, B., 1999. Monitoring soil quality of arable land: Microbiological indicators. *Acta Agric. Scand. - Sect. B Soil Plant Sci.* 49, 1–24. doi:Doi 10.1080/09064719950135669
- Sylvia, D.M., Fuhrmann, J.J., Hartel, P.G., Zuberer, D. a, Darmstadt, T.U., Hall, P., 1998. Principles and Applications of Soil Microbiology 550.
- Tiemann, L.K., Grandy, A.S., Atkinson, E.E., Marin-Spiotta, E., Mcdaniel, M.D., 2015. Crop rotational diversity enhances belowground communities and functions in an agroecosystem. *Ecol. Lett.* 18, 761–771. doi:10.1111/ele.12453
- Wienhold, B.J., Pikul, J.L., Liebig, M.A., Mikha, M.M., Varvel, G.E., Doran, J.W., Andrews, S.S., 2006. Cropping system effects on soil quality in the Great Plains: Synthesis from a regional project.

Renew. Agric. Food Syst. 21, 49–59. doi:10.1079/RAF2005125

Yang, Y., Guo, J., Chen, G., Yin, Y., Gao, R., Lin, C., 2009. Effects of forest conversion on soil labile organic carbon fractions and aggregate stability in subtropical China. *Plant Soil* 323, 153–162. doi:10.1007/s11104-009-9921-4

Zelles, L., 1999. Fatty acid patterns of phospholipids and lipopolysaccharides in the characterisation of microbial communities in soil: a review. *Biol. Fertil. Soils* 29, 111–129.

Zou, X.M., Ruan, H.H., Fu, Y., Yang, X.D., Sha, L.Q., 2005. Estimating soil labile organic carbon and potential turnover rates using a sequential fumigation-incubation procedure. *Soil Biol. Biochem.* 37, 1923–1928. doi:10.1016/j.soilbio.2005.02.028

9. Tables and figures

Table 1A. Effect of crop rotation and nutrient management on selected soil attributes at the 5 to 10 cm soil increment depth from Breton site. Within a column, treatment means with different letters differ, $P < 0.05$.

Crop rotation	Bulk Density (g cm ⁻³)	Porosity	sat. Water Content	θ_{FC}	θ_{PWP}	PAW	θ_s	θ_r	n	α (hPa ⁻¹)	S-index	RMSE Θ (cm ³ cm ⁻³)	RMSE K (cm d ⁻¹)
Forest	0.77 c	0.71 a	0.59 a	0.30 a	0.08 c	0.23 a	0.62 a	0.001	1.17 a	0.35 a	0.030 a	0.021	0.094
SEM	0.085	0.032	0.015	0.008	0.003	0.010	0.016		0.008	0.046	0.002		
5-yr rotation	1.28 b	0.52 b	0.47 b	0.29 ab	0.09 b	0.19 b	0.47 b	0.001	1.18 a	0.08 b	0.024 b	0.015	0.127
SEM	0.017	0.007	0.007	0.005	0.002	0.005	0.007		0.004	0.011	0.000		
2-yr rotation	1.40 a	0.47 c	0.44 c	0.27 b	0.11 a	0.16 c	0.43 c	0.001	1.19 a	0.06 b	0.022 b	0.010	0.111
SEM	0.048	0.018	0.013	0.005	0.005	0.005	0.013		0.006	0.016	0.000		
P-value	<0.001	<0.001	<0.001	0.03	<0.001	<0.001	<0.001		0.35	<0.001	<0.001		
Phases of 5-yr rotation													
5-yr-Hay	1.27 a	0.52 a	0.46 a	0.27 a	0.09 a	0.18 a	0.46 a	0.001	1.19 a	0.08 a	0.024 a	0.012	0.148
SEM	0.024	0.009	0.010	0.008	0.003	0.011	0.010		0.009	0.021	0.001		
5-yr-Wheat	1.31 a	0.50 a	0.47 a	0.29 a	0.09 a	0.20 a	0.47 a	0.001	1.18 a	0.08 a	0.023 a	0.015	0.123
SEM	0.033	0.012	0.013	0.007	0.005	0.007	0.015		0.005	0.020	0.001		
P-value	0.33	0.34	0.45	0.11	0.93	0.17	0.70		0.34	0.79	0.65		
Nutrient managements													
Manure	1.27 b	0.52 a	0.47 a	0.28 ab	0.10 a	0.18 ab	0.46 ab	0.001	1.17 b	0.10 a	0.022 b	0.014	0.157
SEM	0.034	0.013	0.009	0.006	0.004	0.007	0.008		0.003	0.021	0.000		
Balanced fertilization	1.33 ab	0.50 ab	0.47 a	0.29 a	0.09 a	0.19 a	0.47 a	0.001	1.19 a	0.08 a	0.024 a	0.013	0.127
SEM	0.039	0.014	0.012	0.006	0.005	0.008	0.015		0.008	0.019	0.001		
Control	1.41 a	0.47 b	0.42 b	0.26 b	0.10 a	0.16 b	0.42 b	0.001	1.20 a	0.05 a	0.022 ab	0.009	0.076
SEM	0.037	0.014	0.010	0.006	0.007	0.009	0.013		0.004	0.012	0.001		
P-value	0.04	0.04	0.003	0.03	0.22	0.03	0.02		0.004	0.21	0.03323		

θ_{FC} : field capacity water content; θ_{PWP} : permanent wilting point water content; PAW: plant available water; θ_s : saturated volumetric water content; θ_r : residual water content; n: a shape parameter related to the curve smoothness; α : a negative inverse of the air entry potential; S-index: the slope at the inflection point; RMSE: root mean square error of modelled θ and K data.

Table 1B. Effect of crop rotation and nutrient management on selected soil attributes at the 5 to 10 cm soil increment depth from Breton site. Within a column, treatment means with different letters differ, $P < 0.05$. Ks: saturated hydraulic conductivity; Unsat. K: hydraulic conductivity at 100 hPa; SOC: soil organic carbon; STN: soil total nitrogen; C:N: carbon to nitrogen ratio; MBC: microbial biomass carbon.

Crop rotation	Ks (cm d ⁻¹)	unsat. K at 100 hPa	Pore Volume (cm ³ cm ⁻³)				pH	STN (% m/m)	SOC (% m/m)	C:N	MBC nmol g ⁻¹ soil	Dm
			>100	100-50	50-9	<9						
			(μm diameter)									
Forest	2506 a	0.027 a	0.30 a	0.03 a	0.07 a	0.30 a	5.00 b	0.21 a	3.62 a	17.3 a	1849 b	0.920 b*
SEM	1238	0.008	0.035	0.001	0.005	0.008	0.17	0.020	0.41	0.42	207	0.049
5-yr rotation	110 b	0.039 a	0.14 b	0.03 a	0.06 a	0.29 ab	5.15 b	0.19 a	2.19 b	11.2 b	2641 a	0.969 ab*
SEM	31	0.005	0.008	0.002	0.002	0.005	0.12	0.009	0.11	0.12	176	0.030
2-yr rotation	76 b	0.037 a	0.11 b	0.02 a	0.06 a	0.27 b	6.17 a	0.13 b	1.47 c	11.4 b	1912 b	0.991 a
SEM	22	0.009	0.016	0.002	0.002	0.005	0.11	0.023	0.28	0.34	153	0.047
P-value	<0.001	0.62	<0.001	0.15	0.42	0.03	<0.001	0.003	<0.001	<0.001	0.01	0.01
Phases of 5-yr rotation												
5-yr-Hay	134 a	0.041 a	0.15 a	0.03 a	0.07 a	0.27 a	4.89 a	0.19 a	2.20 a	11.3 a	2627 a	0.956 a*
SEM	56	0.010	0.011	0.002	0.003	0.008	0.21	0.017	0.21	0.19	268	0.035
5-yr-Wheat	119.a	0.043 a	0.12 a	0.03 a	0.06 a	0.29 a	5.17 a	0.17 a	1.92 a	10.7 b	2718 a	0.976 a*
SEM	61	0.009	0.015	0.002	0.003	0.007	0.18	0.008	0.09	0.12	322	0.033
P-value	0.86	0.91	0.21	0.47	0.12	0.11	0.32	0.45	0.23	0.01	0.83	0.12
Nutrient managements												
Manure	112 a	0.019 b	0.15 a	0.02 a	0.06 a	0.28 ab	5.80 a	0.21 a	2.43 a	11.3 a	3018 a	0.987 a
SEM	49	0.003	0.015	0.002	0.002	0.006	0.15	0.007	0.10	0.24	324	0.044
Balanced fertilization	132 a	0.044 a	0.1 a	0.03 a	0.07 a	0.28 a	4.80 b	0.15 b	1.64 b	10.9 a	2258 ab	0.965 a*
SEM	60	0.009	0.012	0.002	0.003	0.006	0.26	0.011	0.12	0.17	177	0.029
Control	76 a	0.065 a	0.11 a	0.03 a	0.07 a	0.26 b	5.64 a	0.13 b	1.53 b	11.3 a	1982 b	0.985 a
SEM	25	0.010	0.015	0.003	0.003	0.006	0.18	0.023	0.28	0.32	199	0.035
P-value	0.74	<0.001	0.09	0.10	0.15	0.03	0.004	0.002	0.004	0.49	0.02	0.26

* indicates that the Dm value is significantly different from 1 at $P < 0.05$ or it is fractal.

Table 2A. Effect of crop rotation type on selected soil attributes at the 5 to 10 cm soil depth increment from Lethbridge site. Within a column, treatment means with different letters differ, $P < 0.05$.

Crop rotation	Bulk Density (g cm ⁻³)	Porosity	sat. Water Content	θ_{FC}	θ_{PWP}	PAW	θ_s	θ_r	n	α	S-index	RMSE Θ (cm ³ cm ⁻³)	RMSE K (cm d ⁻¹)
				(cm ³ cm ⁻³)							(hPa ⁻¹)		
6-yr rotation	1.39 b	0.48 a	0.47 a	0.27 a	0.14 b	0.14 a	0.47 a	0.004 a	1.20 a	0.05 a	0.026 a	0.007	0.23
SEM	0.02	0.01	0.007	0.01	0.00	0.00	0.01	0.00	0.008	0.01	0.00		
2-yr rotation	1.48 a	0.44 b	0.43 b	0.28 a	0.15 a	0.13 a	0.44 a	0.006 a	1.20 a	0.04 a	0.023 a	0.008	0.27
SEM	0.01	0.01	0.013	0.01	0.00	0.01	0.01	0.00	0.007	0.01	0.00		
P-value	0.007	0.006	0.02	0.84	0.006	0.24	0.06	0.94	0.77	0.17	0.12		
Phases of 2-yr rotation													
2-yr-Wheat	1.46 a	0.45 a	0.43 a	0.27 a	0.15 a	0.12 a	0.43 a	0.008 a	1.19 a	0.03 a	0.022 a	0.008	0.31
SEM	0.01	0.004	0.018	0.011	0.003	0.014	0.016	0.008	0.009	0.006	0.000		
2-yr-Fallow	1.50 a	0.43 a	0.44 a	0.28 a	0.15 a	0.13 a	0.46 a	0.004 a	1.20 a	0.04 a	0.024 a	0.010	0.21
SEM	0.02	0.009	0.020	0.010	0.009	0.014	0.020	0.004	0.008	0.003	0.002		
P-value	0.19	0.12	0.57	0.62	0.92	0.72	0.29	0.67	0.90	0.52	0.21		
Phases of 6-yr rotation													
6-yr-Fallow	1.38 a	0.48 a	0.50 a	0.27 ab	0.14 a	0.13 ab	0.52 a	0.011 a	1.21 a	0.07 a	0.028 a	0.010	0.75
SEM	0.02	0.01	0.016	0.014	0.008	0.009	0.021	0.011	0.024	0.020	0.003		
6-yr-Wheat₁	1.32 a	0.50 a	0.48 a	0.26 ab	0.13 a	0.13 ab	0.47 a	0.005 a	1.19 a	0.08 a	0.025 a	0.007	0.54
SEM	0.01	0.009	0.017	0.002	0.001	0.004	0.009	0.003	0.012	0.012	0.003		
6-yr-Wheat₂	1.50 a	0.43 a	0.45 a	0.31 a	0.14 a	0.17 a	0.45 a	0.0001 a	1.19 a	0.02 a	0.024 a	0.008	0.17
SEM	0.02	0.01	0.012	0.013	0.009	0.009	0.013	0.000	0.010	0.006	0.002		
6-yr-Alfalfa₂	1.38 a	0.48 a	0.47 a	0.26 b	0.13 a	0.13 ab	0.48 a	0.009 a	1.24 a	0.04 a	0.029 a	0.005	0.11
SEM	0.01	0.02	0.011	0.011	0.004	0.012	0.011	0.008	0.019	0.008	0.002		
6-yr-Alfalfa₃	1.44 a	0.46 a	0.44 a	0.27 ab	0.14 a	0.13 b	0.44 a	0.0005 a	1.19 a	0.04 a	0.023 a	0.006	0.12
SEM	0.02	0.02	0.019	0.007	0.004	0.005	0.018	0.001	0.007	0.013	0.001		
P-value	0.18	0.15	0.09	0.05	0.21	0.05	0.06	0.78	0.34	0.11	0.22		

θ_{FC} : field capacity water content; θ_{PWP} : permanent wilting point water content; PAW: plant available water; θ_s : saturated volumetric water content; θ_r : residual water content; n: a shape parameter related to the curve smoothness; α : a negative inverse of the air entry potential; S-index: the slope at the inflection point; RMSE: root mean square error of modelled θ and K data.

Table 2B. Effect of crop rotation on selected soil attributes at the 5 to 10 cm soil depth increment from Lethbridge site. Within a column, treatment means with different letters differ, P < 0.05. Ks: saturated hydraulic conductivity; Unsat. K: hydraulic conductivity at 100 hPa; SOC: soil organic carbon; STN: soil total nitrogen; C:N: carbon to nitrogen ratio; MBC: microbial biomass carbon.

Crop rotation	Ks (cm d ⁻¹)	unsat. K at 100 hPa	Pore Volume (cm ³ cm ⁻³)				pH	STN (% m/m)	SOC (% m/m)	C:N	MBC nmol g ⁻¹ soil	Dm
			>100	100-50	50-9	<9						
				(µm diameter)								
6-yr rotation	104 a	0.070 a	0.08 a	0.03 a	0.09 a	0.27 a	7.20 a	0.16 a	1.94 a	11.9 a	707 a	0.984 a*
SEM	47	0.01	0.01	0.00	0.00	0.01	0.089	0.00	0.09	0.44	36	0.016
2-yr rotation	57 a	0.077 a	0.05 a	0.03 a	0.08 a	0.28 a	7.29 a	0.13 b	1.61 b	12.0 a	576 a	0.986 a*
SEM	19	0.03	0.01	0.00	0.00	0.01	0.086	0.00	0.08	0.37	50	0.015
P-value	0.51	0.73	0.17	0.29	0.27	0.81	0.5667	<0.001	0.03	0.91	0.05	0.83
Phases of 2-yr rotation												
2-yr-Wheat	47 a	0.042 a	0.07 a	0.03 a	0.08 a	0.27 a	7.25 a	0.14 a	1.67 a	12.1 a	535 a	0.987 a*
SEM	17	0.017	0.010	0.002	0.004	0.011	0.128	0.005	0.14	0.717	52	0.019
2-yr-Fallow	139 a	0.125 a	0.03 a	0.03 a	0.08 a	0.28 a	7.33 a	0.13 a	1.54 a	11.8 a	617 a	0.984 a
SEM	54	0.052	0.023	0.004	0.010	0.010	0.131	0.006	0.09	0.308	87	0.012
P-value	0.12	0.14	0.21	0.23	0.86	0.62	0.64	0.36	0.47	0.67	0.45	0.81
Phases of 6-yr rotation												
6-yr-fal	99 a	0.072 a	0.09 a	0.05 a	0.09 a	0.27 ab	7.19 a	0.14 c	1.73 a	12.0 a	625 a	0.993 a
SEM	52	0.009	0.042	0.006	0.005	0.014	0.168	0.003	0.057	0.270	36	0.019
6-yr-wh1	1083 a	0.050 a	0.11 a	0.03 ab	0.09 a	0.26 ab	7.24 a	0.15 bc	2.11 a	13.5 a	655 a	0.989 a*
SEM	292	0.008	0.013	0.002	0.006	0.002	0.213	0.006	0.283	1.362	87	0.005
6-yr-wh2	35 a	0.052 a	0.03 a	0.02 b	0.07 a	0.31 a	7.12 a	0.18 ab	1.84 a	10.2 a	737 a	0.985 a*
SEM	23	0.022	0.017	0.002	0.009	0.013	0.270	0.006	0.190	0.657	36.	0.004
6-yr-alf2	329 a	0.093 a	0.08 a	0.04 ab	0.10 a	0.26 b	7.06 a	0.19 a	2.06 a	11.0 a	792 a	0.975 a
SEM	139	0.023	0.016	0.004	0.005	0.011	0.282	0.006	0.258	1.034	141	0.025
6-yr-alf3	562 a	0.074 a	0.08 a	0.02 b	0.09 a	0.27 ab	7.40 a	0.15 bc	1.96 a	12.7 a	723 a	0.979 a
SEM	326	0.026	0.016	0.003	0.008	0.007	0.052	0.008	0.188	0.693	69	0.017
P-value	0.19	0.58	0.40	0.013	0.29	0.04	0.82	<0.001	0.71	0.12	0.64	0.42

* indicates that the Dm value is significantly different from 1 at P<0.05 or it is fractal.

Table 3. Multi-response permutation procedure results for microbial community structure (PLFA) in both sites. Only comparisons that were found to be significantly different are presented.

Comparisons	T	A	p
Breton			
Among treatments	-7.198	0.146	<0.001 *
2-yr R-Wheat vs. 5-yr R-Hay	-3.982	0.094	0.003 *
2-yr R-Wheat vs. Forest	-5.054	0.158	0.001 *
5-yr R-Wheat vs. Forest	-5.214	0.160	<0.001 *
5-yr R-Hay vs. Forest	-4.455	0.133	0.002 *
Lethbridge			
Among treatments	-4.335	0.148	<0.001*
2-yr R-Fallow vs. 6-yr R-Alfalfa ₃	-3.578	0.163	0.006 *
2-yr R-Fallow vs. 6-yr R-Fallow	-3.242	0.174	0.001 *

T: separation among groups; P: probability value; A: homogeneity within groups

Table 4. Distinctive indicator species analysis for microbial community structure (PLFA) associated with treatments in Breton site. Each value represents the mean indicator with standard deviation in parentheses, and the highest indicator value is in bold. Only PLFAs that were found to be significantly different among groups are presented.

PLFA	Taxa biomarker	Indicator Value					Monte Carlo P < 0.05
		Mean	2-yr R-Wheat	5-yr R-Wheat	5-yr R-Hay	Forest	
16:1 ω 9c	Gram -	18.3 (6.64)	29	7	15	0	0.049
19:0 Cyc ω 8c	Gram -	26.0 (4.56)	2	26	42	7	<0.001
20:4 ω 6c (6,9,12,15)	protozoa	21.2 (6.11)	1	3	12	43	0.005
15:00	general bacteria	19.7 (6.59)	1	0	7	67	<0.001
16:1 ω 11c	Gram -	26.2 (4.2)	8	17	11	36	0.023
18:3 ω 6c (6,9,12)	fungi	17.1 (7.07)	1	0	8	52	0.002

Table 5. Distinctive indicator species analysis for microbial community structure (PLFA) associated with treatments in Lethbridge site. Each value represents the mean indicator with standard deviation in parentheses, and the highest indicator value is in bold. Only PLFAs that were found to be significantly different among groups are presented.

PLFA	Taxa biomarker	Indicator Value								Monte Carlo
		Mean	2-yr R-Wheat	2-yr R-Fallow	6-yr R-Fallow	6-yr R-Wheat ₁	6-yr R-Wheat ₂	6-yr R-Alfalfa ₂	6-yr R-Alfalfa ₃	P < 0.05
14:0 ISO	Gram +	19.9 (7.25)	0	0	37	37	0	2	9	0.035
18:1 ω 5c	Gram -	15.6 (0.38)	14	8	16	15	17	15	14	0.002

Table 6. Pearson correlation coefficients (r-values) for relationships among soil properties in both sites.

	<i>MBC</i>	<i>C:N</i>	<i>SOC</i>	<i>TSN</i>	<i>pH</i>	<i><9 μm</i>	<i>9-50 μm</i>	<i>50-100 μm</i>	<i>>100 μm</i>	<i>Ks</i>	<i>S-index</i>	<i>α</i>	<i>n</i>	<i>θs</i>	<i>PAW</i>	<i>Sat. WC</i>	<i>BD</i>
Breton																	
<i>Dm</i>	0.27 n	-0.51**	-0.36*	-0.13 n	0.30 n	0.02 n	-0.25 n	-0.21 n	-0.44 **	-0.35 *	-0.46**	-0.51**	0.02 n	-0.47**	-0.12 n	-0.39*	0.44*
<i>BD</i>	0.15 n	-0.74**	-0.71**	-0.46**	0.33*	-0.32 n	-0.23 n	-0.33 n	-0.95**	-0.76**	-0.77**	-0.88**	0.26 n	-0.92**	-0.53**	-0.90**	
<i>Sat. WC</i>	-0.09 n	0.66**	0.63**	0.43**	-0.37*	0.58**	0.15 n	0.36*	0.77**	0.61**	0.77**	0.79**	-0.37*	0.97**	0.73**		
<i>PAW</i>	0.03 n	0.40*	0.43**	0.33*	-0.47**	0.87**	-0.01 n	0.18 n	0.31 n	0.23 n	0.50**	0.33*	-0.20 n	0.64**			
<i>n</i>	-0.33*	-0.21 n	-0.38*	-0.38*	-0.14 n	-0.22 n	0.40*	-0.03 n	-0.28 n	-0.15 n	0.27 n	-0.41*					
<i>S-index</i>	-0.35*	0.57**	0.42*	0.18 n	-0.49**	0.32 n	0.43**	0.41*	0.66**	0.54**							
<i>Ks</i>	-0.32 n	0.54**	0.43**	0.19 n	-0.12 n	0.12 n	0.32 n	0.03 n	0.77**								
<i>9-50 μm</i>	-0.45**	0.16 n	-0.004 n	-0.13 n	-0.33*	-0.09 n											
<i>TSN</i>	0.29 n	0.28 n	0.85**														
<i>SOC</i>	-0.02 n	0.72**															
<i>C:N</i>	-0.40*																
Lethbridge																	
<i>Dm</i>	-0.17 n	-0.07 n	-0.25 n	-0.29 n	-0.13 n	-0.14 n	-0.30 n	0.08 n	0.28 n	-0.09 n	-0.03 n	0.27 n	0.03 n	-0.005 n	-0.14 n	-0.04 n	-0.19 n
<i>BD</i>	-0.02 n	-0.09 n	-0.07 n	-0.01 n	0.27 n	0.61**	-0.26 n	-0.55**	-0.85**	-0.38*	-0.53**	-0.75**	-0.39*	-0.62**	0.28 n	-0.65**	
<i>Sat. WC</i>	-0.10 n	0.12 n	0.22 n	0.22 n	-0.01 n	-0.12 n	0.55**	0.75**	0.19 n	0.02 n	0.80**	0.41*	0.49*	0.97**	0.19 n		
<i>PAW</i>	0.11 n	0.09 n	0.43*	0.53**	0.18 n	0.85**	-0.22 n	-0.23 n	-0.49*	-0.23 n	-0.005 n	-0.34 n	-0.17 n	0.10 n			
<i>n</i>	-0.22 n	-0.07 n	0.12 n	0.26 n	-0.05 n	-0.42*	0.64**	0.69**	0.12 n	-0.43*	0.90**	-0.01 n					
<i>S-index</i>	-0.19 n	0.02 n	0.21 n	0.29 n	-0.01 n	-0.30 n	0.70**	0.83**	0.12 n	-0.32 n							
<i>Ks</i>	0.39*	-0.02 n	-0.07 n	-0.07 n	-0.16 n	-0.32 n	-0.21 n	-0.15 n	0.56**								
<i>9-50 μm</i>	-0.37*	0.11 n	0.17 n	0.14 n	-0.09 n	-0.36 n											
<i>TSN</i>	0.35 n	-0.004 n	0.66**														
<i>SOC</i>	-0.11 n	0.74**															
<i>C:N</i>	-0.45*																

* and ** indicate significant correlation at $P < 0.05$ and $P < 0.01$, respectively.

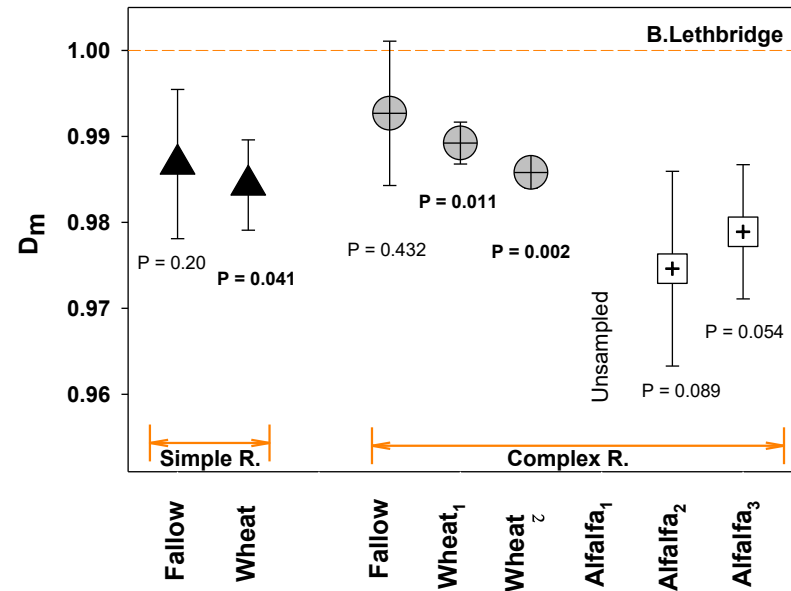
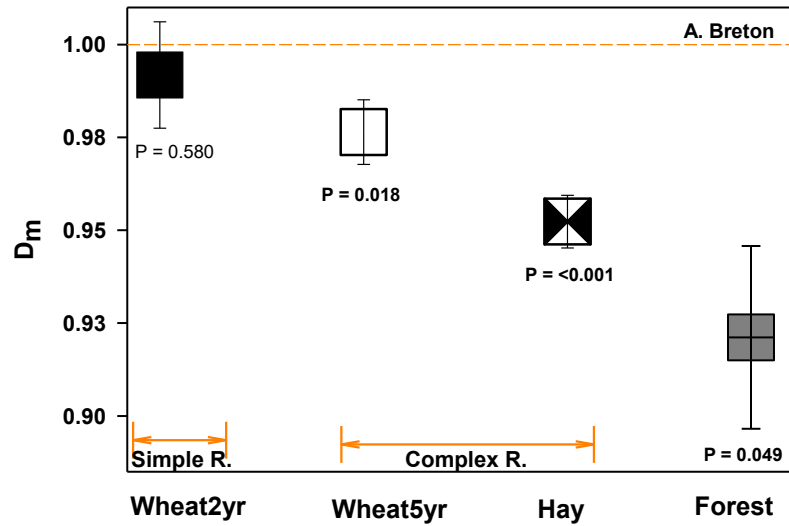


Fig. 1. Mass fractal dimension (D_m , unitless) of the natural log transformed aggregate mass (g) versus natural log normalized aggregate volume (cm^3) for phases within simple and complex rotations and adjacent forest (A. Breton, B. Lethbridge). D_m values are derived as slopes of linear regressions. Shown p-values are for regression coefficients against one as the non-fractal constant for mass vs. volume; $H_0: \beta_1 = 1$. Lower D_m values imply increasing development of hierarchical aggregation, and hence improved soil quality. Figures A and B have different y-axis scales.

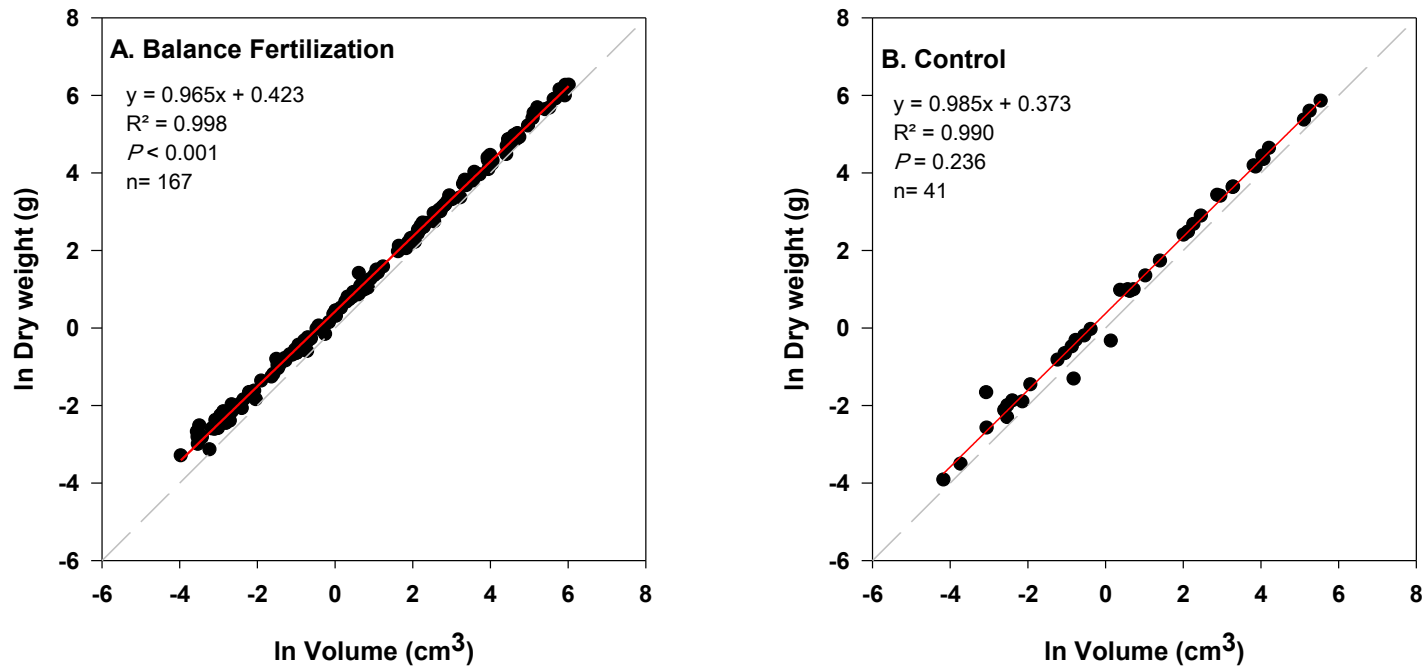


Fig. 2. Mass fractal dimension (D_m , unitless) of the natural log transformed aggregate mass (g) versus natural log normalized aggregate diameter (cm) for two nutrient managements (A. balanced fertilization, B. control). The n value is the number of scanned aggregates. D_m values are derived as slopes of linear regressions. Shown p -values are for regression coefficients against one as the non-fractal constant for mass vs. volume; $H_0: \beta_1 = 1$.

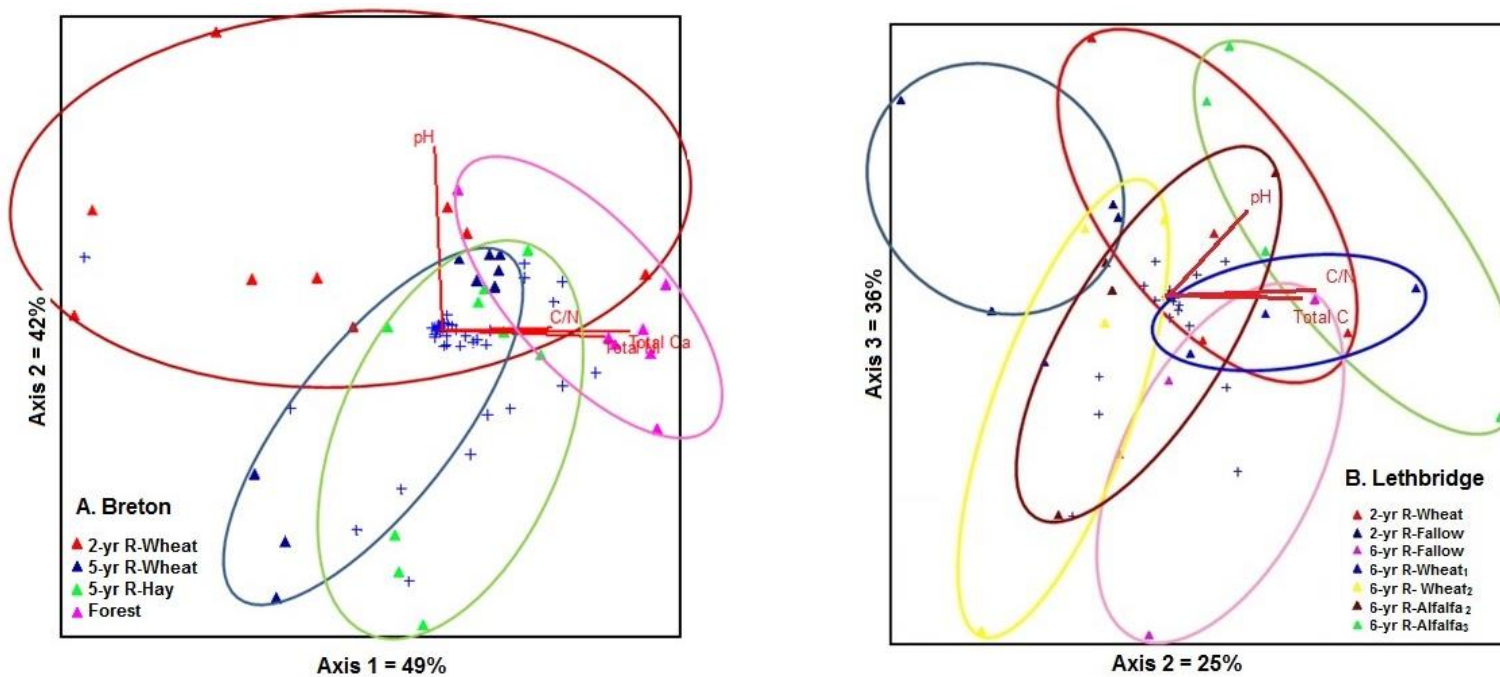


Fig. 3. NMS ordination biplots for phospholipid fatty acid (PLFA) analysis for phases within simple and complex rotations and adjacent forest (A. Breton, B. Lethbridge). 89 iterations, stress= 13, and 2-dimensional solution for Breton and 69 iterations, stress= 11, 3-dimensional solution for Lethbridge.

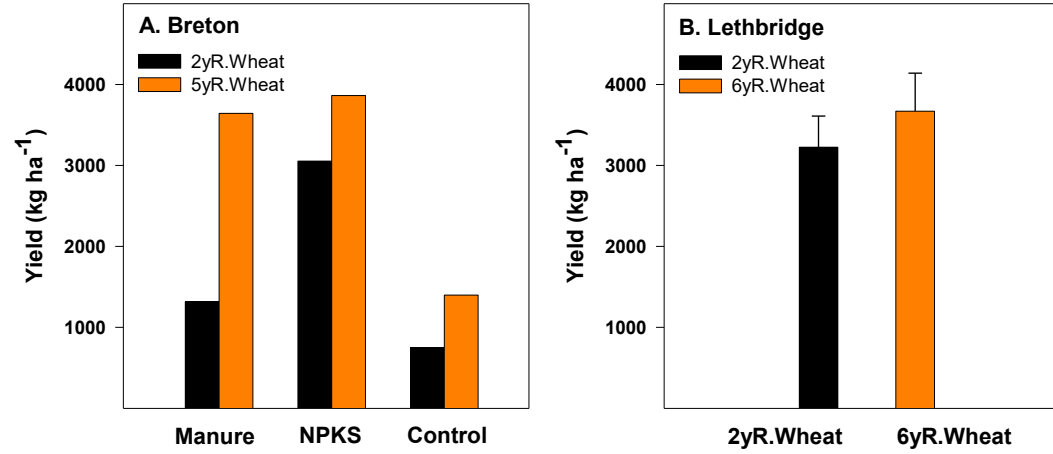


Fig. 4. Wheat grain yield (kg dry matter ha⁻¹) for simple and complex rotations in 2014 (A. Breton site, B. Lethbridge site). The wheat grain yield in complex rotation of Lethbridge site is the yield of first year of wheat at the mentioned rotation. There are three nutrient regimes in Breton, and the NPKS is referred in this study as balanced fertilization.

10. Figure captions

Fig. 1. Mass fractal dimension (D_m , unitless) of the natural log transformed aggregate mass (g) versus natural log normalized aggregate volume (cm^3) for phases within simple and complex rotations and adjacent forest (A. Breton, B. Lethbridge). D_m values are derived as slopes of linear regressions. Shown p-values are for regression coefficients against one as the non-fractal constant for mass vs. volume; $H_0: \beta_1 = 1$. Lower D_m values imply increasing development of hierarchical aggregation, and hence improved soil quality. Figures A and B have different y-axis scales.

Fig. 2. Mass fractal dimension (D_m , unitless) of the natural log transformed aggregate mass (g) versus natural log normalized aggregate diameter (cm) for two nutrient managements (A. balanced fertilization, B. control). The n value is the number of scanned aggregates. D_m values are derived as slopes of linear regressions. Shown p-values are for regression coefficients against one as the non-fractal constant for mass vs. volume; $H_0: \beta_1 = 1$.

Fig. 3. NMS ordination biplots for phospholipid fatty acid (PLFA) analysis for phases within simple and complex rotations and adjacent forest (A. Breton, B. Lethbridge). 89 iterations, stress= 13, and 2-dimensional solution for Breton and 69 iterations, stress= 11, 3-dimensional solution for Lethbridge.

Fig. 4. Wheat grain yield ($\text{kg dry matter ha}^{-1}$) for simple and complex rotations in 2014 (A. Breton site, B. Lethbridge site). The wheat grain yield in complex rotation of Lethbridge site is the yield of first year of wheat at the mentioned rotation. There are three nutrient regimes in Breton, and the NPKS is referred in this study as balanced fertilization.

CHAPTER TWO

**Spatial Heterogeneities of Plant Available Water, Soil Organic Carbon, and Microbial Biomass
under Divergent Land Uses: Comparing Regression-Kriging, Cokriging, and Regression-Cokriging
Approaches**

1. Abstract

Improved knowledge of the spatial patterns of soil organic carbon (SOC), microbial biomass carbon (MBC), and plant available water (PAW) can underpin the identification and inventory of beneficial ecosystem functions and services in predominant land-use system types. However, little research has been done to address and account for the field variability of these key soil properties. This study characterized the spatial heterogeneities of PAW, SOC concentration, and MBC and evaluated their spatial prediction using ordinary kriging (OK), regression-kriging (RK), cokriging (coK), and regression-cokriging (RcoK) geostatistical approaches. Using a nested cyclic sampling design, we sampled a total of 112 point locations (5–10 cm soil depth increment) in two fields: a native grassland (NG) site and an irrigated cultivated (IC) site located near Brooks, Alberta. Converting the native grassland to irrigated cultivated land altered soil pore distribution by reducing macroporosity (by 25 %) which also led to lower saturated water content and half of the hydraulic conductivity in IC compared to NG. This land-use conversion also decreased the relative abundance of Gram-negative bacteria, while increasing the MBC concentration (601 vs. 812 nmol g⁻¹ soil) in particular the proportion of Gram-positive bacteria. Across field sites and measured properties, the best fitted spatial model was Gaussian. The IC showed stronger degree of spatial dependence and longer range of spatial auto-correlation (~ 23 % increase) revealing a homogenization of the spatial variability of soil properties likely as a result of intensive, repeated agricultural activities. Comparison of OK, RK, coK, and RcoK approaches indicated that cokriging (coK) method had the best performance as demonstrated by profound improvements in the accuracy of spatial estimations of PAW, SOC concentration, and MBC. It seems that the combination of kriging with certain terrain covariates such as elevation and depth-to-water delivers enhanced capability for effectively incorporating explicit ancillary

information into predictive soil mapping. Overall, identification and depiction of spatial patterns of soil properties in agricultural lands can generate a bird's eye view for land owners to design and improve management practices which lead to sustainable production.

Keywords: geostatistics, grassland, PLFA, predictive mapping, secondary variable, soil properties, uncertainty

2. Introduction

Site-specific land management endeavors to decipher and interpret spatial and temporal variabilities within fields in order to optimize profitability, sustainability, and environmental protection (Duffera et al., 2007; Lowenberg-DeBoer and Swinton, 1997). Heterogeneity in soil properties across the landscape can represent a management challenge to producers and policymakers in particular when land-use changes commonly occur (Nyamadzawo et al., 2008; Robertson et al., 1993). Not only there is a paucity of information regarding the comparative impacts of contrasting land use systems on soil functions but also the required information about whether different land-use types influence the spatial variation of soil properties is still elusive. Therefore, there is a need for comprehensive understanding of the spatial structure of soil properties that are linked with relevant ecosystem functions across competing land uses types (e.g., native grassland versus cultivated land).

Soil classification and survey have been traditionally used to document and characterize the spatial variation by generating maps of soil classes that represents soil properties estimated within a defined region or generalized mapping unit (Webster, 1985). Different geostatistical methods have been recently applied to interpolate soil properties from sparse sampling points into continuous surfaces by modeling the spatial correlation with minimum variance (Cambardella et al., 1994; Hengl et al., 2004; Lark, 2002; Wang et al., 2009). Qiu et al. (2016) demonstrated the use of spatial sampling and variography in an annual crop field to identify fertility management zones which can greatly improve nutrient use efficiencies relative to any uniform management. Moreover, earlier studies have revealed that the spatial variability of soil properties across the landscape of an ecosystem may be controlled by the underlying variabilities in topography (Su et al., 2006), vegetation types (Nyamadzawo et al., 2008; Stutter et al., 2004),

cultivation (Wang et al., 2013), texture (Qiu et al., 2016) and parent material (Liu et al., 2006; Stutter et al., 2004). However, insufficient attention has been paid to deciphering and comparing the spatial structure of specific soil properties such as SOC, MBC, and PAW which are implicitly related to key ecosystem functions such as soil carbon sequestration, nutrient transformations and pore water release.

When a spatial interpolation is only based directly on available measured data, ordinary kriging (OK) is commonly applied. This OK approach uses weighted averages to estimate unsampled locations as a linear combination of statistically-neighboring observations (Mirzaee et al., 2016; Wang et al., 2013). By contrast, regression-kriging (RK) method is the summation of regression values and kriging values derived from the regression residuals (Hengl et al., 2004; Odeh et al., 1995). The RK method has been often employed to map soil properties through using such predictor variables when other data of correlated environmental variables are available (Eldeiry and Garcia, 2010; Hengl et al., 2007, 2004; Knotters et al., 1995; Motaghian and Mohammadi, 2011; Odeh et al., 1995). Several studies have demonstrated the advantage of RK compared to OK (Hengl et al., 2004; Mirzaee et al., 2016; Motaghian and Mohammadi, 2011; Odeh et al., 1995). Conversely, other reports have found that RK technique outperform neither OK (Eldeiry and Garcia, 2010; Li, 2010) nor cokriging (coK) (Motaghian and Mohammadi, 2011). These inconsistencies across the existing literature substantiate the need for further comparison of these various geostatistical approaches under a wide range of ecosystems and for multiple biophysical attributes.

When the spatial distribution of a secondary variate (e.g., terrain covariates such as elevation) has been sampled more intensely than the primary variate, cokriging (coK) method can be implemented (Davis, 2002). Incorporating those co-variables into interpolation

procedures may provide an opportunity to obtain higher prediction accuracy while using limited existing data from the primary variate. Moreover, if the primary variate is difficult or expensive to measure, cokriging can greatly improve interpolation estimates without the need for more intensely measurements of the primary variate (Wang et al., 2013). The performance of coK with different auxiliary variables has been previously examined while focusing on soil attributes (Ceddia et al., 2015; Hernández-Stefanoni et al., 2011; Simbahan et al., 2006; Wang et al., 2013). These studies reported the advantage of coK method as it accounts for both the auto correlations and cross correlations among all involved variables including the target variable and the secondary variables, which is not fully achieved in RK method.

Recently, several studies have focused on hybrid geostatistical procedures, which typically combine two conceptually different approaches (i.e., deterministic and stochastic) to model spatial variation of soil properties (Hengl et al., 2007; Mirzaee et al., 2016). One of these hybrid promising geostatistical methods is regression-cokriging (RcoK) which is a combination of regression values and cokriging conducted on the regression residuals simultaneously incorporating covariates. However, compared with other methods such as OK, coK, and RK, the RcoK has been rarely evaluated for modeling purposes of the field variation of soil properties.

More precise maps of the spatial variability of soil attributes in native prairie and cultivated lands may facilitate the strategic implementation of best management practices which can lead to sustainable production systems embedded in multifunctional landscapes (Knotters et al., 1995; Wang et al., 2013). Such improved mapping applications will further facilitate the incorporation and extrapolation of this new, spatially-explicit knowledge into valid predictions for comparable landscapes and land-use systems. The aims of this study were: i) to upscale new spatial knowledge of key soil biophysical attributes (i.e., PAW, SOC concentration, and MBC)

from point measurement to field landscapes by extracting their spatial patterns and examining the influence of contrasting land use types (native grassland versus cultivated land) on multiple soil properties, and ii) to compare the ability of different geostatistical approaches (i.e., OK, coK, RK, and RcoK) for predicting PAW, SOC concentration, and MBC concentration while evaluating terrain remotely-sensed data as potential co-variables.

3. Materials and Methods

3.1. Study sites

This study was conducted in two fields: a native grassland (NG) (north-west corner: 50° 53' 54.4" N, 111° 57' 40.2" W) and an irrigated cultivated (IC) land (north-west corner: 50° 54' 26.5" N, 111° 58' 41.1" W) sites at the University of Alberta Mattheis Research Ranch located within the dry mixed grass prairie natural sub-region of Alberta, Canada. The climate is continental, sub-humid, characterized by long cold winters and short summers (Mollard et al., 2014). Mean annual precipitation and temperature are 354 mm and 4.2 °C, respectively (Hewins et al., 2016). The sites had a Rego Brown Chernozemic soil classification based on Agricultural Region of Alberta Soil Inventory Database (AGRASID, 2015) with a loamy sand texture. The granulometric distribution for native grassland soil was: sand (1000–50 µm size diameter) 865, silt (50–2 µm) 75, and clay (<2 µm) 60 g kg⁻¹ soil and for irrigated cultivated land soil was: sand 831, silt 101, and clay 68 g kg⁻¹ soil.

The native grassland (NG) was dominated by crested wheat grass (*Gropyron cristatum*), smooth brome grass (*Bromus inermis*), and kentucky blue grass (*Poa pratensis*). This NG site also had various native species present such as *Poa sandbergii*, *Stipa comate*, *Carex praticola*, *Equisetum hyemale*, *Artemesia frigida*, *Artemesia ludoviniaca*, *Heterotheca villosa*, and *Achillea millefolium*. The land is currently used as cattle ranch on a rotational grazing basis for approximately 6 months each year, beginning in early May. The cultivated land (IC) site is irrigated by a center pivot system with annual crops such as wheat and oat grown under conventional tillage practices for at least two decades, and this site was seeded to introduced pasture for grazing in spring 2014. The dominant plant species in this recently established pasture were alfalfa, red clover, kentucky blue grass, and crested wheat grass.

3.2. Soil sample collection

Collection of all field samples took place on 6 and 7 June 2015 at both sites. Using a cyclic sampling design (Hudelson and Clayton, 2015; Orr et al., 2014), a 170 m×100 m (1.7 ha) plot was established at each site for data collection (Fig. 1). From the right upper corner to the left upper corner, the sampling intervals were 10, 35, 85, and 100 m distances, and from the top boundary of the field plot to the bottom boundary, distances were 10, 35, 85, 95, 120, and 170 m (for a total of 36 measurement points). A cyclic sampling design can increase the sampling efficiency by optimizing the placement of sampling points to provide the most information for geostatistical analysis with the number of samples possible (Bogaert and Russo, 1999). This design maximizes sampling efficiency by reducing over-sampling at small lag distances (Orr et al., 2014). Moreover, allowing for the possibility of important variability occurring and very fine spatial scales, a nested design was also employed within the overall cyclic sampling pattern. For this nest, a cycle of {0.5, 2, 4.5 m} was applied in both cardinal directions (i.e., west to east and north to south) ($n = 20$). There are also two additional sampling points which were strategically located in the plot to increase the sampling efficiency and to capture the most information for geostatistical analysis. There were 56 sampling points in each site for a total of 112 measured points in this study. A differential global positioning system device was used to locate the sampling points (latitude and longitude) with better than 20 cm accuracy. This sampling protocol allows us to measure lag distances between 0.5 and 197 m in the plot. Also, our nested cyclic sampling design demonstrated to have sufficient pairs of data points (at least 20 pairs per lag class) even for active lag distances of up to 140 m; this facilitates the adequate development of variogram models when assuming uniform size of lag classes as narrow as 5 m distance interval (Fig. 2).

3.3. Soil sample analysis

One undisturbed soil sample was collected using stainless steel cylindrical cores (8 cm inner diameter) in each sampling point to quantify water retention and hydraulic conductivity. For chemical and microbial analyses, one additional disturbed soil sample was taken in each sampling point by composing 4 subsamples taken using a 2 cm inner diameter push probe. Disturbed samples were put in Whirl-Pak[®] (Nasco, Fort Watkins, Wisconsin) sterile sampling bags and were preserved and transported in an icebox to the laboratory. Samples for microbial characterization were kept frozen at -86°C until they were freeze-dried in preparation for analysis. All soil samples were taken at the selected sampling points at the depth increment of 5-10 cm.

Using the undisturbed cores, water retention was determined with the evaporation method (Schindler et al., 2010) using a HYPROP device (UMS GmbH, Munich, Germany). Matric potential was automatically recorded by two tensiometers at two depths within the saturated soil cores. The gravimetric water content of the samples was recorded twice daily for up to 14 days. Data points of the retention and unsaturated hydraulic conductivity curves were calculated with the HYPROP 2011 software (UMS GmbH, Munich, Germany) based on the mean tension potential of the two tensiometers and water contents as detailed in Kiani et al. (2016b).

The soil water retention for moderate to dry moisture ranges was evaluated with a WP4-T potentiometer (Decagon Devices, Inc., Pullman WA, USA) based on the chilled-mirror dew point technique (Schelle et al., 2013). Seven different amounts of water were added to 5 g dry weight of soil in plastic cups. The cups were closed tightly and samples allowed equilibrating for 24 hours. When the water potential of the sample was in equilibrium with the vapor pressure of the WP4-T measurement chamber, water tension was recorded. Sample weight was determined

immediately after measurement and related to the oven-dry weight (at 105 °C) to obtain the corresponding water content. The constrained van Genuchten (1980) model was fitted to the results from the evaporation method (HYPROP) and WP4-T measurements. At the end of each measurement campaign, the soil samples were oven dried at 105 °C for 24 h to derive bulk density and total porosity assuming a particle density of 2.65 g cm⁻³.

Macroporosity was computed from the soil water retention data subtracting the saturated water content from the water content at field capacity (FC; -33 kPa water potential) which corresponds to pore diameters larger than 9 µm. Plant available water was also calculated as the differential volumetric water content between field capacity (-33 kPa) and permanent wilting point (PWP; -1500 kPa).

With the aim of extracting an integrated indicator of soil quality, S-index was calculated as the magnitude of the slope of the soil water retention curve at the inflection point when the curve was expressed as gravimetric water content versus natural logarithm of pore water tension head (Dexter, 2004).

After grinding a portion of the composited, disturbed samples, we determined the concentrations of soil organic carbon (SOC) and soil total nitrogen (STN) by dry combustion method using a Costech ECS 4010 Elemental Analyzer (Costech Analytical Technologies Inc., Valencia, CA, USA). The SOC density was calculated by multiplying SOC concentration (g C kg⁻¹ soil) × bulk density (g cm⁻³) × soil thickness (cm) × 10 (conversion factor). Soil pH was measured using a 1:2 soil to water ratio (Mclean, 1982).

Using composited samples, we characterized soil microbial communities using phospholipid fatty acid (PLFA) analysis. Polar lipids were extracted from freeze-dried samples using a modified Bligh and Dyer protocol (Hannam et al., 2006). The standardized X: Y ω Z

nomenclature for fatty acids was used to identify PLFAs, where X is the number of carbon atoms, Y is the number of double bonds, and Z is the position of the first double bond from the aliphatic end (ω) of the molecule. Prefixes “i” and “a” indicate branching at the second and third carbon atom, respectively, from the ω end, and the suffix “c” corresponds to a c transfiguration. Adding them together, all of the PLFA biomarkers were considered to be representative of the total PLFA concentration of the microbial community in our soils.

Candidate terrain covariates were derived from airborne LiDAR (Light Detection and Ranging) measurements with vertical accuracy of 30 cm. Available LiDAR spatial resolution was 2 m x 2 m with horizontal accuracy of 50 cm. The LiDAR method uses light in the form of a pulsed laser to measure variable distances to the Earth. A LiDAR measurement system basically consists of a laser, a scanner, and a specialized GPS receiver. Topographic LiDAR typically uses a near-infrared laser to map the land (Gatziolis and Andersen, 2008). The LiDAR-derived data in our study included terrain elevation (Fig. 4), curvature, slope, aspect, hill shade, and depth to water (DTW) using ArcGIS 10.3 (ArcGIS[®]). DTW was obtained from the wet-areas delineation algorithms across the landscape, using the flow channels and shorelines (Murphy et al., 2011).

3.3. Classical statistical analysis

The datasets were analyzed to determine the descriptive parameters, i.e., maximum, minimum, mean, median, and standard deviation (SD). The Kolmogorov–Smirnov test, together with skewness and kurtosis values, was used to evaluate the normality of the datasets. For data that failed the normality test, a suitable transformation was performed to achieve a normal distribution for use in further statistical analyses.

A two-sample t-test (α critical value = 0.05) using R software determined whether the means of soil properties differed significantly under different land use types. Spearman rank

correlations were used to determine the existence and strength of relationships among soil properties and with covariates.

All PLFAs with < 20 carbons were used for analysis of the microbial communities. Data groupings were tested for significant differences in the NMS analysis using a multi-response permutation procedure (MRPP). In addition to the probability value (P), the MRPP test generates a T value, which indicates separation among groups, with a larger T reflecting a stronger separation, and an A value, which is an index of within-group homogeneity compared to a random expectation, with a larger A indicating greater homogeneity. Moreover, indicator species analyses were performed using the data groupings shown to be different by MRPP. This statistical method generates an indicator value based on the abundance and frequency of a particular PLFA in a given data grouping. A larger indicator value represents a stronger relationship between the PLFA and the given data grouping. The statistical significance of the indicator value was tested against a randomized Monte Carlo test. All analyses were conducted using PCORD software (version 5, MjM Software Design, Gleneden Beach, OR, USA).

The approach by Metcalfe et al (2008) was used to find the optimal sample size (N_{opt}) for each measured soil properties:

$$N_{opt} = \left[\frac{t_{\alpha} CV}{D} \right]^2 \quad [1]$$

where t_{α} is the Student's t-value at a chosen critical level ($\alpha = 0.05$ in this study). CV is the coefficient of variation, equal to the standard deviation normalized by the sample mean (given in %). Also known as mean value accuracy, D is essentially the margin of error, expressed as percentage of the mean. We assessed D of 5, 10, 20, or 40% in our data. Upon conducting sampling using N_{opt} samples, a 95% of the time, the true mean value could be found within $\pm 5, 10, 20, \text{ or } 40\%$ from the estimated mean.

3.4. Geostatistical analysis

Geostatistics uses a semivariogram to quantify and model spatial autocorrelation, and subsequently, to provide parameters for optimal spatial interpolation, which is known as kriging method (Webster and Oliver, 2007). Our measured data was used to calculate the experimental semivariogram, which is then, fitted by authorized theoretical models, i.e. linear, Gaussian, spherical and exponential. The best-fitted model was considered to be the one having the smallest residual sum of squares (RSS) and the largest coefficient of determination (R^2). Three major parameters could be derived from the fitted model, i.e. nugget (C_0), sill ($C+C_0$) and autocorrelation range, which can characterize the spatial structure of variables of interest at a given scale. The total variance (sill, $C+C_0$) is expressed as the summary of the structural variance (C , variance explained by spatial autocorrelation) and the nugget effect (C_0 , variance occurring at a smaller scale than the field sampling and from the experimental error) (Liu et al., 2013). The spatial autocorrelation range represents the maximum distance within which variables exhibit internal spatial dependence. To determine the magnitude of spatial dependence, the percentage of total variance (sill) explained by random variance (C_0) was calculated as a nugget ratio (Cambardella et al., 1994).

In our study, regression (R), ordinary kriging (OK), regression-kriging (RK), cokriging (coK), and regression-cokriging (RcoK) methods were used for the spatial interpolation of PAW, SOC concentration, and MBC in the 5–10 cm soil depth increment across our native grassland and cultivated land sites. The general equation of OK (Eq. [2]) and coK (Eq. [3]) methods are (Webster and Oliver, 2007):

$$\hat{Z}(X_i) = \sum_{i=1}^N \lambda_i Z(X_i) \quad [2]$$

$$\hat{Z}(X_i) = \sum_{i=1}^N a_i Z(X_i) + \sum_{i=1}^N b_i Z(X_j) \quad [3]$$

where $\hat{Z}(X_i)$, $Z(X_i)$, $Z(X_j)$, and N are the predicted value, primary variable, secondary variable, and the number of soil samples, respectively. The λ_i , a_i , and b_i , are kriging weights. The RK (Eq. 4) (Odeh et al., 1995) and RcoK (Eq. 5) combined a deterministic component (i.e., linear regression) as first step followed by stochastic spatial interpolation:

$$\hat{Z}(X_i) = Z(R_i) + \sum_{i=1}^N \lambda_i e(S_i) \quad [4]$$

$$\hat{Z}(X_i) = Z(R_i) + \sum_{i=1}^N c_i e(S_i) + \sum_{i=1}^N d_i e(S_j) \quad [5]$$

where the $Z(R_i)$ is the estimation data by regression model, $e(S_i)$ is the interpolated residuals, and the $e(S_j)$ is the secondary variable. The λ_i , c_i , and d_i are the kriging weights. The residuals for each soil property were obtained by subtracting the measured data from the estimated values (derived from the regression) (Heuvelink et al., 2016). Then, variograms (and cross-variogram) were fitted on the regression residuals to inform optimal kriging or cokriging.

The criteria used for contrasting the performance of the evaluated geostatistical methods were coefficient of determination (R^2), standard error of prediction (SE predict), mean prediction error (MPE), and root mean square prediction error (RMSPE) calculating as follows:

$$SE \text{ predict} = SD \sqrt{1 - r^2} \quad [6]$$

$$MPE = \frac{1}{N} \times \sum_{i=1}^N [\hat{Z}(X_i) - Z(X_i)] \quad [7]$$

$$RMSPE = \sqrt{\frac{1}{N} \times \sum_{i=1}^N [\hat{Z}(X_i) - Z(X_i)]^2} \quad [8]$$

where SD is the standard deviation of the measured data. The geostatistical analysis was performed with the GS+ software (version 10.0) and the distribution contour plots were produced with SigmaPlot software (version 11.0) without using any data smoothing function.

4. Results

4.1. Classical statistical analyses of soil properties

The overall means of Van Genuchten (VG) parameters for our soil moisture retention curves consistently differed between native grassland (NG) and irrigated cultivated (IC) land (Table 1). Saturated water content was 11% higher in native grassland ($P < 0.05$), while PAW was found to be three times greater in cultivated land, and this outcome was driven by a 1.3-times significantly higher water content at field capacity (FC) for IC than in NG soils (Table 1). Additionally, a reciprocal 1.3-times greater presence of draining pores (macropores; $> 9 \mu\text{m}$ diameter) in these sandy soils under perennial native grasses (NG $>$ IC) implies faster water infiltration, conductivity, redistribution and percolation across the NG soil profiles. A clear significant difference was also found in S-indexes (i.e., slope of moisture curves at their inflection point) between native grassland and irrigated cultivated land, with magnitudes of 0.11 for NG vs. 0.06 for IC ($P < 0.05$; Table 1). Regarding the fitting performance of our VG models, root mean square errors for the moisture curve of each land use system ranged from 0.003 to $0.020 \text{ cm}^3 \text{ cm}^{-3}$ indicating effective fitting of the VG models to measured data.

Our NG soil exhibited two-fold faster hydraulic conductivity under unsaturated conditions (unsat. K at -10 kPa water tension) than the IC soil ($P < 0.05$; Table 1). Conversely, this clear effect of land use on water movement capacity did not translate into differences in hydraulic conductivity at saturation. Root mean square error values of modelled hydraulic conductivity (K) were high across all our data sets (0.21 cm day^{-1} ; data not shown) indicating modest fitting which is in part a result of extrapolation into the saturated zone of the water retention curve.

The MBC concentration was significantly greater in cultivated land with a concentration of 812 nmol g⁻¹ versus 601 nmol g⁻¹ in the native grassland soils ($P < 0.05$; Table 1). Separation between native grassland and cultivated land was significant for the PLFA data (as a proxy to microbial community structure) as evidenced by our MRPP analyses (all $P_s < 0.001$). Similarly, the A value, which indicates within-group homogeneity, was 0.04 for the microbial communities between two sampling sites. Although the A value shows that within-group variability is considerable, the large T value (15.6) indicates distinctive separation between two groups. The indicator species analysis detected six significant PLFAs in our native grassland soils, but no specific biomarker was detected for the cultivated soils (Table 5). In further detail, the presence of Gram-negative bacteria associated with 15:1 i, 17:1 a, and 17:1 ω 8c PLFAs, and also a unique actinobacteria biomarker (17:0 10 methyl) were evident only in the native grasslands.

Although both SOC concentration and SOC density showed no statistically differences between land uses, STN concentrations were significantly higher in the cultivated land (Table 1). As a result, soil C:N ratio mirrored this difference between land use systems; this parameter was 12% narrower in IC soil than PG ($P < 0.05$; Table 1), perhaps revealing less limiting nitrogen status in IC soils after decades of intense cropping history including N fertilization and introduction of legumes.

4.2. Variographic analyses of soil properties

The mean and median were used as central tendency estimates, while the minimum, maximum, skewness, kurtosis, and standard deviation (SD) values were used as descriptors of variability from each separate site. We observed that water content at FC, PAW, sat. K, SOC, STN, and MBC were highly positively skewed (Table 1) as shown by distinctive asymmetry in their distributions. In addition, the distribution of water content at FC, PAW, sat. K, SOC, and

STN peaked more than a Gaussian distribution according to the Kurtosis values. The highly skewed distributions of PAW and SOC particularly in our native grassland may be in part considered evidence of spatial heterogeneity with extreme values characteristic of landscapes where agricultural management (e.g., tillage, irrigation) have not smoothed natural variation features. The relatively high variability of terrain curvature (at 2 m by 2 m resolution and using eight surrounding neighbors) in the native grassland site can support this notion. Likewise, the standard deviation of terrain elevation in NG was double in NG vs. IC (Table 1 and Fig. 4). The recurrent, random addition of cattle manure during field grazing in NG may have also led to accumulation patches of enriched SOC as well.

As part of our variogram development, active lag distance values were found to be from 60 to 110 m throughout the fitting procedures. The class intervals were applied in a way to have at least 20 pairs in each class, and at least 3 classes within the domain of the autocorrelation range. The typical size of the lag class interval ranged from 4 to 10 m. For model selection purposes, each experimental variogram, secondary variogram, and cross-variogram was fitted with a Gaussian, spherical, and exponential models, and the optimal model was chosen to attain both lower RSS and higher R^2 (Table 4). Overall, Gaussian model had the best fitting results for almost all variograms and cross-variograms.

Candidate predictors for PAW, SOC concentration, and MBC were pre-screened based on Spearman correlation coefficients among the available data and each of the dependent variables of interest, a low variance inflation factor (VIF), and their significance of predictors in the regression models (Table 2). The optimal predictor for PAW was SOC in both land uses (Fig. 3). With respect to SOC concentration, all S-index, α , porosity, and Sat. WC (with VIFs < 2) were suitable predictors in native grassland, while θ_{FC} was best predictor for SOC concentration in cultivated land. The optimum set of predictors for MBC was C:N ratio, S-index, and Sat. WC

in the NG soils, whereas C:N ratio was the best predictor for MBC in our IC soils (Table 2; Fig. 3).

With the aim of selecting suitable covariates, we assessed our three soil properties of interest (i.e., SOC concentration, PAW, and MBC) alongside with highly correlated terrain variables (Table 3) to examine which candidate covariate(s) led to the lowest RSS and highest R^2 as derived through fitted cross-variograms. Using covariates consistently resulted in a substantial reduction in RSS of the variographies for all assessed soil properties. Of the assessed terrain attributes, the best covariate for PAW was terrain slope in native grassland and elevation in cultivated land (Fig. 4). Interestingly, DTW was the optimal covariate for both SOC concentration and MBC in both land-use systems implying an overarching influence of terrain wetness on these two key soil biological responses irrespective of the land management scenarios.

The autocorrelation range was typically 40 to 126 m (Table 4), and the longest autocorrelation ranges were observed with coK and RcoK methods where terrain covariates contributed to these spatial prediction. Congruently, the nugget ratio exhibited prominent reductions when applying the terrain covariates (Table 4), likely indicating also tighter spatial structure and increased predictability.

The standard error of the predictions had the lowest value in coK and highest value in RK for all soil variables (Table 4). Furthermore, both coK and RcoK methods had low RMSPE (Table 4), which suggests that the two approaches are similarly good interpolators. The goodness of fit (R^2 values) between the measured and predicted data also indicated that coK performed best across all variables at both land uses. Moreover, correlation analyses showed that the associations between variables' regression residuals and selected terrain covariates were very

weak or even inexistent when compared to the relatively stronger correlations between the same terrain covariates and our observed experimental values; this divergence correlation result was particularly evident for PAW in NG and for SOC in IC (Table 2). Because the regression residuals trended losing relatedness to the observed values, the cokriging step within the RcoK method could not contribute effectively to further reduce the uncertainty of prediction when compared to the coK approach which provided consistently lower uncertainty as detailed above (Table 4).

Of the evaluated geostatistical approaches, OK had the weakest fit in the native grassland, while in the cultivated land, R had the lowest performance. This might suggest that in the cultivated land, the variation in soil properties is more spatially structured which could not be sufficiently captured with linear regression approaches. In further details, the mapped means of PAW, SOC concentration, and MBC (Fig. 5) changed amply within different distance ranges over our NG field, which indicates that the correlations of the covariates with the primary variate vary with spatial locations in this relatively heterogeneous prairie site. Moreover, similar patterns were observed for the cultivated land (data not shown). We also found that OK, RK, coK, and RcoK approaches differed with respect to their spatial patterns of prediction errors. The estimated uncertainty of soil PAW was very high with OK and RK method, but clearly reduced with both coK and RcoK (Fig. 6). As indicated above, PAW typically exhibits high spatial variability by nature, and hence, approaches that demonstrate systematically reductions in PAW uncertainty are avidly sought-after for improving predictive mapping.

The optimal number of samples for various soil properties was calculated on the basis of power function (Eq. [1]; Table 1). The Nopts varied over the measured variables and land uses. Based on an α critical value of 5%, bulk density, porosity, saturated water content, C:N ratio, and

pH needed the least amount of minimum samples (i.e., 6-29 samples), while the saturated and unsaturated hydraulic conductivity, plant available water, and microbial biomass carbon required the largest amount of samples (≥ 153 samples) at both field sites. Overall, the cultivated land's optimal number of samples was higher than in native grassland for all of the soil properties except for PAW, SOC, and STN which exhibited the reverse outcome.

5. Discussion

5.1. Soil quality changes in contrasting land use systems.

Compared to cultivated land, native grassland had greater saturated water content and doubled the hydraulic conductivity (at -10 kPa water potential). This outcome directly reflects the higher abundance of macropores in native grassland soils (Table 1) which can readily intake, store and transport ample amounts of water at low tensions. However, in an apparent incongruency, plant available water (PAW) was almost triple in the irrigated cultivated land (0.069 vs. 0.024 m³ m⁻³) which can be largely attributing to a greater volume of smaller-size pores in these IC soils. This cultivated land was formerly used as a cropland continuously for more than two decades, and it had been recently converted to introduced pasture in the summer prior to our field sampling. Our results can imply that previous annual cropping activities, such as tillage and recurrent equipment traffic, can have led to soil compaction which is known to alter soil pore distribution by reducing macroporosity (Pagliai et al., 2004). Moreover, animal treading may further compress large pores into relatively smaller pores near the ground surface (Drewry et al., 2008). We postulate that this creation of smaller and more frequent size pores as a long term response to management change could have increased PAW in the cultivated land.

A greater MBC in cultivated land could further support our hypothetical explanation for higher volume of smaller pores in IC (Table 1). Even in coarse-textured soils, microorganisms can influence the formation aggregates and stabilization of structure (Six et al., 2004) provided that microbes inhabit the pore space between microaggregates (20-250 µm size) (Chenu, 1989). It seems plausible that a facilitation of increased microaggregation mediated by microbial activity in combination with small pores derived from soil compaction resulted in higher PAW and higher water content at field capacity in our cultivated land soil. Daynes et al. (2013) also

showed the PAW increased in the presence of living plant roots and soil microbes because of maximization in the distribution of relatively finer pores that are capable of holding water available for vegetation.

The S-index value is a promising indicator of soil physical quality. It is well established that an S-index ≥ 0.05 indicates “very good” soil physical or structural quality, and $0.035 \leq$ S-index < 0.050 indicates “good physical quality” (Dexter, 2004; Tormena et al., 2008). Our S-index results showed good to very good soil structural quality ($0.031 \leq$ S-index ≤ 0.197) for native grasslands (Table 1). On the other hand, it has been documented that well-sorted loamy sand texture as found in our field sites is typically associated with a narrow pore-size distribution, lack of inter-aggregate spaces, and a low accumulation of organic C (relative to fine and medium textured soils) (Reynolds et al., 2009). As a result, the soil water release curve in grassland is very steep at its inflection point (n was 1.5 times higher in NG). As also concluded by Dexter et al (2008), large S-index values for soils exhibiting no continuous pore networks (e.g., well-graded sands and sandstones) mainly reflect soil matrix attributes rather than soil structural characteristics. Consequently, it appears that S-index should be interpreted cautiously, and in conjunction with other indicators, when attempting to quantify the physical quality of rigid to moderately expansive soils (Reynolds et al., 2009). Additionally, it is noteworthy that although our NG soil has higher S-index compared to the IC soils, microbial biomass carbon was substantially lower in NG soils (Table 1). Kiani et al. (2016b) also reported the same trend in long-term cropping systems, concluding that specific beneficial soil functions (such nutrient cycling vs. water availability vs. structure development) can be influenced in different directions by same land managements; this finding emphasizes the importance of integrally assessing

several soil quality indicators simultaneously for inferring multiple soil functions and the status of ecosystem services and soil quality in land-use systems.

Our native grassland soil was characterized by the presence of Gram-negative bacteria, actinobacteria, and anaerobic bacteria as main biomarkers (Table 5). Steenwerth et al. (2002) also indicated Gram-negative bacteria and 16:1 2OH as unique biomarkers of grazed perennial grassland. They reported greater abundance of Gram-positive (i17:1) in cultivated sites than in perennial grasslands which is also consistent with our findings (data not shown). It seems that converting the native grassland to cultivated land decreased the relative abundance of Gram-negative bacteria, while increasing the proportion of Gram-positive bacteria. These results are consistent with Geisseler et al (2016) who also reported higher Gram-negative bacteria in natural grassland and higher Gram-positive bacteria in cropland.

Differences in microbial community structure between grassland and cultivated land are most likely related to variations in the quantity and quality of carbon substrates being supplied to the soil (Khalili et al., 2016; Grayston et al., 2004). The grassland and cultivated land have differences in plant community composition that are likely to exert strong selective pressures on the soil microbial community. Soil microbial biomass carbon was also significantly higher in the cultivated land than the native grassland (Table 1). Khalili et al. (2016) reported that total microbial biomass was significantly greater in grasslands than shrublands. In general, different vegetation types may result in differences in soil aeration, soil moisture and the quality of resources available to microbes. Grazing and associated manure and urine addition may also impact the large abundance of MBC in cultivated land. Our study extends the existing literature by documenting clear differences in soil pore water interactions and microbial functions across competing land uses types.

5.2. Gaussian model fits better for PAW, SOC, and MBC variographies.

Autocorrelation range values of measured soil properties assessed at 5–10 cm soil layer varied between the two sites (Table 4). Focusing on results from OK approach, the autocorrelation range values for SOC concentration and PAW were generally higher for cultivated land soil and both variables had lower CV in cultivated land as well (Table 4). A similar observation was also reported by Wang et al (2009) for soil total nitrogen when they compared the spatial patterns of STN under farmland and grassland systems at a watershed scale. In our results, this trend was reverse for MBC as its autocorrelation range was longer in native grassland, and the goodness of fit (r^2) for semivariogram model was very low for NG (< 0.1). Variability in range values could arise from features such as landscape position and history of management (Webster, 1985).

The OK approach revealed that PAW, SOC concentration, and MBC were strongly spatially dependent in cultivated land (nugget ratio $< 18\%$; Table 4) entailing that predictable field segments can capture a significant proportion of the spatial variability (Duffera et al., 2007). These soil properties were less spatially dependence in native grassland (Table 4). Glendell et al (2014) also found a stronger degree of spatial dependence of total carbon and C:N ratio in agricultural land ($< 24\%$) than in grasslands (37 to 71%). The stronger degree of spatial dependence and longer auto-correlation range in cultivated lands indicates a homogenization of the spatial variability of soil properties (Glendell et al., 2014; Li et al., 2010; Qiu et al., 2016). This effect could be a result of intensive, long term agricultural activities such as tillage, irrigation, fertilization, and harvest which were applied uniformly across this field.

Spatial structures varied across the assessed parameters. Of the three key soil properties of our interest (i.e., PAW, SOC, and MBC), SOC exhibited the strongest spatial dependency at

both field sampling sites (Table 4). Such strong spatial dependency may be controlled by the variations in both intrinsic and extrinsic factors such as heterogeneity of soil development, soil texture, type of vegetation, land use and management (Cambardella et al., 1994; Stutter et al., 2004; Qiu et al., 2016). In our study, spatial dependence was more likely associated with the differences in land use management and vegetation. A similar inference was also reported by Nyamadzawo et al. (2008) as they found that the strong spatial dependency of total carbon concentration was associated with the land management and vegetation in their reclaimed minesoils seeded to grass and trees.

In general, the best fitted model option for PAW, SOC concentration, and MBC was Gaussian model based on the output with lower RSS and higher R^2 (Table 4). In our study, the type of optimal theoretical models did not differ between the grassland and the cultivated land except for SOC concentration in the cultivated land for which the spherical model had better fitting outcome. Glendell et al (2014) reported spherical model as the best fit for soil total carbon for both agricultural land and grassland. Other studies also showed that spherical model fits better when conducting SOC concentration variography (Cambardella et al., 1994; Glendell et al., 2014; Nyamadzawo et al., 2008; Wang et al., 2013).

5.3. Co-kriging approach enhances spatial predictions.

In our study, we systematically explored several geostatistical methods to provide a detailed spatial-resolution prediction and visualization of PAW, SOC concentration, and MBC in soils of native grasslands and the cultivated lands. Comparison of R, OK, RK, coK and RcoK approaches based on their R^2 and standard error of prediction indicated that coK method had the best performance, demonstrating a profound improvement in the accuracy of spatial estimations of SOC concentration and MBC when DTW was incorporated as a covariate (Table 4). Soil

moisture availability directly impacts the activity of microorganisms in a way that their activity decreases as the soil becomes dry (Curtin et al., 2012). With regards to SOC, previous studies also showed a significant positive relationship between water availability and SOC (Kiani et al., 2016b). Water availability could increase the production of plant biomass and residues that can be incorporated into the soil and feedback in the long-term into additional organic carbon accrual. Furthermore, when focusing on PAW, the coK method had also the best performance among the evaluated approaches when terrain slope and elevation were the selected covariates for native grassland and cultivated land, respectively. The MPE also showed that bias estimation was considerably reduced when the coK was applied for spatial prediction (Table 4). Our results are consistent with earlier reports showing a clear advantage of coK over ordinary kriging for predicting spatial variation of SOC stock (Ceddia et al., 2015), saturated hydraulic conductivity (Motaghian and Mohammadi, 2011), and topsoil gravel and subsoil clay (Odeh et al., 1995). Furthermore, the low correlation values ($\rho < 0.2$) between the predicted standard deviations derived from coK method and the terrain covariates shows that the remaining spatial uncertainties of PAW, SOC concentration, and MBC are very unrelated to characteristics of the landscapes at both sites (Table 3). This unique finding can reinforce the notion that other key determinant factors different than topography such as vegetation type, parent material and management system are also main underlying causes for our observed spatial variability patterns.

At our sites, PAW, SOC concentration, and MBC were not only strongly spatially dependent but they had also autocorrelation ranges exceeding 70 m based on the coK approach, which can indicate spatial relatedness that can bridge several separated segments across larger landscapes. Such relatively large autocorrelation range values encompassing several spatial

segments or map units can suggest that these soils are related to one another by their similar landscape positions or landforms on the wider terrain (Cambardella et al., 1994).

Graphic visualization of the mean and uncertainty for predicted values across our field sites provides opportunities to identify spatial patterns and to conduct comparisons amongst geostatistical approaches (Hengl et al., 2004). Overall, our mean maps for selected soil properties (PAW, SOC concentration, and MBC) showed similarities in estimated values when comparing OK with coK method, and RK with RcoK (data not shown); however, a major difference became evident when contrasting standard deviation maps derived from OK and RK versus those from coK and RcoK (Fig. 6). It is noticeable that the incorporation of covariates substantially reduces the estimated uncertainty of the predictions by about half. In further details, OK and RK uncertainty maps showed abrupt textural changes with sharp increases in predicted standard deviation particularly in field areas distant from our measured points. Conversely, coK and RcoK maps exhibited much lower, coherent uncertainty patterns across the space even in areas away from our measured sampling points. Our study is one of the few available reports evaluating various combinations of regression and kriging or cokriging for modeling the spatial structure of key soil properties at field scale and across competing land-use systems.

Relative to basic OK, both coK and RcoK procedures performed similarly well ($r^2s > 0.7$) and were both capable of greatly improving accuracy and precision of prediction for PAW, SOM, and MBC (Table 4 and Fig. 5 and 6). However, considering the fact that mappers aiming at implementing RcoK will need to physically measure or have access to predictor data layers such as C:N ratio or saturated water content (sat. WC), coK approach appears to be a more reasonable, readily deployable approach. Moreover, our coK estimates at field scale were based on terrain attributes derived from LiDAR data which is current available and can effectively

cover extensive areas, whereas RcoK entails access or generation of additional predictor data which can demand abundant resources and time. Overall, these results encourage further development of cokriging models in conjunction with rigorous selection of effective terrain covariates.

If there would have been no covariates available for our study sites, OK would be the more accurate method for native grassland, whereas RK for cultivated land, based on their relatively lower RMSPE results (Table 4). Eldeiry and Garcia (2010) reported that OK performed better than RK for generating accurate soil salinity maps when applied to LANDSAT images. They concluded that the better performance of OK over RK may be attributed to the fact that autocorrelation among soil salinity data are higher than cross correlation between soil salinity and the LANDSAT bands. On the other hand, other studies found that RK was a more suitable method than OK for accurately mapping the spatial distribution of soil properties such as soil organic matter (Mirzaee et al., 2016), subsoil clay and topsoil gravel (Odeh et al., 1995). This is plausible because the regression predictors in these studies accounted for substantial proportion of soil properties variability in the spatial models (Hengl et al., 2004; Hernández-Stefanoni et al., 2011). However, we detected no advantage of RK over OK under all scenarios in our study. These inconsistencies across existing studies may be driven by the nature and spatial scale of the selected regression predictors; for example, higher performance of RK has been reported when predictor data were extracted from satellite images at relatively coarse spatial resolution (Hengl et al., 2004; Mirzaee et al., 2016; Odeh et al., 1995).

Our geostatistical analyses suggest that the regression component per se had not much contribution in reducing mapping uncertainty based on the spatial context of our study (Table 4). Moreover, we can infer that the prediction improvement derived from using RcoK was mostly

due to the contributing effect of terrain covariates at high spatial resolution [i.e., $2\text{ m} \times 2\text{ m}$ cell, and 30 cm accuracy for ground elevation (Fig. 4)]. In general, the combination of specific terrain covariates with kriging techniques provided an enhanced ability for incorporating ancillary information into predictive soil mapping. It is suggested to undertake additional validation of our findings in new, independent field sites; such efforts will evaluate the robustness and usefulness of our derived spatial models over comparable landscapes and leading to the optimization of these predictive mapping tools.

5.4. Optimization of field sampling designs

Our intensive field measurements were used to derive guidelines for improving future sampling designs. As predictable, the minimum sample sizes required to detect certain confident interval increased with increasing targeted mean value accuracy (Table 1) (Fóti et al., 2014; Herbst et al., 2009). Our sampling size ($n= 56$) was adequate for quantifying SOC and MBC at 90% confidence interval in native grasslands; about 50 samples are required as a minimum size for detecting mean differences of 10% in these properties in this land-use system. For PAW in NG, desirable precision of estimations will required a much larger sample size. By contrast, at our cultivated land site, suitable sample sizes for identifying mean differences of 10% were just 33 for SOC, as high as 145 for MBC, and up to 230 for PAW. Conversely, after studying a topographically-uniform annual cropland in New Zealand, Qiu et al. (2016) reported a much lower minimum sample size for their SOC measurements where 11 samples were needed to achieve a 95% confidence interval. These contrasting results highlight the compound impact of landscape heterogeneity on increasing sampling requirements for attaining precise quantification of soil properties. Amongst the soil properties assessed in our study, the largest minimum sample size requirements were estimated for saturated hydraulic conductivity, followed by PAW, and

MBC which is in part driven by the inherently ample spatial variability of these properties. As a recommendation when designing an efficient collection of independent soil samples in future field samplings, distances between the closest sampling locations should be larger than our autocorrelation ranges (Table 4).

6. Conclusion

This study examined several geostatistical methods for capturing and predicting field spatial variability of PAW, SOC concentration, and MBC. Our results showed that combining kriging with selected terrain covariates (coK) accounted for 74 to up to 94% of the variation for PAW, SOC concentration, and MBC in particular when incorporating DTW, elevation, or slope as contributing covariates. Moreover, analysis of accuracy also supported the usefulness of integrating such high spatial-resolution topographic information derived from remote sensing into geostatistical coK and RcoK methods as these approaches resulted in profound improvements of prediction ability compared to OK and RK methods.

Gaussian was established as the more effective variographic model across most of our datasets. The cultivated land (IC) emerged with stronger degrees of spatial dependence and longer auto-correlation range perhaps suggesting a homogenization or smoothing of the spatial variability of soil properties as a result of intensive agricultural activities which have been repeated in the long term under this land use system. Conversion of native grassland to cultivated lands also altered detrimentally the soil structural characteristics through substantially lowering macroporosity, saturated water content, and S-index, and reducing in half the hydraulic conductivity under unsaturated conditions. This land use conversion also appears to decrease the relative abundance of Gram-negative bacteria, while increasing MBC concentration and the proportion of Gram-positive bacteria. Overall, identification of spatial patterns of soil properties in agricultural lands provides holistic visualization tools to land owners for implementing and improving management practices which will eventually lead to more sustainable production. Such knowledge will also underpin the design of multi-functional landscapes that account for and target areas of greater intensity and convergence “hot spots” of diverse ecosystem services.

There is a need to continue developing explicit spatial upscaling information of specific soil properties that are linked to key ecosystem functions under a broader variety of land-use systems, at other soil depths than in our study, and in fine-textured soils.

7. Acknowledgement

This project was jointly supported by our funding partners Alberta Livestock and Meat Agency (ALMA) Sustainability, and Rangeland Research Institute (RRI) University of Alberta. The authors acknowledge Germar Lohstraeter (Alberta Agriculture & Forestry), Don Armitage (Mattheis Research Ranch) and Jela Burkus for the technical support to perform this study. The authors also wish to thank Lewis Fausak, Karin Lindquist, and Kris Guenette for their assistance during field sampling at the Mattheis sites and laboratory analyses.

8. References

- AGRASID. Agricultural Region of Alberta Soil Inventory Database. 2015.
URL:[http://www1.agric.gov.ab.ca/\\$department/deptdocs.nsf/all/sag3249](http://www1.agric.gov.ab.ca/$department/deptdocs.nsf/all/sag3249).
- Bogaert, P., Russo, D., 1999. Optimal spatial sampling design for the estimation of the variogram based on a least squares approach. *Water Resour Res.* 4, 1275–1289.
- Cambardella, C. a., Moorman, T.B., Parkin, T.B., Karlen, D.L., Novak, J.M., Turco, R.F., Konopka, a. E., 1994. Field-Scale Variability of Soil Properties in Central Iowa Soils. *Soil Sci. Soc. Am. J.* 58, 1501. doi:10.2136/sssaj1994.03615995005800050033x
- Ceddia, M.B., Villela, A.L.O., Pinheiro, T.F.M., Wendroth, O., 2015. Spatial variability of soil carbon stock in the Urucu river basin, Central Amazon-Brazil. *Sci. Total Environ.* 526, 58–69. doi:10.1016/j.scitotenv.2015.03.121
- Chenu, C., 1989. Influence of a fungal polysaccharide, scleroglucan, on clay microstructures. *Soil Biol. Biochem.* 21, 299–305. doi:10.1016/0038-0717(89)90108-9
- Curtin, D., Beare, M.H., Hernandez-Ramirez, G., 2012. Temperature and Moisture Effects on Microbial Biomass and Soil Organic Matter Mineralization. *Soil Sci. Soc. Am. J.* 0, 0. doi:10.2136/sssaj2012.0011
- Davis, J.C., 2002. *Statistics and Data Analysis in Geology* (3rd ed.), John Wiley and Sons, New York, p. 638.
- Daynes, C.N., Field, D.J., Saleeba, J.A., Cole, M.A., McGee, P.A., 2013. Development and stabilisation of soil structure via interactions between organic matter, arbuscular mycorrhizal fungi and plant roots. *Soil Biol. Biochem.* 57, 683–694. doi:10.1016/j.soilbio.2012.09.020
- Dexter, a R., 2004. Soil physical quality Part I. Theory, effects of soil texture, density, and organic mailer, and effects on root growth. *Geoderma* 120, 201–214. doi:10.1016/j.geodermaa.2003.09.005
- Dexter, A.R., Czyz, E.A., Richard, G., Reszkowska, A., 2008. A user-friendly water retention function that takes account of the textural and structural pore spaces in soil. *Geoderma* 143, 243–253. doi:10.1016/j.geoderma.2007.11.010

- Drewry, J.J., Cameron, K.C., Buchan, G.D., 2008. Pasture yield and soil physical property responses to soil compaction from treading and grazing - A review. *Aust. J. Soil Res.* 46, 237–256. doi:10.1071/SR07125
- Duffera, M., White, J.G., Weisz, R., 2007. Spatial variability of Southeastern U.S. Coastal Plain soil physical properties: Implications for site-specific management. *Geoderma* 137, 327–339. doi:10.1016/j.geoderma.2006.08.018
- Eldeiry, A. a., Garcia, L. a., 2010. Comparison of Ordinary Kriging, Regression Kriging, and Cokriging Techniques to Estimate Soil Salinity Using LANDSAT Images. *J. Irrig. Drain. Eng.* 136, 355–364. doi:10.1061/(ASCE)IR.1943-4774.0000208
- Fóti, S., Balogh, J., Nagy, Z., Herbst, M., Pintér, K., Péli, E., Koncz, P. and Bartha, S., 2014. Soil moisture induced changes on fine-scale spatial pattern of soil respiration in a semi-arid sandy grassland. *Geoderma* 213, 245–254. doi:10.1016/j.geoderma.2013.08.009
- Fortin, M., Payette, S., 2002. How to test the significance of the relation between spatially autocorrelated data at the landscape scale: a case study using fire and forest maps. *Ecoscience* 9, 213–218. doi:10.1111/j.1538-4632.2009.00766.x
- Gatziolis, D., Andersen, H.E., 2008. A Guide to LIDAR Data Acquisition and Processing for the Forests of the Pacific Northwest. Gen. Tech. Rep. PNW-GTR-768 1–40. doi:Gen. Tech. Rep. PNW-GTR-768
- Geisseler, D., Lazicki, P.A., Scow, K.M., 2016. Mineral nitrogen input decreases microbial biomass in soils under grasslands but not annual crops. *Appl. Soil Ecol.* 106, 1–10. doi:10.1016/j.apsoil.2016.04.015
- Glendell, M., Granger, S.J., Bol, R., Brazier, R.E., 2014. Quantifying the spatial variability of soil physical and chemical properties in relation to mitigation of diffuse water pollution. *Geoderma* 214-215, 25–41. doi:10.1016/j.geoderma.2013.10.008
- Grayston, S.J., Campbell, C.D., Bardgett, R.D., Mawdsley, J.L., Clegg, C.D., Ritz, K., Griffiths, B.S., Rodwell, J.S., Edwards, S.J., Davies, W.J. and Elston, D.J., 2004. Assessing shifts in microbial community structure across a range of grasslands of differing management intensity using CLPP, PLFA and community DNA techniques. *Applied Soil Ecology*, 25, 63–84.

- Griffith, D. a, Griffith, D. a, 2013. Establishing Qualitative Geographic Sample Size in the Presence of Spatial Autocorrelation Establishing Qualitative Geographic Sample Size in the Presence of Spatial Autocorrelation 5608, 37–41. doi:10.1080/00045608.2013.776884
- Hannam, K. D., Quideau, S. A., Kishchuk, B. E., 2006. Forest floor microbial communities in relation to stand composition and timber harvesting in northern Alberta. *Soil Biology and Biochemistry*, 38, 2565- 2575.
- Hengl, T., Heuvelink, G.B.M., Rossiter, D.G., 2007. About regression-kriging: From equations to case studies. *Comput. Geosci.* 33, 1301–1315. doi:10.1016/j.cageo.2007.05.001
- Hengl, T., Heuvelink, G.B.M., Stein, A., 2004. A generic framework for spatial prediction of soil variables based on regression-kriging. *Geoderma* 120, 75–93. doi:10.1016/j.geoderma.2003.08.018
- Herbst, M., Prolingheuer, N., Graf, a., Huisman, J. a., Weihermüller, L., Vanderborght, J., 2009. Characterization and Understanding of Bare Soil Respiration Spatial Variability at Plot Scale. *Vadose Zo. J.* 8, 762. doi:10.2136/vzj2008.0068
- Hernández-Stefanoni, J.L., Alberto Gallardo-Cruz, J., Meave, J.A., Dupuy, J.M., 2011. Combining geostatistical models and remotely sensed data to improve tropical tree richness mapping. *Ecol. Indic.* 11, 1046–1056. doi:10.1016/j.ecolind.2010.11.003
- Heuvelink, G.B.M., Kros, J., Reinds, G.J., De Vries, W., 2016. Geostatistical prediction and simulation of European soil property maps. *Geoderma Reg.* 7, 201–215. doi:10.1016/j.geodrs.2016.04.002
- Hewins, D.B., Broadbent, T., Carlyle, C.N., Bork, E.W., 2016. Extracellular enzyme activity response to defoliation and water addition in two ecosites of the mixed grass prairie. *Agric. Ecosyst. Environ.* 230, 79–86. doi:10.1016/j.agee.2016.05.033
- Hudelson, B.D., Clayton, M.K., 2015. Confidence Intervals for Autocorrelations Based on Cyclic Samples 90, 753–757.
- Khalili, B., Ogunseitan, O.A., Goulden, M.L., Allison, S.D., 2016. Interactive effects of precipitation manipulation

- and nitrogen addition on soil properties in California grassland and shrubland. *Appl. Soil Ecol.* 107, 144–153.
doi:10.1016/j.apsoil.2016.05.018
- Kiani, M., Hernandez-Ramirez, G., Quideau, S., Smith, E., Janzen, H., Larney, F., Puurveen, D., 2016b. Quantifying the sensitive soil quality indicators across contrasting long-term land management systems: crop rotations and nutrient Regimes
- Knotters, M., Brus, D.J., Voshaar, J.H.O., 1995. a Comparison of Kriging, Co-Kriging and Kriging Combined With Regression for Spatial Interpolation of Horizon Depth With Censored Observations. *Geoderma* 67, 227–246.
doi:10.1016/0016-7061(95)00011-c
- Lark, R.M., 2002. Optimized spatial sampling of soil for estimation of the variogram by maximum likelihood. *Geoderma* 105, 49–80. doi:10.1016/S0016-7061(01)00092-1
- Li, J., Richter, D. deB, Mendoza, A., Heine, P., 2010. Effects of land-use history on soil spatial heterogeneity of macro- and trace elements in the Southern Piedmont USA. *Geoderma* 156, 60–73.
doi:10.1016/j.geoderma.2010.01.008
- Li, Y., 2010. Can the spatial prediction of soil organic matter contents at various sampling scales be improved by using regression kriging with auxiliary information? *Geoderma* 159, 63–75.
doi:10.1016/j.geoderma.2010.06.017
- Liu, D., Wang, Z., Zhang, B., Song, K., Li, X., Li, J., Li, F., Duan, H., 2006. Spatial distribution of soil organic carbon and analysis of related factors in croplands of the black soil region, Northeast China. *Agric. Ecosyst. Environ.* 113, 73–81. doi:10.1016/j.agee.2005.09.006
- Liu, Z.-P., Shao, M.-A., Wang, Y.-Q., 2013. Spatial patterns of soil total nitrogen and soil total phosphorus across the entire Loess Plateau region of China. *Geoderma* 197-198, 67–78. doi:10.1016/j.geoderma.2012.12.011
- Lowenberg-DeBoer, J., Swinton, S.M., 1997. Economics of site-specific management in agronomic crops. state site-specific Manag. *Agric.* 369–396.
- Mclean, E.O., 1982. Soil pH and lime requirement. *Methods Soil Anal.* 9, 595– 624.

doi:10.2134/agronmonogr9.2.2ed.c12

Metcalfe, D., Meir, P., Aragao, L.E.O., da Costa, A., Almeida, S., Braga, A., Gonçalves, P., Athaydes, J., Malhi, Y. and Williams, M., 2008. Sample sizes for estimating key ecosystem characteristics in a tropical terra firme rainforest. *For. Ecol. Manage.* 255, 558–566. doi:10.1016/j.foreco.2007.09.026

Mirzaee, S., Ghorbani-Dashtaki, S., Mohammadi, J., Asadi, H., Asadzadeh, F., 2016. Spatial variability of soil organic matter using remote sensing data. *Catena* 145, 118–127. doi:10.1016/j.catena.2016.05.023

Mollard, F.P.O., Naeth, M.A., Cohen-Fernandez, A., 2014. Impacts of mulch on prairie seedling establishment: Facilitative to inhibitory effects. *Ecol. Eng.* 64, 377–384. doi:10.1016/j.ecoleng.2014.01.012

Murphy, P.N., Ogilvie, J., Meng, F.R., White, B., Bhatti, J.S. and Arp, P.A., 2011. Modelling and mapping topographic variations in forest soils at high resolution: A case study. *Ecological Modelling* 222(14),2314–2332.

Motaghian, H.R., Mohammadi, J., 2011. Spatial estimation of saturated hydraulic conductivity from terrain attributes using regression, kriging, and artificial neural networks. *Pedosphere* 21, 170–177. doi:10.1016/S1002-0160(11)60115-X

Odeh, I.O.A., McBratney, A.B., Chittleborough, D.J., 1995. Further results on prediction of soil properties from terrain attributes: heterotopic cokriging and regression-kriging. *Geoderma* 67, 215–226. doi:10.1016/0016-7061(95)00007-B

Orr, C.H., Predick, K.I., Stanley, E.H., Rogers, K.L., 2014. Spatial autocorrelation of denitrification in a restored and a natural floodplain. *Wetlands* 34, 89–100. doi:10.1007/s13157-013-0488-8

Pagliai, M., Vignozzi, N., Pellegrini, S., 2004. Soil structure and the effect of management practices. *Soil Tillage Res.* 79, 131–143. doi:10.1016/j.still.2004.07.002

Qiu, W, Curtin, D., Johnstone, P., Beare, M., Hernandez-Ramirez G. (2016): Small-Scale Spatial Variability of Plant Nutrients and Soil Organic Matter: an Arable Cropping Case Study, *Communications in Soil Science and Plant Analysis* <http://dx.doi.org/10.1080/00103624.2016.1228945>

- Reynolds, W.D., Drury, C.F., Tan, C.S., Fox, C.A., Yang, X.M., 2009. Use of indicators and pore volume-function characteristics to quantify soil physical quality. *Geoderma* 152, 252–263. doi:10.1016/j.geoderma.2009.06.009
- Robertson, G.P., Crum, J.R., Ellis, B.G., 1993. The spatial variability of soil resources following long-term disturbance. *Oecologia* 96, 451–456. doi:10.1007/BF00320501
- Schelle, H., Heise, L., Jänicke, K., Durner, W., 2013. Water retention characteristics of soils over the whole moisture range: A comparison of laboratory methods. *Eur. J. Soil Sci.* 64, 814–821. doi:10.1111/ejss.12108
- Schindler, U., Durner, W., von Unold, G., Muller, L., 2010. Evaporation Method for Measuring Unsaturated Hydraulic Properties of Soils: Extending the Measurement Range. *Soil Sci Soc Am J* 74, 1071–1083. doi:10.2136/sssaj2008.0358
- Simbahan, G.C., Dobermann, A., Goovaerts, P., Ping, J., Haddix, M.L., 2006. Fine-resolution mapping of soil organic carbon based on multivariate secondary data. *Geoderma* 132, 471–489. doi:10.1016/j.geoderma.2005.07.001
- Six, J., Bossuyt, H., Degryze, S., Denef, K., 2004. A history of research on the link between (micro)aggregates, soil biota, and soil organic matter dynamics. *Soil Tillage Res.* 79, 7–31. doi:10.1016/j.still.2004.03.008
- Steenwerth, K.L., Jackson, L.E., Calderón, F.J., Stromberg, M.R., Scow, K.M., Caldero, F.J., 2002. Soil microbial community composition and land use history in cultivated and grassland ecosystems of coastal California. *Soil Biol. Biochem.* 34, 1599–1611. doi:10.1016/S0038-0717(02)00144-X
- Stutter, M.I., Deeks, L.K., Billett, M.F., 2004. Spatial Variability in Soil Ion Exchange Chemistry in a Granitic Upland Catchment. *Soil Sci. Soc. Am. J.* 68, 1304. doi:10.2136/sssaj2004.1304
- Su, Z.-Y., Xiong, Y.-M., Zhu, J.-Y., Ye, Y.-C., Ye, M., Zhi-yaol, S.U., Yong-mei, X., Jian-yun, Z.H.U., Yong-chang, Y.E., Mai, Y.E., 2006. Soil Organic Carbon Content and Distribution in a Small Landscape of Dongguan, South China. *Pedosphere* 16, 10–17. doi:10.1016/S1002-0160(06)60020-9
- Tormena, C.A., Silva, Á.P. Da, Imhoff, S.D.C., Dexter, A.R., 2008. Quantification of the soil physical quality of a tropical oxisol using the S index. *Sci. Agric.* 65, 56–60. doi:10.1590/S0103-90162008000100008

- Wang, K., Zhang, C., Li, W., 2013. Predictive mapping of soil total nitrogen at a regional scale: A comparison between geographically weighted regression and cokriging. *Appl. Geogr.* 42, 73–85. doi:10.1016/j.apgeog.2013.04.002
- Wang, Y., Zhang, X., Huang, C., 2009. Spatial variability of soil total nitrogen and soil total phosphorus under different land uses in a small watershed on the Loess Plateau, China. *Geoderma* 150, 141–149. doi:10.1016/j.geoderma.2009.01.021
- Webster, R., 1985. Quantitative Spatial Analysis of Soil in the Field, in: Stewart, B.A. (Ed.), *Advances in Soil Science*. Springer New York, New York, NY, pp. 1–70. doi:10.1007/978-1-4612-5090-6_1

9. Tables and figures

Table 1. Descriptive statistics of soil properties at native grassland (NG) and irrigated cultivated land (IC) and optimal sample sizes at various confidence intervals.

Attributes	Sites	Mean	Median	Min	Max	Kurtosis	Skewness	SD	Optimum sample size			
									D=5%	D=10	D=20	D=40
Bulk density (g cm ⁻³)	NG	1.44 a	1.44	1.14	1.63	-0.30	-0.41	0.11	9	2	1	0
	IC	1.43 a	1.43	1.09	1.65	-0.40	-0.39	0.14	14	4	1	0
Porosity (m ³ m ⁻³)	NG	0.455 a	0.46	0.38	0.57	-0.24	0.42	0.042	13	3	1	0
	IC	0.460 a	0.46	0.38	0.59	-0.37	0.34	0.051	19	5	1	0
Sat. WC (m ³ m ⁻³)	NG	0.474 a	0.47	0.34	0.57	1.81	-0.50	0.041	12	3	1	0
	IC	0.422 b	0.43	0.29	0.56	-0.20	-0.20	0.058	29	7	2	0
θFC (m ³ m ⁻³)	NG	0.118 b	0.11	0.08	0.37	29.85	4.82	0.039	168	42	11	3
	IC	0.154 a	0.14	0.07	0.36	3.89	1.63	0.051	168	42	11	3
θPWP (m ³ m ⁻³)	NG	0.094 a	0.10	0.00	0.16	5.18	-1.07	0.023	94	23	6	1
	IC	0.085 a	0.08	0.01	0.17	0.04	0.57	0.034	249	62	16	4
PAW (m ³ m ⁻³)	NG	0.024 b	0.01	0.00	0.21	12.09	3.08	0.035	3431	858	214	54
	IC	0.069 a	0.05	0.01	0.27	1.95	1.25	0.053	921	230	58	14
Macroporosity (m ³ m ⁻³)	NG	0.355 a	0.36	0.20	0.44	3.78	-1.36	0.044	23	6	1	0
	IC	0.268 b	0.27	0.14	0.45	2.59	0.20	0.075	121	30	8	2
α (hPa ⁻¹)	NG	0.020 b	0.02	0.01	0.02	2.81	1.29	0.002	14	4	1	0
	IC	0.024 a	0.02	0.01	0.07	6.17	1.98	0.011	339	85	21	5
n	NG	3.04 a	3.06	1.22	4.72	-0.22	0.08	0.77	99	25	6	2
	IC	1.97 b	1.97	1.24	3.16	-0.54	0.37	0.48	91	23	6	1
θ _r (m ³ m ⁻³)	NG	0.091 a	0.10	0.00	0.14	5.12	-1.90	0.025	120	30	7	2
	IC	0.072 b	0.07	0.00	0.17	-0.77	0.20	0.046	625	156	39	10
θ _s (m ³ m ⁻³)	NG	0.468 a	0.47	0.34	0.56	1.62	-0.62	0.041	12	3	1	0
	IC	0.427 b	0.44	0.30	0.53	-0.29	-0.30	0.053	24	6	1	0
S-index	NG	0.106 a	0.106	0.031	0.197	0.82	0.37	0.031	133	33	8	2
	IC	0.055 b	0.054	0.023	0.099	-0.84	0.26	0.019	190	47	12	3
Ks (cm d ⁻¹)	NG	6.70 a	3.68	0.46	52.20	13.81	3.36	8.75	2623	656	164	41
	IC	8.36 a	2.39	0.30	120.20	24.92	4.64	18.60	7607	1902	475	119
Unsat. K (cm d ⁻¹)	NG	0.18 a	0.19	0.05	0.35	0.29	0.14	0.06	153	38	10	2
	IC	0.08 b	0.03	0.00	0.40	2.50	1.85	0.10	2710	677	169	42
SOC concentration (% m/m)	NG	1.05 a	0.97	0.66	3.13	19.42	3.75	0.36	182	46	11	3
	IC	1.09 a	1.03	0.70	2.65	10.11	2.56	0.32	131	33	8	2
SOC density (g m ⁻² soil)	NG	748 a	698	497	1878	12.17	2.94	220	133	33	8	2
	IC	779 a	737	473	1961	15.21	2.7	242	148	37	9	2
STN (% m/m)	NG	0.09 b	0.08	0.05	0.28	9.68	2.51	0.04	248	62	15	4
	IC	0.11 a	0.10	0.06	0.24	7.92	2.13	0.03	109	27	7	2
C:N	NG	11.47 a	11.85	9.17	14.20	-1.18	0.05	1.36	22	5	1	0
	IC	10.15 b	9.91	8.18	13.50	0.90	1.10	1.22	22	6	1	0
pH	NG	5.97 a	5.94	5.08	7.42	3.23	0.89	0.37	6	1	0	0
	IC	6.03 a	6.02	5.18	6.86	-0.38	-0.17	0.40	7	2	0	0
MBC (nmol g ⁻¹ soil)	NG	601 b	527	178	1223	0.91	1.01	212	201	50	13	3
	IC	812 a	621	268	2388	2.05	1.49	481	578	145	36	9
Elevation (m)	NG	722.0	721.9	720.6	723.2	-0.88	-0.04	0.5	0	0	0	0
	IC	723.1	723.1	722.5	724.0	-0.19	0.20	0.3	0	0	0	0
Curvature (m ⁻¹)	NG	0.01	0.00	-14.0	31.75	13.52	1.24	2.54	>	> 1000	> 1000	> 1000
	IC	0.01	0.00	-6.5	8.75	0.61	0.16	1.87	>	> 1000	> 1000	> 1000
Slope (°)	NG	2	1	0	8	3.66	1.71	1.1	770	193	48	12
	IC	1	1	0	4	3.71	1.54	0.6	714	178	45	11
Aspect (°)	NG	155	131	0	360	-1.04	0.41	100	648	162	41	10
	IC	177	167	0	360	-1.14	0.12	100	492	123	31	8
Hill shade (°)	NG	179	179	161	194	1.66	-0.34	4	1	0	0	0
	IC	180	179	172	191	1.22	0.20	2	0	0	0	0
DTW (m)	NG	1.03	1.02	0.00	2.36	-0.54	0.12	0.46	314	79	20	5
	IC	0.36	0.33	0.00	1.36	1.23	1.03	0.24	679	170	42	11

NG: native grassland; IC: irrigated cultivated land; SD: standard deviation; D: margin of error (as in Eq. [1]); θFC: field capacity water content; θPWP: permanent wilting point water content; PAW: plant available water; θ_s: saturated volumetric water content; θ_r: residual water content; n: a shape parameter related to the curve smoothness; α: a negative inverse of the air entry potential; S-index: the slope at the inflection point; Ks: saturated hydraulic conductivity; Unsat. K: hydraulic conductivity at 10 kPa; SOC: soil organic carbon; STN: soil total nitrogen; C:N: carbon to

nitrogen ratio; MBC: microbial biomass carbon; DTW: depth to water. Number of samples (N) for soil properties is 56 per site, while N for terrain covariates is 7162 in the NG site and 6194 in the IC site.

Table 2. Spearman correlation coefficients (ρ -values) for relationships among selected soil properties at native grassland (NG) and irrigated cultivated land (IC).

Land use and soil property	Porosity	sat. WC	θ FC	θ PWP	α	n	S-index	unsat. K	pH	C:N	SOC concentration	MBC
Native grassland (NG)												
PAW	0.278*	0.362**	0.547**	-0.326*	0.043 n	-0.932**	-0.796**	0.239 n	-0.074 n	-0.391**	0.605**	0.201 n
SOC concentration	0.451**	0.257 n	0.417**	-0.195 n	-0.138 n	-0.622**	-0.585**	0.155 n	0.0349 n	-0.548**	-	0.329*
MBC	0.197 n	0.234 n	0.142 n	0.016 n	-0.010 n	-0.290*	-0.335*	0.106 n	0.120 n	-0.221 n	0.329*	-
Irrigated cultivated land (IC)												
PAW	0.118 n	-0.13 n	0.543**	-0.556**	0.104 n	-0.934**	-0.690**	0.258 n	0.430**	0.417**	0.393**	-0.283*
SOC concentration	0.164 n	0.282*	0.571**	-0.0002 n	-0.166 n	-0.304*	-0.169 n	0.286*	0.019 n	0.491**	-	-0.168 n
MBC	-0.047 n	0.038 n	-0.335*	0.061 n	0.007 n	0.263*	0.182 n	-0.161 n	-0.208 n	-0.447**	-0.168 n	-

* and ** indicate significant correlation at $P < 0.05$ and $P < 0.01$, respectively.

Table 3. Spearman correlation coefficients (ρ -values) for relationships among soil properties of interest and terrain covariates (as derived from Light Detection and Ranging; LiDAR) at native grassland (NG) and irrigated cultivated land (IC).

Attributes	Elevation	Curvature	Slope	Aspect	Hill shade	DTW
<u>Observed values</u>						
Native grassland						
PAW	-0.199 n	-0.278*	-0.345**	0.320*	0.118 n	-0.212 n
SOC concentration	-0.454**	-0.195 n	-0.216 n	0.131 n	-0.056 n	-0.468**
MBC	-0.053 n	0.052 n	-0.183 n	0.107 n	0.009 n	-0.274*
Irrigated cultivated land						
PAW	-0.547**	0.159 n	0.083 n	0.111 n	0.016 n	0.122 n
SOC concentration	-0.355**	-0.035 n	0.139 n	0.139 n	0.175 n	0.255*
MBC	0.394**	-0.157 n	-0.206 n	0.051 n	0.064 n	-0.476**
<u>Regression residuals</u>						
Native grassland						
PAW	0.196 n	-0.240 n	-0.246 n	0.157 n	0.120 n	0.106 n
SOC concentration	-0.298*	-0.105 n	-0.011 n	-0.098 n	-0.114 n	-0.261*
MBC	-0.027 n	0.068 n	-0.141 n	0.069 n	0.024 n	-0.269*
Irrigated cultivated land						
PAW	-0.443**	0.214 n	0.094 n	0.115 n	-0.072 n	0.108 n
SOC concentration	-0.024 n	0.017 n	0.150 n	0.252 n	0.185 n	0.148 n
MBC	0.168 n	-0.204 n	-0.113 n	0.049 n	0.031 n	-0.295*
<u>Standard deviation of coKriging</u>						
Native grassland						
PAW	-0.006 n	0.001 n	0.008	0.003 n	-0.045**	-0.003 n
SOC concentration	0.036 **	-0.001 n	0.032 **	-0.018 n	-0.001 n	-0.015 n
MBC	-0.003 n	0.003 n	0.015 n	0.005 n	-0.044 **	0.031**
Irrigated cultivated land						
PAW	0.028*	-0.005 n	0.018 n	0.023 n	0.014 n	-0.016 n
SOC concentration	-0.010 n	-0.007 n	0.007 n	-0.013 n	-0.026*	-0.009 n
MBC	0.019 n	-0.003 n	0.006 n	0.19 n	0.003 n	-0.024*

* and ** indicate significant correlation at $P < 0.05$ and $P < 0.01$, respectively.

Table 4. Deterministic and variographic (semivariogram and cross-semivariogram) models, fitting statistical indicators, and resulting validation parameters as a function of five geostatistical approaches in both native grassland (NG) and irrigated cultivated land (IC).

Attributes	Prediction Method	Regression equation; §Predictors; °Covariates	Variography					Validation Parameters			
			Model	Residual SS	r ²	Auto-correlation Range (m)	C0/(C0+C) (%)	R ²	SE predict	MPE	RMSPE
NG											
	R	PAW ^{0.5} = - 0.692 + (1.852 × SOC)	-	-	-	-	-	0.68	1.96	-0.38	2.11
	OK	-	G	116.0	0.70	50	29.4	0.04	1.57	-0.14	3.56
PAW	RK	§SOC	G	2.1×10 ⁻³	0.05	40	26.3	0.68	1.97	-0.17	2.07
	coK	°Slope	G	1.43	0.63	90	18.0	0.85	0.97	-0.02	1.53
	RcoK	SOC *Slope	G	0.32	0.66	79	24.9	0.85	1.33	0.03	1.38
	R	Log ₁₀ (SOC) = -0.192 - (2.055 × S-index) - (20.061 × α) + (0.747 × P) + (0.89 × Sat. WC)	-	-	-	-	-	0.60	0.13	-1.02	1.05
SOC concentration	OK	-	G	0.03	0.43	47	16.0	0.06	0.15	-0.01	0.35
	RK	§S-index, α, P, Sat. WC	G	1.1×10 ⁻³	0.15	60	20.1	0.50	0.19	0.17	0.31
	coK	°DTW	G	2.4×10 ⁻³	0.73	99	9.3	0.92	0.08	-0.01	0.12
	RcoK	(S-index, α, P, Sat. WC) *DTW	G	3.8×10 ⁻⁴	0.67	70	2.6	0.71	0.19	-0.03	0.20
	R	Log ₁₀ (MBC) = 2.573 - (0.0053 × C: N) - (1.179 × S · index) + (0.755 × Sat. WC)	-	-	-	-	-	0.15	66.34	-31.3	196
MBC	OK	-	G	5.4×10 ⁸	0.70	99	41.0	0.11	94.97	-8.41	202
	RK	§C:N, S-index, Sat. WC	G	6.8×10 ⁸	0.56	85	36.8	0.26	105.07	-7.58	181
	coK	°DTW	G	673.0	0.91	113	2.2	0.74	63.47	-4.37	121
	RcoK	(C:N, S-index, Sat. WC) *DTW	G	794.0	0.86	126	1.0	0.80	66.37	-3.52	101
IC											
	R	PAW ^{0.5} = 0.916 + (1.39 × SOC)	-	-	-	-	-	0.20	2.39	-0.77	4.79
	OK	-	G	497.0	0.63	64	13.9	0.40	2.80	-0.40	4.12
PAW	RK	§SOC	G	135.0	0.68	76	35.3	0.29	3.64	-0.14	4.69
	coK	°ELEV	G	0.82	0.72	90	0.1	0.94	1.12	-0.08	1.33
	RcoK	SOC *ELEV	G	1.35	0.58	105	0.1	0.84	1.70	-0.09	2.17
	R	Log ₁₀ (SOC) = -0.149 + (0.0112 * θFC)	-	-	-	-	-	0.26	0.13	-0.03	0.27
SOC concentration	OK	-	S	0.05	0.31	63	0.1	0.74	0.14	0.00	0.16
	RK	§θFC	G	0.03	0.34	67	11.3	0.43	0.22	-0.02	0.25
	coK	*DTW	G	1.05×10 ⁻³	0.20	70	10.1	0.76	0.18	-0.01	0.18
	RcoK	(θFC) *DTW	G	5.3×10 ⁴	0.20	52	1.8	0.67	0.24	-0.01	0.24
	R	Log ₁₀ (MBC) = 3.682 - (0.0844 × C: N)	-	-	-	-	-	0.15	134.43	-97.6	452
MBC	OK	-	G	1.9×10 ¹¹	0.07	35	17.7	0.53	235.00	42.49	330
	RK	§C:N	G	1.1×10 ¹¹	0.34	30	36.2	0.41	270.34	33.22	370
	coK	°DTW	G	1042.0	0.77	80	0.2	0.87	141.74	5.88	184
	RcoK	C:N *DTW	G	777.0	0.74	80	0.3	0.79	168.01	9.76	230

$C_0/(C_0+C)$: nugget to sill ratio; G: gaussian; S: spherical ; R: regression; OK: ordinary kriging; RK: regression-kriging; coK: cokriging; RcoK: regression-cokriging; PAW: plant available water; SOC: soil organic carbon; MBC: microbial biomass carbon; DTW: depth to water; ELEV: elevation; P: porosity; θ_{FC} : field capacity water content; Sat. WC: saturated water content; α : a negative inverse of the air entry potential; S-index: the slope at the inflection point; C:N: carbon to nitrogen ratio. Units for all presented variables are as detailed in Table 1.

Table 5. Distinctive phospholipid fatty acid (PLFA) indicator species analysis associated with whether native grassland (NG) or irrigated cultivated land (IC). Each value represents the mean indicator with standard deviation in parentheses, and the highest indicator value is in bold. Only PLFAs that were found to be significantly different among groups are presented.

PLFA	Taxa biomarker	Indicator Value			Monte Carlo P < 0.05
		Mean	NG	IC	
14:00	Bacteria in general	41.8 (2.65)	53	26	0.0012
15:1 i	Gram -	41.8 (2.62)	50	28	0.0044
17:1 a	Gram -	15.5 (2.86)	31	2	<0.001
17:1ω8c	Gram -	50.4 (0.84)	54	45	<0.001
17:0 10 methyl	Actinobacteria (Gram+)	49.7 (1.31)	53	43	<0.001
16:1 2OH	Anaerobic bacteria	50.3 (1.11)	52	46	0.0226

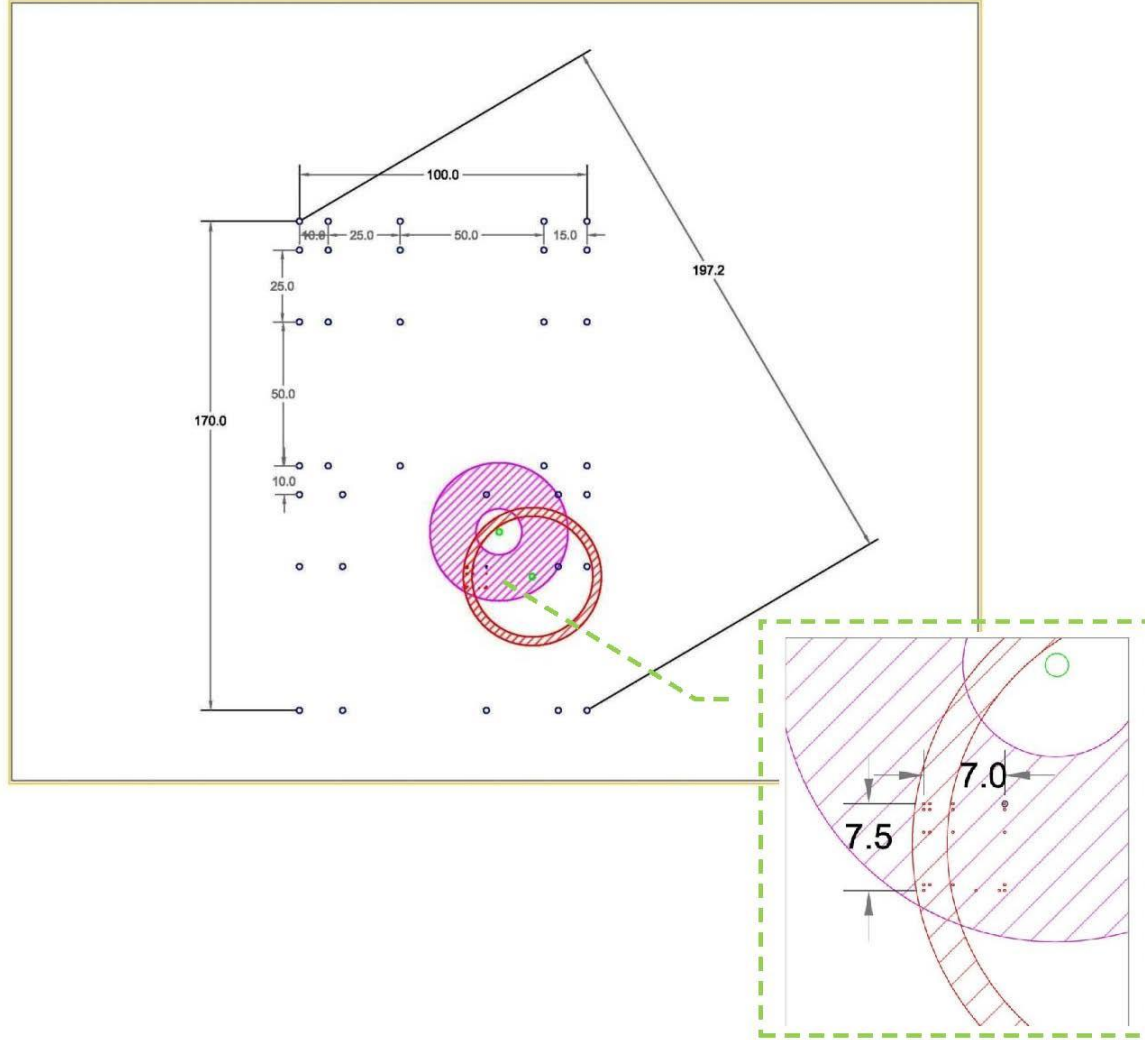


Fig. 1. Nested cyclic sampling design. The sampling intervals were every 10, 35, 85, 100 m for west to east direction and every 10, 35, 85, 95, 120, 170 m for north to south direction ($n = 36$; main panel). A 0.5, 2, 4.5 m cycle was applied in both directions for the smaller scale nest ($n = 20$) as showed in the inset. There are also two additional sampling points (highlighted in green) which were strategically located in the field plots to increase the sampling efficiency.

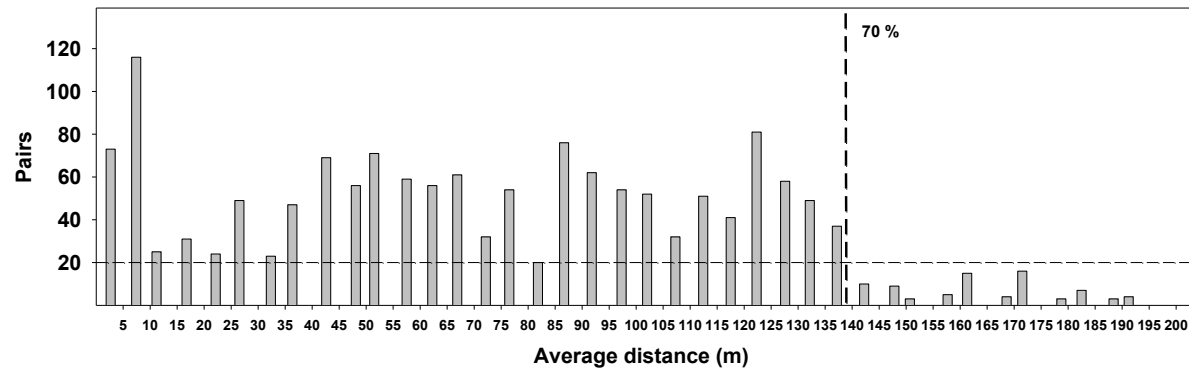


Fig. 2. Number of pairs of measured data points for each lag class assuming a uniform lag class size of 5 m distance interval. The dash line shows the 70% of the total distance which is taken as the maximum allowable active lag distance.

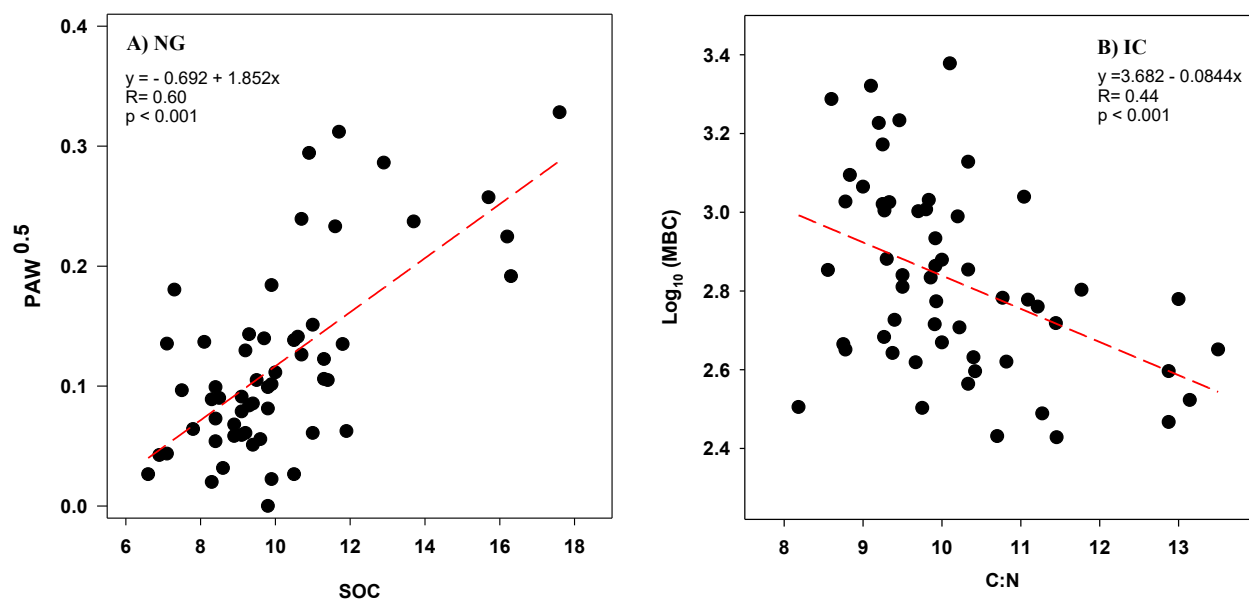


Fig. 3. (A) Square root of plant available water (PAW; $\text{m}^3 \text{m}^{-3}$) versus soil organic carbon concentration (SOC; g C kg^{-1} soil) for native grassland (NG) site, and (B) logarithmic microbial biomass carbon (MBC; nmol g^{-1} soil) versus carbon to nitrogen ratio (C:N; unitless) for irrigated cultivated (IC) site.

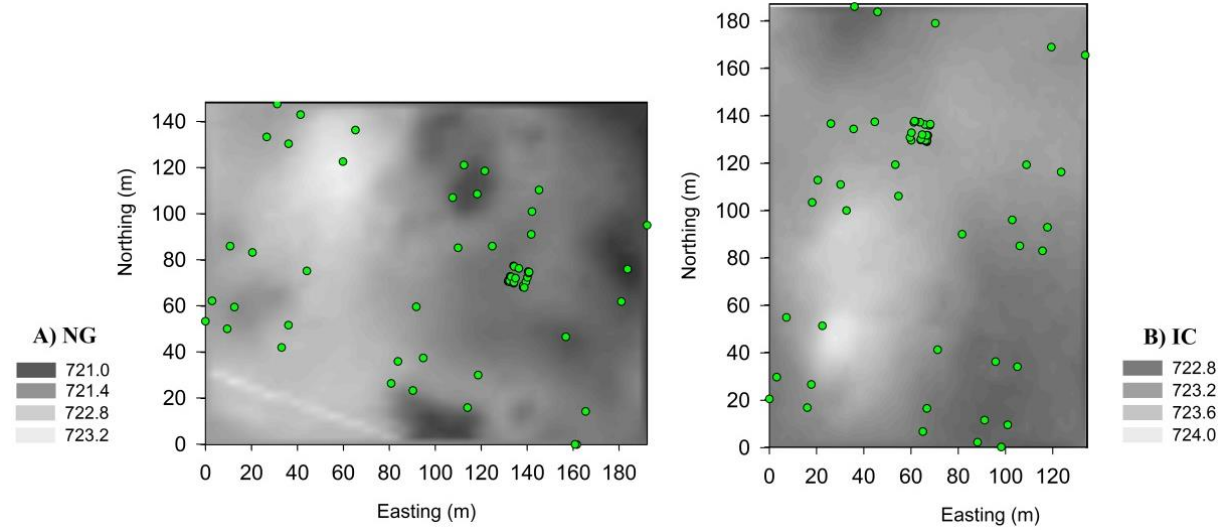


Fig. 4. Terrain elevation derived from airborne LiDAR (Light Detection and Ranging) with vertical accuracy of 30 cm and spatial resolution of 2 m x 2 m [A. native grassland (NG), B. irrigated cultivated land (IC)]. The green dots are the locations of the 56 measured points in each field site. As customary, terrain elevation units are in meters above mean sea level.

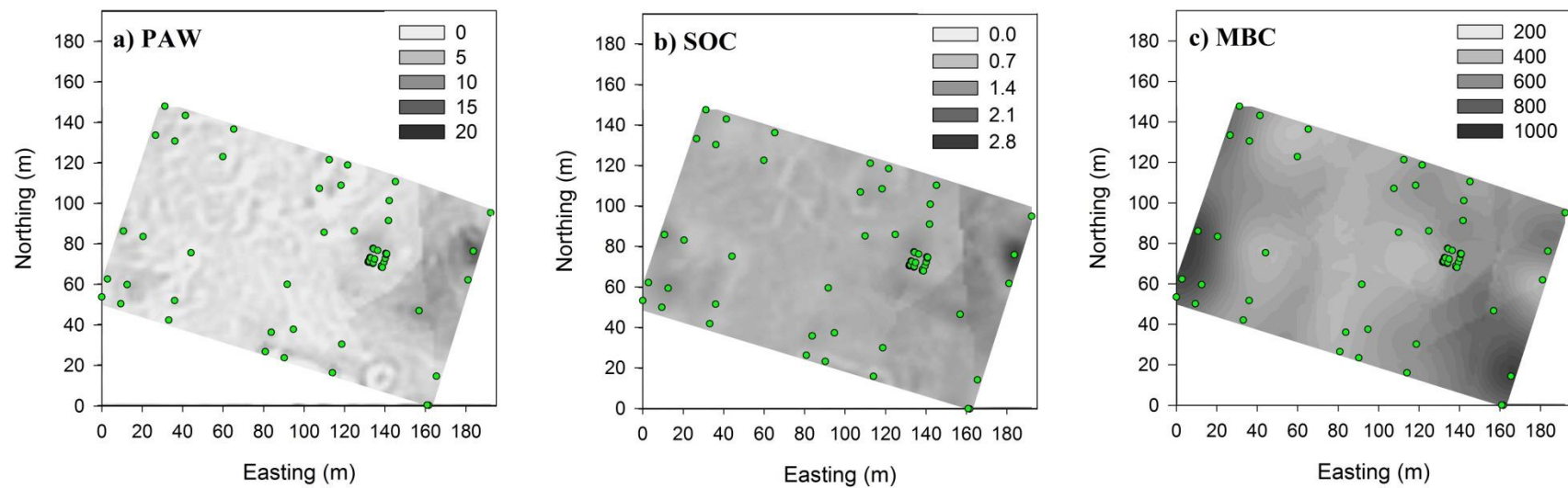


Fig. 5. Mean maps of (a) plant available water (PAW; m³ m⁻³), (b) soil organic carbon concentration (SOC; % m/m), and (c) microbial biomass carbon (MBC; nmol g⁻¹ soil) concentration by cokriging (coK) method in native grassland. The green dots are the locations of 56 measured points.

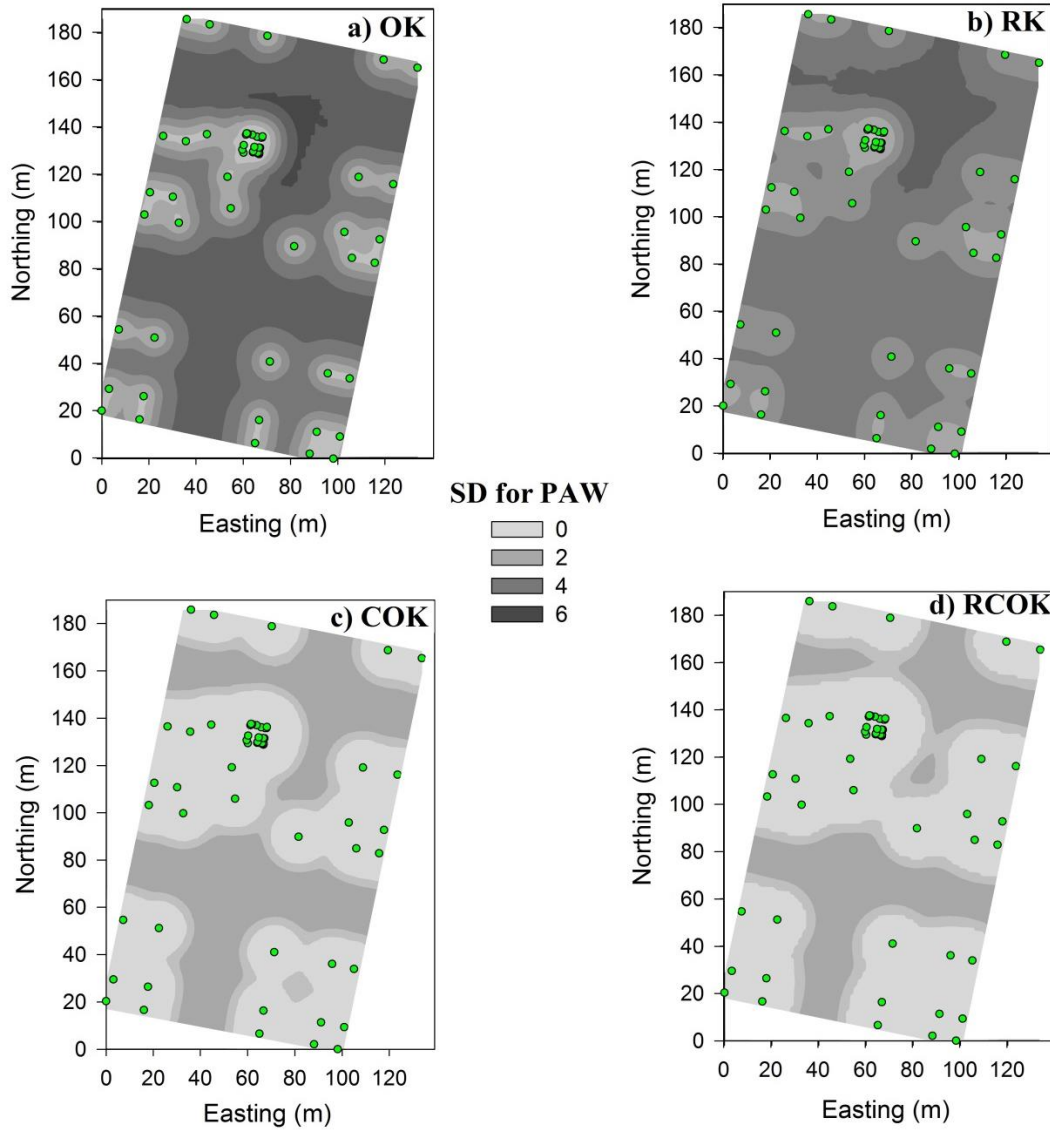


Fig. 6. Generalized visualization of the uncertainty prediction [standard deviation (SD)] for plant available water (PAW; $\text{m}^3 \text{m}^{-3}$) using (a) ordinary kriging (OK), (b) regression-kriging (RK), (c) cokriging (coK), and (d) regression-cokriging (RcoK) approaches in an irrigated cultivated land site. The green dots are the 56 measured points.

10. Figure captions

Fig. 1. Nested cyclic sampling design. The sampling intervals were every 10, 35, 85, 100 m for west to east direction and every 10, 35, 85, 95, 120, 170 m for north to south direction ($n = 36$; main panel). A 0.5, 2, 4.5 m cycle was applied in both directions for the smaller scale nest ($n = 20$) as showed in the inset. There are also two additional sampling points (highlighted in green) which were strategically located in the field plots to increase the sampling efficiency.

Fig. 2. Number of pairs of measured data points for each lag class assuming a uniform lag class size of 5 m distance interval. The dash line shows the 70% of the total distance which is taken as the maximum allowable active lag distance.

Fig. 3. (A) Square root of plant available water (PAW; $\text{m}^3 \text{m}^{-3}$) versus soil organic carbon concentration (SOC; g C kg^{-1} soil) for native grassland (NG) site, and (B) logarithmic microbial biomass carbon (MBC; nmol g^{-1} soil) versus carbon to nitrogen ratio (C:N; unitless) for irrigated cultivated (IC) site.

Fig. 4. Terrain elevation derived from airborne LiDAR (Light Detection and Ranging) with vertical accuracy of 30 cm and spatial resolution of 2 m x 2 m [A. native grassland (NG), B. irrigated cultivated land (IC)]. The green dots are the locations of the 56 measured points in each field site. As customary, terrain elevation units are in meters above mean sea level.

Fig. 5. Maps of (a) plant available water (PAW; $\text{m}^3 \text{m}^{-3}$), (b) soil organic carbon concentration (SOC; g C kg^{-1} soil), and (c) microbial biomass carbon (MBC; nmol g^{-1} soil) concentration by cokriging (coK) method in native grassland. The green dots are the locations of 56 measured points.

Fig. 6. Generalized visualization of the uncertainty prediction [standard deviation (SD)] for plant available water (PAW; $\text{m}^3 \text{m}^{-3}$) using (a) ordinary kriging (OK), (b) regression-kriging (RK), (c) cokriging (coK), and (d) regression-cokriging (RcoK) approaches in an irrigated cultivated land site. The green dots are the 56 measured points.

Conclusion

Different land managements and land use systems significantly influenced various soil properties. Long-term implementation of more diverse and extended crop rotations contributed to soil quality by improving soil aggregation, increasing porosity, and accruing soil organic matter, nitrogen and microbial biomass, which in turn interacted collectively to provide substantial benefits on plant water availability, soil water conductivity, and crop productivity. The various crop phases of the assessed rotations did not caused pronounced differences in terms of most of the measured soil properties, with the only noticeable exception of fractal aggregation which revealed clear differences across phases of the crop rotations. Fallow phases exhibited non-fractal aggregation, while the most fractal soil was found under the perennial leguminous phases of these rotations. Overall, the inclusion of perennial plants in the crop rotation amply benefited soil structural parameters. With respect to nutrient managements, although long-term nutrient additions contributed in general to improving soil functions compared to the control fields that received no nutrient additions, cattle manure addition had even stronger effect specifically on improving nutrient cycling functions while the balanced fertilization benefited directly water availability and overall soil physical condition. Finally, a collective assessment of the measured properties of various land-use systems indicate that conversion of forest to agricultural land and native grassland to cultivated lands alter the soil structural characteristics through substantially lowering macroporosity, saturated water content, and S-index. This land use conversion also appears to increasing MBC concentration in croplands and irrigated cultivated lands compared with forest and native grassland while fungi in the forest soils and gram negative bacteria in native grassland were distinctive biomarkers.

Perennial legumes have heavy tap roots that burrow deep into the ground, lifting soil for better tilth and water holding capacity. Our results demonstrated an improved soil physical structure in soils covered by perennial legumes and grasses compared to annual cropping indicates an overall tendency for increased soil space for roots, air, and water in these soils.

Fractal aggregation (Dm value), S-index, PAW, SOC, and MBC were identified as a valuable representative subset of highly responsive indicators of soil quality which are useful for comparing management options that influence agricultural productivity and sustainability of agroecosystems. Our study found high consistency and sensitivity of Dm approach to specific management options; fractal aggregation approach effectively detected that balanced fertilization was the only nutrient regime exhibiting significantly improved fractal aggregation which may be due to the greater amount of crop residues and roots derived from a higher plant productivity under this nutrient management. These results also demonstrated that fallow phases of both simple and complex rotations were not significantly fractal. It is noteworthy that our two reference ecosystems (i.e., natural forest and native grassland) exhibited improved soil S-index compared to their counterparts (i.e., managed agroecosystems such as irrigated cultivated lands and croplands), but by contrast, the microbial biomass carbon declined in both natural forest and native grasslands. Once more, these findings imply that distinct soil functions are affected by different land use in different directions, emphasizing the importance of considering several soil quality indicators for assessing multiple soil functions. It is suggested to explore the applicability of the mentioned subset of indicators in a wider range of land managements.

The optimal number of samples for detecting management effects on various soil properties varied over the measured variables and land uses at the depth increment of 5-10 cm. It

is suggested to examine the optimal number of samples for various soil properties in other soil depths.

The cultivated land (IC) emerged with stronger degrees of spatial dependence and longer auto-correlation range perhaps suggesting a homogenization or smoothing of the spatial variability of soil properties as a result of intensive agricultural activities repeated in the long term under this specific land use system. Using a nested cyclic sampling design, Gaussian was established as the more effective variographic models across most of our datasets. This study examined several geostatistical methods to predict field spatial variability of PAW, SOC, and MBC concentration. Our results showed that combining kriging with selected terrain covariates accounted for 74 to up to 94% of the variation for PAW, SOC, and MBC in particular when incorporating DTW, elevation, or slope as contributing covariates. Moreover, analysis of accuracy also supported the usefulness at integrating this high spatial-resolution topographic information derived from remote sensing into geostatistical coK and RcoK methods as these approaches resulted in profound improvements of prediction ability compared to OK and RK methods. It is suggested to conduct an additional validation of our findings in independent field sites (independent data sets for interpolation and validation) over comparable landscapes. Overall, more precise maps of the spatial variability of soil attributes in divergent land uses facilitate strategic implementation of best management practices which can lead to sustainable production systems embedded in multifunctional landscapes. It is recommended to continue developing explicit spatial upscaling information for specific soil properties that are linked to key ecosystem functions at other soil depths than in our study, in fine-textured soils, and under a broader variety of land-use systems.

References

- AGRASID. Agricultural Region of Alberta Soil Inventory Database. 2015, URL: [http://www1.agric.gov.ab.ca/\\$department/deptdocs.nsf/all/sag3249](http://www1.agric.gov.ab.ca/$department/deptdocs.nsf/all/sag3249).
- Alberta-Weather Conditions and Forecast, 2016. URL: <http://agriculture.alberta.ca/acis/alberta-weather-data-viewer.jsp>
- Ahamadou, B. and Huang, Q., 2013. Impacts of Agricultural Management Practices on Soil Quality. In *Molecular Environmental Soil Science* (pp. 429-480). Springer Netherlands.
- Ashagrie, Y., Zech, W., Guggenberger, G., Mamo, T., 2007. Soil aggregation, and total and particulate organic matter following conversion of native forests to continuous cultivation in Ethiopia. *Soil Tillage Res.* 94, 101–108. doi:10.1016/j.still.2006.07.005
- Bastida, F., Zsolnay, A., Hernández, T., García, C., 2008. Past, present and future of soil quality indices: A biological perspective. *Geoderma* 147, 159–171. doi:10.1016/j.geoderma.2008.08.007
- Beheshti, A., Raiesi, F., Golchin, A., 2012. Soil properties, C fractions and their dynamics in land use conversion from native forests to croplands in northern Iran. *Agric. Ecosyst. Environ.* 148, 121–133. doi:10.1016/j.agee.2011.12.001
- Bogaert, P., Russo, D., 1999. Optimal spatial sampling design for the estimation of the variogram based on a least squares approach. *Water Resour Res.* 4, 1275–1289.
- Bossuyt, H., Deneff, K., Six, J., Frey, S.D., Merckx, R., Paustian, K., 2001. Influence of microbial populations and residue quality on aggregate stability. *Appl. Soil Ecol.* 16, 195–208. doi:10.1016/S0929-1393(00)00116-5
- Bremer, E., Ellert, K., 2004. Soil quality indicators: a review of implications for agricultural ecosystems in Alberta. Technical report, Symbio Ag Consulting, Lethbridge, Alberta, Canada. AESA.
- Cambardella, C. a., Moorman, T.B., Parkin, T.B., Karlen, D.L., Novak, J.M., Turco, R.F., Konopka, a. E., 1994. Field-Scale Variability of Soil Properties in Central Iowa Soils. *Soil Sci. Soc. Am. J.* 58, 1501.

doi:10.2136/sssaj1994.03615995005800050033x

Ceddia, M.B., Villela, A.L.O., Pinheiro, T.F.M., Wendroth, O., 2015. Spatial variability of soil carbon stock in the Urucu river basin, Central Amazon-Brazil. *Sci. Total Environ.* 526, 58–69.

doi:10.1016/j.scitotenv.2015.03.121

Chakraborty, A., Chakrabarti, K., Chakraborty, A., Ghosh, S., 2011. Effect of long-term fertilizers and manure application on microbial biomass and microbial activity of a tropical agricultural soil. *Biol. Fertil. Soils* 47,

227–233. doi:10.1007/s00374-010-0509-1

Chenu, C., 1989. Influence of a fungal polysaccharide, scleroglucan, on clay microstructures. *Soil Biol. Biochem.*

21, 299–305. doi:10.1016/0038-0717(89)90108-9

Curtin, D., Beare, M.H., Hernandez-Ramirez, G., 2012. Temperature and Moisture Effects on Microbial Biomass and Soil Organic Matter Mineralization. *Soil Sci. Soc. Am. J.* 0, 0. doi:10.2136/sssaj2012.0011

D'Hose, T., Coughon, M., De Vlieghe, A., Vandecasteele, B., Viaene, N., Cornelis, W., Van Bockstaele, E., Reheul, D., 2014. The positive relationship between soil quality and crop production: A case study on the effect of farm compost application. *Appl. Soil Ecol.* 75, 189–198. doi:10.1016/j.apsoil.2013.11.013

Danga, B.O., Ouma, J.P., Wakindiki, I.I.C., Bar-Tal, A., 2009. Chapter 5 Legume-Wheat Rotation Effects on Residual Soil Moisture, Nitrogen and Wheat Yield in Tropical Regions, 1st ed, *Advances in Agronomy*.

Elsevier Inc. doi:10.1016/S0065-2113(08)00805-5

Davis, J.C., 2002. *Statistics and Data Analysis in Geology* (3rd ed.), John Wiley and Sons, New York, p. 638.

Daynes, C.N., Field, D.J., Saleeba, J.A., Cole, M.A., McGee, P.A., 2013. Development and stabilisation of soil structure via interactions between organic matter, arbuscular mycorrhizal fungi and plant roots. *Soil Biol. Biochem.* 57, 683–694. doi:10.1016/j.soilbio.2012.09.020

de Paul Obade, V., Lal, R., 2014. Soil quality evaluation under different land management practices. *Environ. Earth Sci.* 72, 4531–4549. doi:10.1007/s12665-014-3353-z

Dexter, A.R., 2004. Soil physical quality Part I. Theory, effects of soil texture, density, and organic matter, and

- effects on root growth. *Geoderma* 120, 201–214. doi:10.1016/j.geodermaa.2003.09.005
- Dexter, A.R., Czyz, E.A., Richard, G., Reszkowska, A., 2008. A user-friendly water retention function that takes account of the textural and structural pore spaces in soil. *Geoderma* 143, 243–253. doi:10.1016/j.geoderma.2007.11.010
- Di, H.J., Cameron, K.C., Shen, J., Winefield, C.S., Callaghan, M.O., Bowatte, S., He, J., 2013. Molecular Environmental Soil Science. doi:10.1007/978-94-007-4177-5
- Dong, W., Zhang, X., Wang, H., Dai, X., Sun, X., Qiu, W., Yang, F., 2012. Effect of Different Fertilizer Application on the Soil Fertility of Paddy Soils in Red Soil Region of Southern China. *PLoS One* 7, 1–9. doi:10.1371/journal.pone.0044504
- Drewry, J.J., Cameron, K.C., Buchan, G.D., 2008. Pasture yield and soil physical property responses to soil compaction from treading and grazing - A review. *Aust. J. Soil Res.* 46, 237–256. doi:10.1071/SR07125
- Duffera, M., White, J.G., Weisz, R., 2007. Spatial variability of Southeastern U.S. Coastal Plain soil physical properties: Implications for site-specific management. *Geoderma* 137, 327–339. doi:10.1016/j.geoderma.2006.08.018
- Eldeiry, A. a., Garcia, L. a., 2010. Comparison of Ordinary Kriging, Regression Kriging, and Cokriging Techniques to Estimate Soil Salinity Using LANDSAT Images. *J. Irrig. Drain. Eng.* 136, 355–364. doi:10.1061/(ASCE)IR.1943-4774.0000208
- Fóti, S., Balogh, J., Nagy, Z., Herbst, M., Pintér, K., Péli, E., Koncz, P. and Bartha, S., 2014. Soil moisture induced changes on fine-scale spatial pattern of soil respiration in a semi-arid sandy grassland. *Geoderma* 213, 245–254. doi:10.1016/j.geoderma.2013.08.009
- Fortin, M., Payette, S., 2002. How to test the significance of the relation between spatially autocorrelated data at the landscape scale: a case study using fire and forest maps. *Ecoscience* 9, 213–218. doi:10.1111/j.1538-4632.2009.00766.x
- Garrigues, E., Corson, M.S., Angers, D.A., Van Der Werf, H.M.G., Walter, C., 2012. Soil quality in Life Cycle

- Assessment: Towards development of an indicator. *Ecol. Indic.* 18, 434–442.
doi:10.1016/j.ecolind.2011.12.014
- Gatziolis, D., Andersen, H.E., 2008. A Guide to LIDAR Data Acquisition and Processing for the Forests of the Pacific Northwest. Gen. Tech. Rep. PNW-GTR-768 1–40. doi:Gen. Tech. Rep. PNW-GTR-768
- Geisseler, D., Lazicki, P.A., Scow, K.M., 2016. Mineral nitrogen input decreases microbial biomass in soils under grasslands but not annual crops. *Appl. Soil Ecol.* 106, 1–10. doi:10.1016/j.apsoil.2016.04.015
- Glendell, M., Granger, S.J., Bol, R., Brazier, R.E., 2014. Quantifying the spatial variability of soil physical and chemical properties in relation to mitigation of diffuse water pollution. *Geoderma* 214–215, 25–41. doi:10.1016/j.geoderma.2013.10.008
- Grayston, S.J., Campbell, C.D., Bardgett, R.D., Mawdsley, J.L., Clegg, C.D., Ritz, K., Griffiths, B.S., Rodwell, J.S., Edwards, S.J., Davies, W.J. and Elston, D.J., 2004. Assessing shifts in microbial community structure across a range of grasslands of differing management intensity using CLPP, PLFA and community DNA techniques. *Applied Soil Ecology*, 25, 63–84.
- Griffith, D. a, Griffith, D. a, 2013. Establishing Qualitative Geographic Sample Size in the Presence of Spatial Autocorrelation Establishing Qualitative Geographic Sample Size in the Presence of Spatial Autocorrelation 5608, 37–41. doi:10.1080/00045608.2013.776884
- Gülser, C., 2006. Effect of forage cropping treatments on soil structure and relationships with fractal dimensions. *Geoderma* 131, 33–44. doi:10.1016/j.geoderma.2005.03.004
- Hati, K.M., Swarup, A., Mishra, B., Manna, M.C., Wanjari, R.H., Mandal, K.G., Misra, A.K., 2008. Impact of long-term application of fertilizer, manure and lime under intensive cropping on physical properties and organic carbon content of an Alfisol. *Geoderma* 148, 173–179. doi:10.1016/j.geoderma.2008.09.015
- Hebb, C., Schoderbek, D., Hernandez-Ramirez, G., Bork, E., Hewins, D., Carlyle, C., 2016. Soil Physical Quality Varies Among Contrasting Land Uses in Northern Prairie Regions.
- Hengl, T., Heuvelink, G.B.M., Rossiter, D.G., 2007. About regression-kriging: From equations to case studies.

Comput. Geosci. 33, 1301–1315. doi:10.1016/j.cageo.2007.05.001

Hengl, T., Heuvelink, G.B.M., Stein, A., 2004. A generic framework for spatial prediction of soil variables based on regression-kriging. *Geoderma* 120, 75–93. doi:10.1016/j.geoderma.2003.08.018

Herbst, M., Prolingheuer, N., Graf, a., Huisman, J. a., Weihermüller, L., Vanderborght, J., 2009. Characterization and Understanding of Bare Soil Respiration Spatial Variability at Plot Scale. *Vadose Zo. J.* 8, 762. doi:10.2136/vzj2008.0068

Hernandez-ramirez, G., Lawrence-smith, E.J., Sinton, S.M., Schwen, A., Brown, H.E., 2014. Root Responses to Alterations in Macroporosity and Penetrability in a Silt Loam Soil. *Soil Sci. Soc. Am. J.* 78, 1392–1403. doi:10.2136/sssaj2014.01.0005

Hernández-Stefanoni, J.L., Alberto Gallardo-Cruz, J., Meave, J.A., Dupuy, J.M., 2011. Combining geostatistical models and remotely sensed data to improve tropical tree richness mapping. *Ecol. Indic.* 11, 1046–1056. doi:10.1016/j.ecolind.2010.11.003

Heuvelink, G.B.M., Kros, J., Reinds, G.J., De Vries, W., 2016. Geostatistical prediction and simulation of European soil property maps. *Geoderma Reg.* 7, 201–215. doi:10.1016/j.geodrs.2016.04.002

Hewins, D.B., Broadbent, T., Carlyle, C.N., Bork, E.W., 2016. Extracellular enzyme activity response to defoliation and water addition in two ecosites of the mixed grass prairie. *Agric. Ecosyst. Environ.* 230, 79–86. doi:10.1016/j.agee.2016.05.033

Hirmas, D.R., Giménez, D., Subroy, V., Platt, B.F., 2013. Fractal distribution of mass from the millimeter- to decimeter-scale in two soils under native and restored tallgrass prairie. *Geoderma* 207-208, 121–130. doi:10.1016/j.geoderma.2013.05.009

Hudelson, B.D., Clayton, M.K., 2015. Confidence Intervals for Autocorrelations Based on Cyclic Samples 90, 753–757.

Inglett, K.S., Inglett, P.W., Ramesh Reddy, K., Reddy, K.R., 2011. Soil Microbial Community Composition in a Restored Calcareous Subtropical Wetland. *Soil Sci. Soc. Am. J.* 75, 1731–1740. doi:10.2136/sssaj2010.0424

- Karlen, D.L., Andrews, S.S., Weinhold, B.J., Doran, J.W., 2003. Soil quality: Humankind's foundation for survival 171–179.
- Karlen, D.L., Hurley, E.G., Andrews, S.S., Cambardella, C.A., Meek, D.W., Duffy, M.D., Mallarino, A.P., 2006. Crop rotation effects on soil quality at three northern corn/soybean belt locations. *Agron. J.* 98, 484–495. doi:10.2134/agronj2005.0098
- Khalili, B., Ogunseitan, O.A., Goulden, M.L., Allison, S.D., 2016. Interactive effects of precipitation manipulation and nitrogen addition on soil properties in California grassland and shrubland. *Appl. Soil Ecol.* 107, 144–153. doi:10.1016/j.apsoil.2016.05.018
- Kiani, M., Gheysari, M., Mostafazadeh-Fard, B., Majidi, M.M., Karchani, K., Hoogenboom, G., 2016a. Effect of the interaction of water and nitrogen on sunflower under drip irrigation in an arid region. *Agric. Water Manag.* 171, 162–172. doi:10.1016/j.agwat.2016.04.008
- Kiani, M., Hernandez-Ramirez, G., Quideau, S., Smith, E., Janzen, H., Larney, F., Puurveen, D., 2016b. Quantifying the sensitive soil quality indicators across contrasting long-term land management systems: crop rotations and nutrient Regimes.
- Knotters, M., Brus, D.J., Voshaar, J.H.O., 1995. a Comparison of Kriging, Co-Kriging and Kriging Combined With Regression for Spatial Interpolation of Horizon Depth With Censored Observations. *Geoderma* 67, 227–246. doi:10.1016/0016-7061(95)00011-c
- Lark, R.M., 2002. Optimized spatial sampling of soil for estimation of the variogram by maximum likelihood. *Geoderma* 105, 49–80. doi:10.1016/S0016-7061(01)00092-1
- Li, J., Richter, D. deB, Mendoza, A., Heine, P., 2010. Effects of land-use history on soil spatial heterogeneity of macro- and trace elements in the Southern Piedmont USA. *Geoderma* 156, 60–73. doi:10.1016/j.geoderma.2010.01.008
- Li, Y., 2010. Can the spatial prediction of soil organic matter contents at various sampling scales be improved by using regression kriging with auxiliary information? *Geoderma* 159, 63–75. doi:10.1016/j.geoderma.2010.06.017

- Liu, D., Wang, Z., Zhang, B., Song, K., Li, X., Li, J., Li, F., Duan, H., 2006. Spatial distribution of soil organic carbon and analysis of related factors in croplands of the black soil region, Northeast China. *Agric. Ecosyst. Environ.* 113, 73–81. doi:10.1016/j.agee.2005.09.006
- Liu, Z.-P., Shao, M.-A., Wang, Y.-Q., 2013. Spatial patterns of soil total nitrogen and soil total phosphorus across the entire Loess Plateau region of China. *Geoderma* 197-198, 67–78. doi:10.1016/j.geoderma.2012.12.011
- Liu, Z., Zhou, W., Shen, J., Li, S., Ai, C., 2014. Soil quality assessment of yellow clayey paddy soils with different productivity. *Biol. Fertil. Soils* 50, 537–548. doi:10.1007/s00374-013-0864-9
- Lowenberg-DeBoer, J., Swinton, S.M., 1997. Economics of site-specific management in agronomic crops. *state site-specific Manag. Agric.* 369–396.
- Marzaioli, R., D'Ascoli, R., De Pascale, R.A., Rutigliano, F.A., 2010. Soil quality in a Mediterranean area of Southern Italy as related to different land use types. *Appl. Soil Ecol.* 44, 205–212. doi:10.1016/j.apsoil.2009.12.007
- McCauley, A., Jones, C., Jacobsen, J., 2009. Soil pH and Organic Matter. *Nutrient management modules 8, #4449-8.* Montana State University Extension Service, Bozeman, Montana, pp. 1–12.
- McDaniel, M.D., Tiemann, L.K., Grandy, A.S., 2014. Does agricultural crop diversity enhance soil microbial biomass and organic matter dynamics? A meta-analysis. *Ecol. Appl.* 24, 560–570. doi:10.1890/13-0616.1
- Mclean, E.O., 1982. Soil pH and lime requirement. *Methods Soil Anal.* 9, 595–624. doi:10.2134/agronmonogr9.2.2ed.c12
- Metcalf, D., Meir, P., Aragao, L.E.O., da Costa, A., Almeida, S., Braga, A., Gonçalves, P., Athaydes, J., Malhi, Y. and Williams, M., 2008. Sample sizes for estimating key ecosystem characteristics in a tropical terra firme rainforest. *For. Ecol. Manage.* 255, 558–566. doi:10.1016/j.foreco.2007.09.026
- Mirzaee, S., Ghorbani-Dashtaki, S., Mohammadi, J., Asadi, H., Asadzadeh, F., 2016. Spatial variability of soil organic matter using remote sensing data. *Catena* 145, 118–127. doi:10.1016/j.catena.2016.05.023
- Mollard, F.P.O., Naeth, M.A., Cohen-Fernandez, A., 2014. Impacts of mulch on prairie seedling establishment:

- Facilitative to inhibitory effects. *Ecol. Eng.* 64, 377–384. doi:10.1016/j.ecoleng.2014.01.012
- Motaghian, H.R., Mohammadi, J., 2011. Spatial estimation of saturated hydraulic conductivity from terrain attributes using regression, kriging, and artificial neural networks. *Pedosphere* 21, 170–177. doi:10.1016/S1002-0160(11)60115-X
- Munkholm, L.J., Heck, R.J., Deen, B., 2013. Long-term rotation and tillage effects on soil structure and crop yield. *Soil Tillage Res.* 127, 85–91. doi:10.1016/j.still.2012.02.007
- Munkholm, L.J., Schjønning, P., Rasmussen, K.J., Tanderup, K., 2003. Spatial and temporal effects of direct drilling on soil structure in the seedling environment. *Soil Tillage Res.* 71, 163–173. doi:10.1016/S0167-1987(03)00062-X
- Murphy, P.N., Ogilvie, J., Meng, F.R., White, B., Bhatti, J.S. and Arp, P.A., 2011. Modelling and mapping topographic variations in forest soils at high resolution: A case study. *Ecological Modelling* 222(14),2314–2332.
- Naderi-Boldaji, M., Keller, T., 2016. Degree of soil compactness is highly correlated with the soil physical quality index S. *Soil Tillage Res.* 159, 41–46. doi:10.1016/j.still.2016.01.010
- Norman, C.R., Brye, K.R., Gbur, E.E., Chen, P., Rupe, J., 2016. Long-term Management Effects on Soil Properties and Yields in a Wheat-Soybean Double-Crop System in Eastern Arkansas. *Soil Sci.* 181, 1–12.
- Odeh, I.O.A., McBratney, A.B., Chittleborough, D.J., 1995. Further results on prediction of soil properties from terrain attributes: heterotopic cokriging and regression-kriging. *Geoderma* 67, 215–226. doi:10.1016/0016-7061(95)00007-B
- Orr, C.H., Predick, K.I., Stanley, E.H., Rogers, K.L., 2014. Spatial autocorrelation of denitrification in a restored and a natural floodplain. *Wetlands* 34, 89–100. doi:10.1007/s13157-013-0488-8
- O’Sullivan, L., Creamer, R.E., Fealy, R., Lanigan, G., Simo, I., Fenton, O., Carfrae, J., Schulte, R.P.O., 2015. Functional Land Management for managing soil functions: A case-study of the trade-off between primary productivity and carbon storage in response to the intervention of drainage systems in Ireland. *Land use policy*

47, 42–54. doi:10.1016/j.landusepol.2015.03.007

Oweis, T., Hachum, A., Pala, M., 2004. Lentil production under supplemental irrigation in a Mediterranean environment. *Agric. Water Manag.* 68, 251–265. doi:10.1016/j.agwat.2004.03.013

Pagliai, M., Vignozzi, N., Pellegrini, S., 2004. Soil structure and the effect of management practices. *Soil Tillage Res.* 79, 131–143. doi:10.1016/j.still.2004.07.002

Quideau, S.A., Swallow, M.J.B., Prescott, C.E., Grayston, S.J., Oh, S.W., 2013. Comparing soil biogeochemical processes in novel and natural boreal forest ecosystems. *Biogeosciences* 10, 5651–5661. doi:10.5194/bg-10-5651-2013

Reynolds, W.D., Drury, C.F., Tan, C.S., Fox, C.A., Yang, X.M., 2009. Use of indicators and pore volume-function characteristics to quantify soil physical quality. *Geoderma* 152, 252–263. doi:10.1016/j.geoderma.2009.06.009

Robertson, G.P., Crum, J.R., Ellis, B.G., 1993. The spatial variability of soil resources following long-term disturbance. *Oecologia* 96, 451–456. doi:10.1007/BF00320501

Schelle, H., Heise, L., Jänicke, K., Durner, W., 2013. Water retention characteristics of soils over the whole moisture range: A comparison of laboratory methods. *Eur. J. Soil Sci.* 64, 814–821. doi:10.1111/ejss.12108

Schindler, U., Durner, W., von Unold, G., Muller, L., 2010. Evaporation Method for Measuring Unsaturated Hydraulic Properties of Soils: Extending the Measurement Range. *Soil Sci Soc Am J* 74, 1071–1083. doi:10.2136/sssaj2008.0358

Schwen, A., Hernandez-Ramirez, G., Lawrence-Smith, E.J., Sinton, S.M., Carrick, S., Clothier, B.E., Buchan, G.D., Loiskandl, W., 2011. Hydraulic Properties and the Water-Conducting Porosity as Affected by Subsurface Compaction using Tension Infiltrimeters. *Soil Sci. Soc. Am. J.* 75, 822–831. doi:10.2136/sssaj2010.0257

Sharma, K.L., Grace, J.K., Mandal, U.K., Gajbhiye, P.N., Srinivas, K., Korwar, G.R., Hima Bindu, V., Ramesh, V., Ramachandran, K., Yadav, S.K., 2008. Evaluation of long-term soil management practices using key indicators and soil quality indices in a semi-arid tropical Alfisol. *Soil Res.* 46, 368–377. doi:http://dx.doi.org/10.1071/SR07184

- Simbahan, G.C., Dobermann, A., Goovaerts, P., Ping, J., Haddix, M.L., 2006. Fine-resolution mapping of soil organic carbon based on multivariate secondary data. *Geoderma* 132, 471–489. doi:10.1016/j.geoderma.2005.07.001
- Six, J., Bossuyt, H., Degryze, S., Denef, K., 2004. A history of research on the link between (micro)aggregates, soil biota, and soil organic matter dynamics. *Soil Tillage Res.* 79, 7–31. doi:10.1016/j.still.2004.03.008
- Smith, R.G., Gross, K.L., Robertson, G.P., 2008. Effects of crop diversity on agroecosystem function: Crop yield response. *Ecosystems* 11, 355–366. doi:10.1007/s10021-008-9124-5
- Sradnick, A., Murugan, R., Oltmanns, M., Raupp, J., Joergensen, R.G., 2013. Changes in functional diversity of the soil microbial community in a heterogeneous sandy soil after long-term fertilization with cattle manure and mineral fertilizer. *Appl. Soil Ecol.* 63, 23–28. doi:10.1016/j.apsoil.2012.09.011
- Steenwerth, K.L., Jackson, L.E., Calderón, F.J., Stromberg, M.R., Scow, K.M., Caldero, F.J., 2002. Soil microbial community composition and land use history in cultivated and grassland ecosystems of coastal California. *Soil Biol. Biochem.* 34, 1599–1611. doi:10.1016/S0038-0717(02)00144-X
- Stenberg, B., 1999. Monitoring soil quality of arable land: Microbiological indicators. *Acta Agric. Scand. - Sect. B Soil Plant Sci.* 49, 1–24. doi:Doi 10.1080/09064719950135669
- Stutter, M.I., Deeks, L.K., Billett, M.F., 2004. Spatial Variability in Soil Ion Exchange Chemistry in a Granitic Upland Catchment. *Soil Sci. Soc. Am. J.* 68, 1304. doi:10.2136/sssaj2004.1304
- Su, Z.-Y., Xiong, Y.-M., Zhu, J.-Y., Ye, Y.-C., Ye, M., Zhi-yaol, S.U., Yong-mei, X., Jian-yun, Z.H.U., Yong-chang, Y.E., Mai, Y.E., 2006. Soil Organic Carbon Content and Distribution in a Small Landscape of Dongguan, South China. *Pedosphere* 16, 10–17. doi:10.1016/S1002-0160(06)60020-9
- Sylvia, D.M., Fuhrmann, J.J., Hartel, P.G., Zuberer, D. a, Darmstadt, T.U., Hall, P., 1998. Principles and Applications of Soil Microbiology 550.
- Tiemann, L.K., Grandy, A.S., Atkinson, E.E., Marin-Spiotta, E., Mcdaniel, M.D., 2015. Crop rotational diversity enhances belowground communities and functions in an agroecosystem. *Ecol. Lett.* 18, 761–771.

doi:10.1111/ele.12453

Tormena, C.A., Silva, Á.P. Da, Imhoff, S.D.C., Dexter, A.R., 2008. Quantification of the soil physical quality of a tropical oxisol using the S index. *Sci. Agric.* 65, 56–60. doi:10.1590/S0103-90162008000100008

Bogaert, P., Russo, D., 1999. Optimal spatial sampling design for the estimation of the variogram based on a least squares approach. *Water Resour Res.* 4, 1275–1289.

Cambardella, C. a., Moorman, T.B., Parkin, T.B., Karlen, D.L., Novak, J.M., Turco, R.F., Konopka, a. E., 1994. Field-Scale Variability of Soil Properties in Central Iowa Soils. *Soil Sci. Soc. Am. J.* 58, 1501. doi:10.2136/sssaj1994.03615995005800050033x

Ceddia, M.B., Villela, A.L.O., Pinheiro, T.F.M., Wendroth, O., 2015. Spatial variability of soil carbon stock in the Urucu river basin, Central Amazon-Brazil. *Sci. Total Environ.* 526, 58–69. doi:10.1016/j.scitotenv.2015.03.121

Chenu, C., 1989. Influence of a fungal polysaccharide, scleroglucan, on clay microstructures. *Soil Biol. Biochem.* 21, 299–305. doi:10.1016/0038-0717(89)90108-9

Curtin, D., Beare, M.H., Hernandez-Ramirez, G., 2012. Temperature and Moisture Effects on Microbial Biomass and Soil Organic Matter Mineralization. *Soil Sci. Soc. Am. J.* 0, 0. doi:10.2136/sssaj2012.0011

Davis, J.C., 2002. *Statistics and Data Analysis in Geology* (3rd ed.), John Wiley and Sons, New York, p. 638.

Daynes, C.N., Field, D.J., Saleeba, J.A., Cole, M.A., McGee, P.A., 2013. Development and stabilisation of soil structure via interactions between organic matter, arbuscular mycorrhizal fungi and plant roots. *Soil Biol. Biochem.* 57, 683–694. doi:10.1016/j.soilbio.2012.09.020

Dexter, a R., 2004. Soil physical quality Part I. Theory, effects of soil texture, density, and organic matter, and effects on root growth. *Geoderma* 120, 201–214. doi:10.1016/j.geoderma.2003.09.005

Dexter, A.R., Czyz, E.A., Richard, G., Reszkowska, A., 2008. A user-friendly water retention function that takes account of the textural and structural pore spaces in soil. *Geoderma* 143, 243–253. doi:10.1016/j.geoderma.2007.11.010

- Drewry, J.J., Cameron, K.C., Buchan, G.D., 2008. Pasture yield and soil physical property responses to soil compaction from treading and grazing - A review. *Aust. J. Soil Res.* 46, 237–256. doi:10.1071/SR07125
- Duffera, M., White, J.G., Weisz, R., 2007. Spatial variability of Southeastern U.S. Coastal Plain soil physical properties: Implications for site-specific management. *Geoderma* 137, 327–339. doi:10.1016/j.geoderma.2006.08.018
- Eldeiry, A. a., Garcia, L. a., 2010. Comparison of Ordinary Kriging, Regression Kriging, and Cokriging Techniques to Estimate Soil Salinity Using LANDSAT Images. *J. Irrig. Drain. Eng.* 136, 355–364. doi:10.1061/(ASCE)IR.1943-4774.0000208
- Fóti, S., Balogh, J., Nagy, Z., Herbst, M., Pintér, K., Péli, E., Koncz, P. and Bartha, S., 2014. Soil moisture induced changes on fine-scale spatial pattern of soil respiration in a semi-arid sandy grassland. *Geoderma* 213, 245–254. doi:10.1016/j.geoderma.2013.08.009
- Fortin, M., Payette, S., 2002. How to test the significance of the relation between spatially autocorrelated data at the landscape scale: a case study using fire and forest maps. *Ecoscience* 9, 213–218. doi:10.1111/j.1538-4632.2009.00766.x
- Gatziolis, D., Andersen, H.E., 2008. A Guide to LIDAR Data Acquisition and Processing for the Forests of the Pacific Northwest. Gen. Tech. Rep. PNW-GTR-768 1–40. doi:Gen. Tech. Rep. PNW-GTR-768
- Geisseler, D., Lazicki, P.A., Scow, K.M., 2016. Mineral nitrogen input decreases microbial biomass in soils under grasslands but not annual crops. *Appl. Soil Ecol.* 106, 1–10. doi:10.1016/j.apsoil.2016.04.015
- Glendell, M., Granger, S.J., Bol, R., Brazier, R.E., 2014. Quantifying the spatial variability of soil physical and chemical properties in relation to mitigation of diffuse water pollution. *Geoderma* 214-215, 25–41. doi:10.1016/j.geoderma.2013.10.008
- Grayston, S.J., Campbell, C.D., Bardgett, R.D., Mawdsley, J.L., Clegg, C.D., Ritz, K., Griffiths, B.S., Rodwell, J.S., Edwards, S.J., Davies, W.J. and Elston, D.J., 2004. Assessing shifts in microbial community structure across a range of grasslands of differing management intensity using CLPP, PLFA and community DNA techniques. *Applied Soil Ecology*, 25, 63–84.

- Griffith, D. a, Griffith, D. a, 2013. Establishing Qualitative Geographic Sample Size in the Presence of Spatial Autocorrelation Establishing Qualitative Geographic Sample Size in the Presence of Spatial Autocorrelation 5608, 37–41. doi:10.1080/00045608.2013.776884
- Hannam, K. D., Quideau, S. A., Kishchuk, B. E., 2006. Forest floor microbial communities in relation to stand composition and timber harvesting in northern Alberta. *Soil Biology and Biochemistry*, 38, 2565- 2575.
- Hengl, T., Heuvelink, G.B.M., Rossiter, D.G., 2007. About regression-kriging: From equations to case studies. *Comput. Geosci.* 33, 1301–1315. doi:10.1016/j.cageo.2007.05.001
- Hengl, T., Heuvelink, G.B.M., Stein, A., 2004. A generic framework for spatial prediction of soil variables based on regression-kriging. *Geoderma* 120, 75–93. doi:10.1016/j.geoderma.2003.08.018
- Herbst, M., Prolingheuer, N., Graf, a., Huisman, J. a., Weihermüller, L., Vanderborght, J., 2009. Characterization and Understanding of Bare Soil Respiration Spatial Variability at Plot Scale. *Vadose Zo. J.* 8, 762. doi:10.2136/vzj2008.0068
- Hernández-Stefanoni, J.L., Alberto Gallardo-Cruz, J., Meave, J.A., Dupuy, J.M., 2011. Combining geostatistical models and remotely sensed data to improve tropical tree richness mapping. *Ecol. Indic.* 11, 1046–1056. doi:10.1016/j.ecolind.2010.11.003
- Heuvelink, G.B.M., Kros, J., Reinds, G.J., De Vries, W., 2016. Geostatistical prediction and simulation of European soil property maps. *Geoderma Reg.* 7, 201–215. doi:10.1016/j.geodrs.2016.04.002
- Hewins, D.B., Broadbent, T., Carlyle, C.N., Bork, E.W., 2016. Extracellular enzyme activity response to defoliation and water addition in two ecosites of the mixed grass prairie. *Agric. Ecosyst. Environ.* 230, 79–86. doi:10.1016/j.agee.2016.05.033
- Hudelson, B.D., Clayton, M.K., 2015. Confidence Intervals for Autocorrelations Based on Cyclic Samples 90, 753–757.
- Khalili, B., Ogunseitan, O.A., Goulden, M.L., Allison, S.D., 2016. Interactive effects of precipitation manipulation

- and nitrogen addition on soil properties in California grassland and shrubland. *Appl. Soil Ecol.* 107, 144–153.
doi:10.1016/j.apsoil.2016.05.018
- Kiani, M., Hernandez-Ramirez, G., Quideau, S., Smith, E., Janzen, H., Larney, F., Puurveen, D., 2016. Quantifying the sensitive soil quality indicators across contrasting long-term land management systems: crop rotations and nutrient Regimes
- Knotters, M., Brus, D.J., Voshaar, J.H.O., 1995. a Comparison of Kriging, Co-Kriging and Kriging Combined With Regression for Spatial Interpolation of Horizon Depth With Censored Observations. *Geoderma* 67, 227–246.
doi:10.1016/0016-7061(95)00011-c
- Lark, R.M., 2002. Optimized spatial sampling of soil for estimation of the variogram by maximum likelihood. *Geoderma* 105, 49–80. doi:10.1016/S0016-7061(01)00092-1
- Li, J., Richter, D. deB, Mendoza, A., Heine, P., 2010. Effects of land-use history on soil spatial heterogeneity of macro- and trace elements in the Southern Piedmont USA. *Geoderma* 156, 60–73.
doi:10.1016/j.geoderma.2010.01.008
- Li, Y., 2010. Can the spatial prediction of soil organic matter contents at various sampling scales be improved by using regression kriging with auxiliary information? *Geoderma* 159, 63–75.
doi:10.1016/j.geoderma.2010.06.017
- Liu, D., Wang, Z., Zhang, B., Song, K., Li, X., Li, J., Li, F., Duan, H., 2006. Spatial distribution of soil organic carbon and analysis of related factors in croplands of the black soil region, Northeast China. *Agric. Ecosyst. Environ.* 113, 73–81. doi:10.1016/j.agee.2005.09.006
- Liu, Z.-P., Shao, M.-A., Wang, Y.-Q., 2013. Spatial patterns of soil total nitrogen and soil total phosphorus across the entire Loess Plateau region of China. *Geoderma* 197-198, 67–78. doi:10.1016/j.geoderma.2012.12.011
- Lowenberg-DeBoer, J., Swinton, S.M., 1997. Economics of site-specific management in agronomic crops. state site-specific Manag. *Agric.* 369–396.
- Mclean, E.O., 1982. Soil pH and lime requirement. *Methods Soil Anal.* 9, 595– 624.

doi:10.2134/agronmonogr9.2.2ed.c12

Metcalfe, D., Meir, P., Aragao, L.E.O., da Costa, A., Almeida, S., Braga, A., Gonçalves, P., Athaydes, J., Malhi, Y. and Williams, M., 2008. Sample sizes for estimating key ecosystem characteristics in a tropical terra firme rainforest. *For. Ecol. Manage.* 255, 558–566. doi:10.1016/j.foreco.2007.09.026

Mirzaee, S., Ghorbani-Dashtaki, S., Mohammadi, J., Asadi, H., Asadzadeh, F., 2016. Spatial variability of soil organic matter using remote sensing data. *Catena* 145, 118–127. doi:10.1016/j.catena.2016.05.023

Mollard, F.P.O., Naeth, M.A., Cohen-Fernandez, A., 2014. Impacts of mulch on prairie seedling establishment: Facilitative to inhibitory effects. *Ecol. Eng.* 64, 377–384. doi:10.1016/j.ecoleng.2014.01.012

Murphy, P.N., Ogilvie, J., Meng, F.R., White, B., Bhatti, J.S. and Arp, P.A., 2011. Modelling and mapping topographic variations in forest soils at high resolution: A case study. *Ecological Modelling* 222(14),2314–2332.

Motaghian, H.R., Mohammadi, J., 2011. Spatial estimation of saturated hydraulic conductivity from terrain attributes using regression, kriging, and artificial neural networks. *Pedosphere* 21, 170–177. doi:10.1016/S1002-0160(11)60115-X

Odeh, I.O.A., McBratney, A.B., Chittleborough, D.J., 1995. Further results on prediction of soil properties from terrain attributes: heterotopic cokriging and regression-kriging. *Geoderma* 67, 215–226. doi:10.1016/0016-7061(95)00007-B

Orr, C.H., Predick, K.I., Stanley, E.H., Rogers, K.L., 2014. Spatial autocorrelation of denitrification in a restored and a natural floodplain. *Wetlands* 34, 89–100. doi:10.1007/s13157-013-0488-8

Pagliai, M., Vignozzi, N., Pellegrini, S., 2004. Soil structure and the effect of management practices. *Soil Tillage Res.* 79, 131–143. doi:10.1016/j.still.2004.07.002

Qiu, W, Curtin, D., Johnstone, P., Beare, M., Hernandez-Ramirez G. (2016): Small-Scale Spatial Variability of Plant Nutrients and Soil Organic Matter: an Arable Cropping Case Study, *Communications in Soil Science and Plant Analysis* <http://dx.doi.org/10.1080/00103624.2016.1228945>

- Reynolds, W.D., Drury, C.F., Tan, C.S., Fox, C.A., Yang, X.M., 2009. Use of indicators and pore volume-function characteristics to quantify soil physical quality. *Geoderma* 152, 252–263. doi:10.1016/j.geoderma.2009.06.009
- Robertson, G.P., Crum, J.R., Ellis, B.G., 1993. The spatial variability of soil resources following long-term disturbance. *Oecologia* 96, 451–456. doi:10.1007/BF00320501
- Schelle, H., Heise, L., Jänicke, K., Durner, W., 2013. Water retention characteristics of soils over the whole moisture range: A comparison of laboratory methods. *Eur. J. Soil Sci.* 64, 814–821. doi:10.1111/ejss.12108
- Schindler, U., Durner, W., von Unold, G., Muller, L., 2010. Evaporation Method for Measuring Unsaturated Hydraulic Properties of Soils: Extending the Measurement Range. *Soil Sci Soc Am J* 74, 1071–1083. doi:10.2136/sssaj2008.0358
- Simbahan, G.C., Dobermann, A., Goovaerts, P., Ping, J., Haddix, M.L., 2006. Fine-resolution mapping of soil organic carbon based on multivariate secondary data. *Geoderma* 132, 471–489. doi:10.1016/j.geoderma.2005.07.001
- Six, J., Bossuyt, H., Degryze, S., Denef, K., 2004. A history of research on the link between (micro)aggregates, soil biota, and soil organic matter dynamics. *Soil Tillage Res.* 79, 7–31. doi:10.1016/j.still.2004.03.008
- Steenwerth, K.L., Jackson, L.E., Calderón, F.J., Stromberg, M.R., Scow, K.M., Caldero, F.J., 2002. Soil microbial community composition and land use history in cultivated and grassland ecosystems of coastal California. *Soil Biol. Biochem.* 34, 1599–1611. doi:10.1016/S0038-0717(02)00144-X
- Stutter, M.I., Deeks, L.K., Billett, M.F., 2004. Spatial Variability in Soil Ion Exchange Chemistry in a Granitic Upland Catchment. *Soil Sci. Soc. Am. J.* 68, 1304. doi:10.2136/sssaj2004.1304
- Su, Z.-Y., Xiong, Y.-M., Zhu, J.-Y., Ye, Y.-C., Ye, M., Zhi-yaol, S.U., Yong-mei, X., Jian-yun, Z.H.U., Yong-chang, Y.E., Mai, Y.E., 2006. Soil Organic Carbon Content and Distribution in a Small Landscape of Dongguan, South China. *Pedosphere* 16, 10–17. doi:10.1016/S1002-0160(06)60020-9
- Teferi, E., Bewket, W., Simane, B., 2016. Effects of land use and land cover on selected soil quality indicators in the head water area of the Blue Nile basin of Ethiopia. *Environ. Monit Assess.* 188, 83.

- Tormena, C.A., Silva, Á.P. Da, Imhoff, S.D.C., Dexter, A.R., 2008. Quantification of the soil physical quality of a tropical oxisol using the S index. *Sci. Agric.* 65, 56–60. doi:10.1590/S0103-90162008000100008
- Wang, K., Zhang, C., Li, W., 2013. Predictive mapping of soil total nitrogen at a regional scale: A comparison between geographically weighted regression and cokriging. *Appl. Geogr.* 42, 73–85. doi:10.1016/j.apgeog.2013.04.002
- Wang, Y., Zhang, X., Huang, C., 2009. Spatial variability of soil total nitrogen and soil total phosphorus under different land uses in a small watershed on the Loess Plateau, China. *Geoderma* 150, 141–149. doi:10.1016/j.geoderma.2009.01.021
- Webster, R., 1985. Quantitative Spatial Analysis of Soil in the Field, in: Stewart, B.A. (Ed.), *Advances in Soil Science*. Springer New York, New York, NY, pp. 1–70. doi:10.1007/978-1-4612-5090-6_1
- Wienhold, B.J., Pikul, J.L., Liebig, M.A., Mikha, M.M., Varvel, G.E., Doran, J.W., Andrews, S.S., 2006. Cropping system effects on soil quality in the Great Plains: Synthesis from a regional project. *Renew. Agric. Food Syst.* 21, 49–59. doi:10.1079/RAF2005125
- Yang, Y., Guo, J., Chen, G., Yin, Y., Gao, R., Lin, C., 2009. Effects of forest conversion on soil labile organic carbon fractions and aggregate stability in subtropical China. *Plant Soil* 323, 153–162. doi:10.1007/s11104-009-9921-4
- Zelles, L., 1999. Fatty acid patterns of phospholipids and lipopolysaccharides in the characterisation of microbial communities in soil: a review. *Biol. Fertil. Soils* 29, 111–129.
- Zou, X.M., Ruan, H.H., Fu, Y., Yang, X.D., Sha, L.Q., 2005. Estimating soil labile organic carbon and potential turnover rates using a sequential fumigation-incubation procedure. *Soil Biol. Biochem.* 37, 1923–1928. doi:10.1016/j.soilbio.2005.02.028

Appendices

Table A. Deterministic and variographic (semivariogram and cross-semivariogram) models, fitting statistical indicators, and resulting validation parameters for SOC density (g C m^{-2}) as a function of five geostatistical approaches in both native grassland (NG) and irrigated cultivated land (IC).

SOC density	Prediction Method	Regression equation; §Predictors; °Covariates	Variography					Validation Parameters			
			Model	Residual SS	r ²	Auto-correlation Range (m)	C0/(C0+C) (%)	R ²	SE predict	MPE	RMSPE
NG	R	$\text{Log}_{10}(\text{SOC den}) = 2.631 + (0.244 \times \text{STN})$	-	-	-	-	-	0.88	74.93	-2.70	75.87
	OK	-	G	2.2×10^9	0.44	45	26.1	0.03	84.05	-8.06	219.00
	RK	§STN	S	1.5×10^{-3}	0.53	56	45	0.88	74.95	-2.30	75.88
	coK	°DTW	G	707	0.73	81	4	0.87	59.51	0.43	86.52
	RcoK	STN *DTW	G	133	0.20	80	0.4	0.93	54.67	-0.38	55.76
IC	R	$\text{Log}_{10}(\text{SOC den}) = 2.52 + (0.306 \times \text{STN}) + (0.377 \times \text{PAW})$	-	-	-	-	-	0.85	87.89	-5.27	92.67
	OK	-	G	2.1×10^{10}	0.41	65	0.1	0.55	136.93	-5.07	162.93
	RK	§STN, PAW	G	4.3×10^7	0.54	11	7	0.85	90.58	-7.85	94.20
	coK	°ELEV	G	5253	0.41	75	0.2	0.98	31.67	0.22	31.82
	RcoK	(STN, PAW) * ELEV	G	110	0.64	100	0.1	0.99	18.46	-1.72	18.97

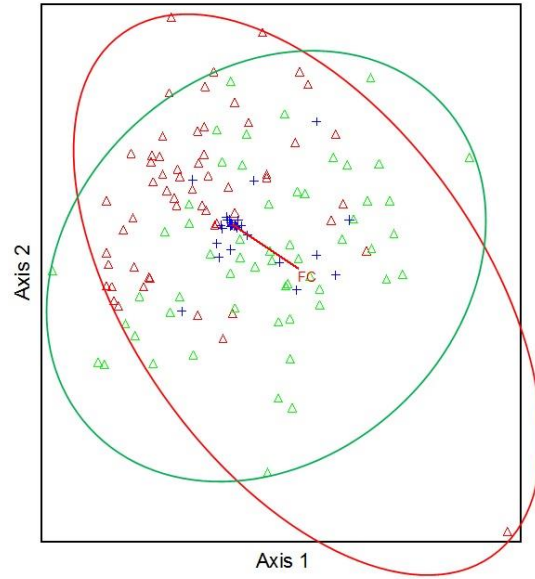


Fig. A. NMS ordination biplots for phospholipid fatty acid (PLFA) analysis for native grassland (NG, red symbol) and irrigated cultivated land (IC, green symbol) at Mattheis sites. 53 iterations, stress= 16, 3-dimensional solution.

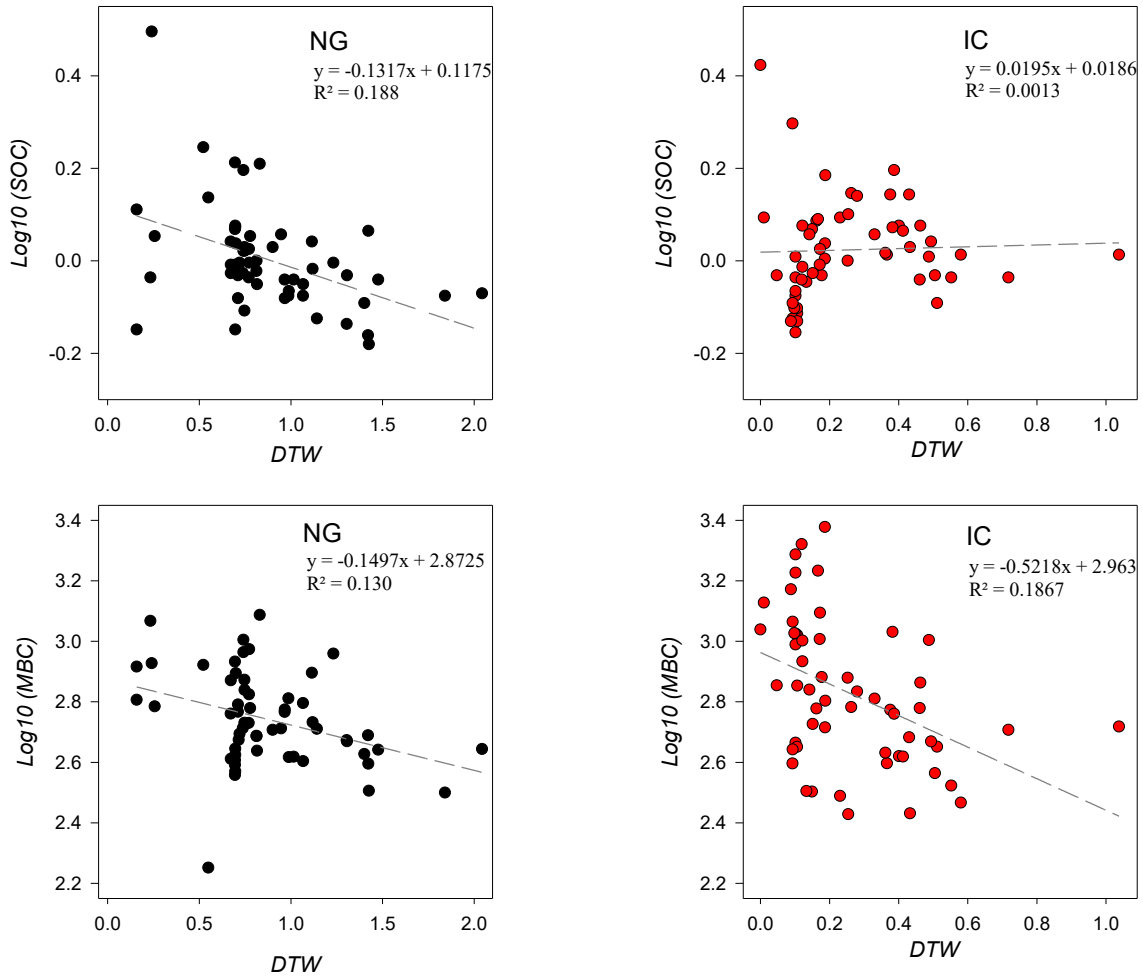


Fig. B. Logarithmic soil organic carbon concentration (SOC; % m/m) versus terrain depth to water (DTW, m) and logarithmic microbial biomass carbon (MBC; nmol g⁻¹ soil) versus DTW for native grassland (NG) and irrigated cultivated (IC) sites. X axes are presented at different scales for the two field sites.